JANUARY 2021 | HydrocarbonProcessing.com

HYDROCARBON PROCESSING®

HYDROCARBON PROCESSING®

JANUARY 2021 | Volume 100 Number 1
HydrocarbonProcessing.com

SPECIAL FOCUS: SUSTAINABILITY

27 **Ras Tanura: The creation of a clean-fuels complex**
M. Halvaci, E. A. Subaie, N. A. Fudhail, C. Pierre and E. Rousseau

29 **FCC NO_x reduction methods: Complying with regulations without capital investment**
P. Hobbins, H. Blair and T. Hochheiser

33 **Cyclic distillation: A novel enhanced technology for processing hydrocarbons and derivatives**
A. A. Kiss, V. N. Maleta, A. Shevchenko and O. Bedryk

39 **Hydrocarbons face toughest challenge yet**
F. Ketelaars

PROCESS OPTIMIZATION

41 **Search for advanced technique of desalter control—TON control for interface level**
K. K. Mandal

44 **Optimize processes with a spreadsheet**
J. Colannino

HEAT TRANSFER

49 **Selection and comparison of thermic fluids in a fired heater**
A. V. Karre and K. T. Valsaraj

53 **Stop oxidation and scale growth with high-emissivity coating**
J. Poth

VALVES, PUMPS AND TURBOMACHINERY

57 **Resolving a chronic water injection pump high vibration through a shaft-lifting technique**
W. A. Alharbi, A. Ghazal and D. Turcan

61 **Modular reed valve technology for reciprocating compressors**
H. P. Bloch

PROCESS CONTROLS, INSTRUMENTATION AND AUTOMATION

65 **How to support condition monitoring with wireless instrumentation networks**
A. Cureton

MAINTENANCE AND RELIABILITY

69 **Improving asset utilization by closing the corrosion window**
J. A. Zurlo

74 **Reasons for vibration issues in boilers and furnaces**
T. Webster

Cover Image: Tüpraş integrates sustainability into all of its processes, from its supply chain to its after-sales operations. Photo courtesy of Tüpraş.

DEPARTMENTS

4 Industry Perspectives
8 Business Trends
14 Global Project Data
15 Construction
76 Innovations
81 Advertiser Index
82 Events

COLUMNS

7 **Editorial Comment**
Will 2021 be a rebound year?

17 **Reliability**
Viewing every maintenance intervention as an upgrade opportunity

19 **Safety**
Do companies have the right tools to make proactive safety decisions?

21 **Risk**
Escaping the "cyclone market" in downstream energy

23 **Valves, Pumps and Turbomachinery**
Use the correct lube oil grade to avoid equipment failures

25 **Corrosion**
Address damage caused by galvanic corrosion

WEB EXCLUSIVE

People

99TH ANNIVERSARY | 1922–2021 |

HP Industry Perspectives

H2TECH

H2Tech: The launch of our newest technical publication

With the increasing prominence of hydrogen technologies circulating into the global market, Gulf Energy Information—publisher of *Hydrocarbon Processing* and *Gas Processing & LNG*—has launched our latest publication: *H2Tech.*

H2Tech will focus primarily on the latest technologies advancing the global hydrogen market. The magazine—to be published quarterly—will be a working technical journal for engineers and other professionals involved in hydrogen production and applications progress. *H2Tech* will focus on hydrogen technology across all spectrums—from green (via renewable energy) to blue (via natural gas with carbon capture) to brown (via coal gasification) and beyond.

The publication's scope also encompasses distribution, storage and end-use applications, including pipeline transport, fuel cells and electric vehicles, gas-to-power, industrial feedstock, synthetic fuels, chemicals and more. Cutting-edge advances in infrastructure and equipment—e.g., pipeline networks, turbines, instrumentation, electrolyzers, refueling stations, compression and turbomachinery, sensors, etc.—will be well represented.

Our worldwide readership includes operating and technology companies, power producers, equipment manufacturers, renewable and conventional energy producers, transportation developers, energy efficiency experts and regulatory and environmental officials. The *H2Tech* website and weekly e-newsletter will provide our audience with up-to-date technical information and news on hydrogen projects, process technologies and regulatory incentives within this fast-growing industry.

As the hydrogen economy and infrastructure expands for fuel, chemical and industrial applications, the industry needs a comprehensive, technical publication for the engineering and scientific communities. *H2Tech* will keep these professionals engaged, informed and up to date with technological advances and major trends affecting the hydrogen market worldwide.

H2Tech will be complimented by a global, virtual technical conference—H2Tech Solutions. The free technical event—to be held May 18–19, 2021—will bring together engineers, technologists and managers working to advance fuel, chemical and industrial applications for hydrogen. More information on topics and abstract submissions can be found at H2-TechSolutions.com.

It is now up to you! If you are interested in writing a technical article, column, trends/analysis piece or executive viewpoint for *H2Tech*, contact Editors@H2-Tech.com. HP

HYDROCARBON PROCESSING®
www.HydrocarbonProcessing.com

P. O. Box 2608
Houston, Texas 77252-2608, USA
Phone: +1 (713) 529-4301
Fax: +1 (713) 520-4433
Editors@HydrocarbonProcessing.com

PUBLISHER Catherine Watkins

EDITOR-IN-CHIEF/ ASSOCIATE PUBLISHER Lee Nichols

EDITORIAL

Executive Editor	Adrienne Blume
Managing Editor	Mike Rhodes
Digital Editor	Stephanie Bartels
Technical Editor	Sumedha Sharma
Reliability/Equipment Editor	Heinz P. Bloch
Contributing Editor	Alissa Leeton
Contributing Editor	ARC Advisory Group
Contributing Editor	Anthony Sofronas

MAGAZINE PRODUCTION / +1 (713) 525-4633

Vice President, Production	Sheryl Stone
Manager, Advertising Production	Cheryl Willis
Manager, Editorial Production	Angela Bathe Dietrich
Assistant Manager, Editorial Production	Melissa DeLucca
Graphic Designer	Krista Norman
Artist/Illustrator	David Weeks

ADVERTISING SALES
See Sales Offices, page 81.

CIRCULATION / +1 (713) 520-4498 / Circulation@GulfEnergyInfo.com
Director, Circulation Suzanne McGehee

SUBSCRIPTIONS
Subscription price (includes both print and digital versions): One year $399, two years $679, three years $897. Airmail rate outside North America $175 additional a year. Single copies $35, prepaid.

Hydrocarbon Processing's Full Data Access subscription plan is priced at $1,995. This plan provides full access to all information and data *Hydrocarbon Processing* has to offer. It includes a print or digital version of the magazine, as well as full access to all posted articles (current and archived), process handbooks, the *HPI Market Data* book, Construction Boxscore Database project updates and more.

Because *Hydrocarbon Processing* is edited specifically to be of greatest value to people working in this specialized business, subscriptions are restricted to those engaged in the hydrocarbon processing industry, or service and supply company personnel connected thereto.

Hydrocarbon Processing is indexed by Applied Science & Technology Index, by Chemical Abstracts and by Engineering Index Inc. Microfilm copies available through University Microfilms, International, Ann Arbor, Mich. The full text of *Hydrocarbon Processing* is also available in electronic versions of the Business Periodicals Index.

DISTRIBUTION OF ARTICLES
Published articles are available for distribution in a PDF format or as professionally printed handouts. Contact Foster Printing at Mossberg & Co. for a price quote and details about how you can customize with company logo and contact information.

For more information, contact Jill Kaletha with Foster Printing at Mossberg & Co. at +1 (800) 428-3340 x 149 or jkaletha@mossbergco.com.

Hydrocarbon Processing (ISSN 0018-8190) is published monthly by Gulf Energy Information, 2 Greenway Plaza, Suite 1020, Houston, Texas 77046. Periodicals postage paid at Houston, Texas, and at additional mailing office. POSTMASTER: Send address changes to Hydrocarbon Processing, P.O. Box 2608, Houston, Texas 77252.

Gulf Energy Information

BPA WORLDWIDE

President/CEO	John Royall
CFO	Alan Millis
Vice President, Upstream and Midstream	Andy McDowell
Vice President, Finance and Operations	Pamela Harvey
Vice President, Production	Sheryl Stone
Vice President, Downstream	Catherine Watkins

Publication Agreement Number 40034765 Printed in USA

Other Gulf Energy Information titles include: *Gas Processing™, Petroleum Economist®, World Oil®, Pipeline & Gas Journal* and *Underground Construction.*

LEE NICHOLS, EDITOR-IN-CHIEF/ASSOCIATE PUBLISHER
Lee.Nichols@HydrocarbonProcessing.com

Will 2021 be a rebound year?

Needless to say, 2020 was an unprecedented year. The global pandemic had, and continues to have, detrimental effects on the global HPI. Global lockdowns and travel restrictions had severe, negative impacts on refined fuels and petrochemical product demand. This led to the following consequences: a significant decline in global GDP, decreased refinery utilization rates, shuttered refining and petrochemical production capacity, delayed final investment decisions (FIDs) on capital projects, deferred maintenance activity, work stoppages on capital projects, rethinking major capital investments and a spike in personnel layoffs.

Fuel demand. In the U.S. EIA's "Short-Term Energy Outlook" (December), crude oil demand was forecast to average approximately 92.4 MMbpd in 2020. This represents a decline in oil consumption of 8.8 MMbpd vs. 2019 levels.

However, with the easing of lockdowns and travel restrictions, refined products demand has increased from the significant decline witnessed in 2020. The EIA forecasts that global oil demand will increase by nearly 6 MMbpd in 2021 (**FIG. 1**). Although oil consumption will not reach the levels seen in 2019, an increase in consumption rates is a welcome outlook.

Petrochemical. The petrochemical sector has also been significantly affected by the COVID-19 pandemic.

Travel restrictions and lockdowns have led to a significant drop in global GDP. According to the "World Economic Outlook" from the International Monetary Fund (IMF) in October 2020, global GPD was projected to have decreased by 4.4% in 2020.

The IMF predicts that global GPD will expand by 5.2% in 2021. Increases in GDP tend to lead to increases in petrochemical demand. For example, polyethylene (PE) is linked directly to GDP. A slowdown in global economies equates to a slowdown in petrochemical consumption, especially for PE; however, the easing of restrictions and lockdowns—along with the distribution of a COVID-19 vaccine—should lead to an increase in petrochemical consumption.

Looking ahead to 2021. As we begin a new year, we hope the worst is behind us and that the industry can focus on supplying refined fuels and petrochemical products to an ever-changing market. Despite the challenges the HPI has faced over the past year, its resilience is a testament to the hard-working nature of its people and the necessity of its products to the global market. HP

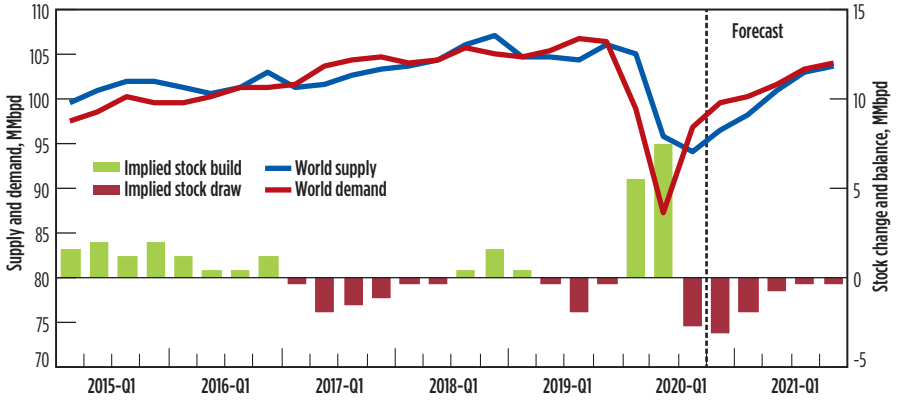

FIG. 1. World oil production and consumption forecast. Source: U.S. EIA.

INSIDE THIS ISSUE

26 Sustainability. Many companies are optimizing operations for greater safety, reliability, efficiency and environmental and social awareness. This month's Special Focus section details major trends in sustainability initiatives globally, as well as technologies to help increase sustainable operations.

41 Optimization. The desalter must operate with maximum efficiency. This article provides a case study on how implementing total opening non-linear control is enabling desalters at Nayara Energy Ltd.'s Vadinar refinery to operate at maximum efficiency.

53 Heat Transfer. This article examines how a high-emissivity coating can stop oxidation and scale growth of radiant tubes and increase conductive heat transfer to process fluids.

65 Process Controls, Instrumentation and Automation. A pervasive sensing approach is being embraced as companies deploy wider IIoT solutions within their digital transformation efforts. This article provides seven practical examples on how it is optimizing operations and safety in refineries and petrochemical plants.

69 Maintenance and Reliability. Many refineries face periods of severe corrosion and fouling in their crude unit distillation overhead systems. Applying a collection of new tools enables additional visibility, faster response and more informed decisions regarding which corrective actions to take for greatest effect. As illustrated in this work, several refiners are applying one or more of these techniques for positive impact on their bottom line, whilst achieving safer, more reliable operations.

M. VAN WAGENBERG, IBASC, Easton, Maryland

Case EPC-2020: Increasing competitiveness and profits

Before the challenges of the COVID-19 pandemic, there were already issues within the energy market (especially in the oil and gas industry) that exposed challenges in the engineering, procurement and construction (EPC) sector. Low-cost competition by EPC firms from Asia was already putting margins under stress. Apart from the alarmingly low quarterly results from many publicly traded EPC firms, several articles pointed at fundamental problems—one of them being productivity.

The gap in global energy consumption and low oil prices has decimated investments. An anticipated stream of projects in LNG liquefaction and other areas has dried up. It has been argued that Western EPC firms need to create more value added in hydrocarbons to sustain their position. Regardless, owners assign projects based on costs, and success will be a result of value and productivity.

In this hypothetical case (EPC-2020), the market will be explored and, from that basis, guidelines can be drawn on how to make an EPC firm more competitive and increase its profit to a healthier 5%–6% of sales.

Development in market segments/demands on a project level, 2020–2024. The basis for Case EPC-2020 to cope with the current situation is to assess the market up to 2024. Demand analysis leads to the overview of markets that is shown in **TABLE 1.**

In the oil, gas, chemicals and power (OGCP) markets, bids can only be satisfactory if they demonstrate substantially lower costs, with one exception: power needs to innovate to combine hydrocarbon and non-hydrocarbon technologies, and government will support that in regions. If an EPC firm can deliver on innovation, then projects in sustainable energy will have a better profit margin. While investments in chemicals are solid, a contraction in other segments can lead to the need for low-cost bids.

In the downstream OGCP segment, productivity gains and, in some cases, innovation are needed. Another other segment—life science, chemical specialties and manufacturing (LSCSM)—focuses its engineering capacity to balance its capabilities; this segment may experience a very limited contraction. The investments in pharmaceuticals seem stable, especially in Europe. National policies are relevant. A trend in new products and e-commerce leads to facilities for manufacturing, e-commerce and data warehousing. However, competition will be fierce, since EPC firms with unused resources from OGCP will switch to this segment. The probability for a bid to improve will be flexible—some owners will ask EPC firms to execute the project with flexibility in time/scope, while remaining efficient. Lead time, as a project demand, is hardly mentioned. As such, it is not listed as a key point for improvement. Circumstances may make lead time a competitive edge in the future.

Lower cost demand on EPC firms. The main demand in both segments is to lower costs, which requires two generic steps:

1. Create purposeful offices, each with a single market focus and goal: to create competition
2. Untangle complex matrix organizations, limit corporate structure and size offices for full staffing.

Then, there are steps within each of the two primary market segments. These include:

- Productivity gains in engineering to improve 15% in 24 mos by adjusting division of labor and IT
- Ensure cooperation in market segments that require solutions that fit national interests
- Map engineering processes to a project demand, and tune for costs, innovation or flexibility
- Implement early warning and early correction alerts on a project level
- Lock in products that result from IT improvements, and then sell and monetize.

TABLE 1. Market overview

	OGCP				LSCSM			
	Costs	Lead-time	Quality	Innovation	Costs	Lead-time	Quality	Innovation
U.S.	X			(X)	X			
Europe	X			X	X		X	
Asia/Middle East/Africa	X				N.A.			

* Markets are typified with the objective of illustrating how EPC firms are to cope with segments
** Cost of engineering
*** Some EPC firms focus on sub-markets offshore, exploration
**** Assumes that the UK remains a de-facto partner in the EU

Slim corporate structure implementation. If markets have common demands and are stable, a central core organization enhances savings. The corporate savings are usually found in centralizing staff (e.g., human resources, finance, quality and sales). If markets become less predictable, the best course will be defined by those who are in close touch with those demands. Technology-driven corporations have implemented a slim corporate structure, pushing decisions toward units that make products for specific markets. In addition, owners regroup to improve decision making in market segments to create a better focus on a single segment. Similarly sized corporations (5,000–20,000 employees) exist that rely on local decision making, while centralizing strategic functions. Therefore, detailed steps define operations that fit regional market demand. With decentralized resources, and with a regional focus, the size must be enough to include human resources, sales, standards/quality and finance—an office with 1,000 employees can provide this.

Another aspect is that offices that are comparable in size may still run a development portfolio and compete on performance and capabilities. Simultaneously, capital and strategy remain corporate tasks, co-developed for each segment/region with the office leadership. The corporate function would then be limited to 1.25% of sales. Each organization has a simplified task (one region, one set of projects). Savings is a result of coordination among offices being removed—this adds 1% profit (i.e., 1% of sales).

More efficient engineering and lower failure risks. The first step for increasing productivity is to check the division of labor. This has been at the core of efforts to increase productivity. Reducing cost by incorporating new sets of tasks and tools is a productivity gain.

The combinations of tasks are based on the lowest cost to execute (i.e., design), iterate (i.e., redo, an essential part of design) and review. This distinction is a reminder that, apart from "execute" as a cost item, "iteration" and "review" are costs, as well. Salary cost is a less flexible component, except for replacing person X with education A by a less salaried person Y with training B. The other cost component is IT tooling. New task structures should save 25%–50% in certain areas, adding up to 15%–20% in savings. This will add 1%–2% to the profit margin.

Another step is to map the engineering process for each project onto the specific demand on that project, such as cost of engineering, lead time, innovation and quality. Often, choices to fine-tune toward the project demands are informally addressed (such as selecting a project manager and senior engineers with proven records to keep costs low or to drive quality). Leadership should implement a structured way to create behavior tuned to that demand. This can add 1% to profits.

The next step is an early warning and early correction approach to avoid cost increases later into the project. Several reports show that 30% of new projects end in failure. The costs of these failures on average represent 2% of sales for EPC firms. These firms have implemented preemptive risk strategies to reduce these losses. The author suggests using an early warning and early correction approach that centers on weekly assessments of non-financial factors, such as iterations that depict the quality of the functioning of the engineering process. Each factor ensures performance that the project demands. This approach achieves a 50% reduction of failures, which adds up to 1% profit.

The final step is to monetize new products that can be delivered by the EPC firm. With limited effort, the delivery of products [e.g., the computer numerical control (CNC) code for fabrication of structural parts] can be added. In LNG, this can save 1%–2% on capital expenditure costs, which can add 0.5% of profit.

These steps are not the only ones that EPC firms can choose to increase profit. Several others exist. Performance improvement practices—such as a lean set of practices to reduce organizational waste—are widely used.

Examples for Case EPC-2020. As previously discussed, the steps are:

- Improve division of labor
- Mapping process onto demand project
- Early warning and correction.

Although the missions of these steps are identical (i.e., add profit), the specifics for each vary, since each has a focus on a set of projects—either downstream OGCP or only LSCSM in one region. Possibilities to change the division of labor plus mappings onto each project demand are only geared toward that specific market segment. Each decentralized office will, in the coming years, take steps to lower engineering costs. In addition, a project demand may be innovation or flexibility.

Improve division of labor. In many sectors of industry outside of the hydrocarbon industry, IT has enabled the ability to revisit the division of labor. In the electronics industries, a very tight integration between 3D modeling and production was implemented decades ago. This allowed for folding several functional engineers into one new design function, thus enhancing productivity. That reduces efforts to coordinate between disciplines.

In EPC plant design, the division of labor is still high. The reason is that resources can be easily swapped from project to project. IT tools ease the integration of disciplinary functions. This allows a search for areas where the productivity increases substantially by using one 3D model. It also provides rules to simplify decision making so that tasks can be further automated, and to recreate one new function out of three. For example, in LNG liquefaction, there are several functional sections in the plant in which piping and structural works can be based on design parameters across functional borders, where rules can automate several design decisions (as in electronic design). In those areas, a new task structure can be created that covers an integrated area of piping, structural, and civil works and controls.

Another area is smaller projects where the services are limited and the decisions are clear, such as the replacement of pump units with some piping and limited structural and civil works. Here, a new integrated task structure can be created, combining tasks so that one person can execute them. Savings in scheduling, decision making and coordination more than compensate for IT costs, as the productivity output in that area will increase twofold.

Mapping process onto demand. What is informally accepted, but not addressed in a more structural way, is that the demand on a project influences the way the engineering process should be specifically handled, and the way that tasks should be timed. It is understood that lead-time demands will require a few more senior engineers (i.e., more resources). This is especially important during the first months of the project to create

a solid design basis as soon as possible, so the next project can enable work in parallel during detailed engineering.

It is well understood that, if the client wants a better solution for a function in the plant (e.g., less energy consumption), one must allow for more resources for innovation, and those engineers can iterate more over an extended period to explore alternatives.

Two variables can be adjusted in volume and time. If one is to create improvements that cross different disciplines, such as controls and mechanical works, then alignment between these two disciplines must be set, as well. This can be accomplished by assigning the engineers in the same time frame. This is a third variable.

Approximately seven more variables can be systematically mapped onto the demand. By addressing these variables at each project, one will create a smoother functioning of the process and reduce the probability of project failures by more than 50%. Project failures cut 2% of sales. This mapping will reduce that by more than 50%.

Early warning and early correction. Another potential area to improve project performance is to have an early warning system in place, such that corrections can be instantly made. Several EPC firms have introduced a strict risk-assessment system before bids can take place, which reduces the risk of losses on projects. Others more closely monitor project costs. Unfortunately, during the first weeks and months of a project, costs are not the best tell-tales for later problems.

For that matter, there are other engineering process indicators that will give solid early warnings, while pointing at steps to handle those situations. For example, within the "mapping process onto demand," the early assignment of senior personnel is essential to hammer out all basics before detailed engineering commences. If those senior staff members do not fully participate in the project, this constitutes an early warning. The correction is to prescribe early reviews for topics related to the progress of senior personnel.

Another example is an innovative project. One measure is to gauge if a healthy iteration takes place in the disciplines that are working on aspects that need innovation. Usually, the disciplines process, mechanical and controls are key players—thus, one measures the iteration in those areas. If the expected level is not at par, then the correction is to prescribe reviews. One can also order alternative designs, and possibly assign junior engineers to enable more iteration to catch up.

The third example for "mapping process onto demand" is the demand for quality. It was mentioned that this could require more alignment between controls and mechanical. If monitoring indicates a lack of alignment, then the correction would be to add more supervision and to reschedule so the engineers would work in the same time frame. The quality results can then be supervised.

The more personnel that monitor early assessments and warning signs, the less possibility of failures occurring and additional hours being spent to complete the task. The estimated savings on overall sales are expected to be between 0.7% and 1.3% of sales.

Monetize new products. The EPC firm prepares data that have a value outside the EPC firm's delivery of documents. The 3D model's main products to be delivered to fabricators are the piping isometrics and drawings for steel. If fabrication is computer numerical control (CNC), the fabricator assigns the job to CNC machines and prepares the NC program—at a cost of up to 15%. With adjustments, the 3D model can produce CNC code for a machine, instead of issuing isometrics, which can save up to 2% on LNG projects. On a $1-B project, that represents $10 MM–$20 MM. To monetize this, one must agree upon the delivery of NC code.

Other areas in OGCP projects exist where contractors benefit from receiving outputs that are easily retrieved from the 3D model. Onsite tank fabrication and sequencing, positioning of parts for assembly, and many civil tasks can use laser-guided positioning, which can be derived from the 3D model. Tasks such as checking quality and progress can benefit, as well. In LSCSM projects, the structural parts to be CNC machined for a building are probably fewer in number. However, there are clusters that benefit from it. Within life sciences projects, the 3D interior model can provide input to CNC production of lab furniture, paneling and ducting. The CNC production reduces the lead time, which supports flexibility. These services are to be monetized and translated into 0.5% profit.

Path to increased profit. The market characteristics that define the focus for the EPC firm and the demands for each of the projects have been reviewed. For EPC firms, it is mostly the cost of engineering, although other areas can be innovation (power) or flexibility (life sciences). These market aspects drive adjustments for the hypothetical EPC-2020 case.

A suggestion is a reduced corporate level where the core tasks are capital and strategy. Coming from an integrated corporate model, this dissolves an elaborate management structure that does not fit current market conditions. It reduces corporate costs to 1.25% of sales. Equal offices of 1,000 employees provide a size for adequate staffing and a focus on a product/market segment.

Three steps to improve project performance and reduce failures are improving the division of labor, mapping process onto the demand of each project, and incorporating early warning and early correction systems. Improving the division of labor leads to several savings: 1%–2% of overall sales. Improving the mapping of several variables onto the project scope guarantees the functional performance and keeps projects in line without using contingencies. It can add 1% or more to profit. OGCP and LSCSM projects have a failure rate that now reduces the company profit by 2%. A root cause for failure is an optimistic lump-sum bid, another by acknowledgment of issues when it is too late to correct. Finally, new products (resulting from 3D and other applications) increase income and profit by 0.5%.

The reduction of corporate costs (1%), adjustments in division of labor (1%–2%), the mapping onto the project demand (1%), reduction of failures (1%) and sales of new high-margin products (0.5%) result in pushing up profits on sales from 2% to an aspired 6%. HP

MAURITS VAN WAGENBERG has extensive experience in tracking the health of engineering organizations and of the engineering execution of complex plants. He has worked more than 30 yr in the field of improving engineering performance and on project risk analysis. He has performed comparative analysis among organizations and developed ways to fine-tune engineering execution toward specific project needs. He has a PhD in industrial organization and is president of IBASC, an engineering management and research firm.

LEE NICHOLS, EDITOR-IN-CHIEF/
ASSOCIATE PUBLISHER
Lee.Nichols@HydrocarbonProcessing.com

Global Project Data

Hydrocarbon Processing's Construction Boxscore Database is tracking nearly 1,400 projects around the world. The Asia-Pacific region accounts for 37% of active projects market share, followed by the U.S. (17%) and the Middle East (14%). The Asia-Pacific region was also the leader in new project announcements in 2020, accounting for more than 40% of market share. However, new project announcements were down in 2020 vs. 2019. In total, new project announcements declined from 358 in 2019 to 238 in 2020, representing a decrease of approximately 34% year-over-year.

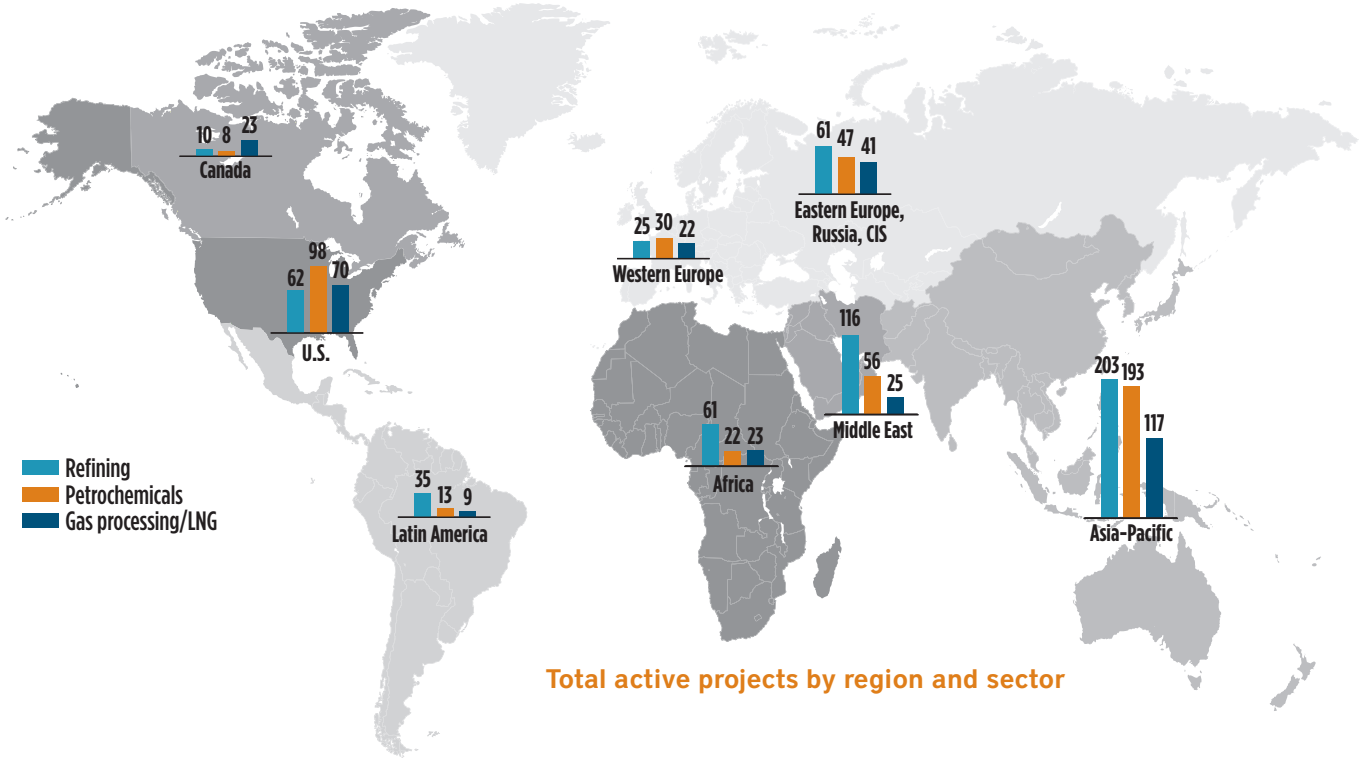

Total active projects by region and sector

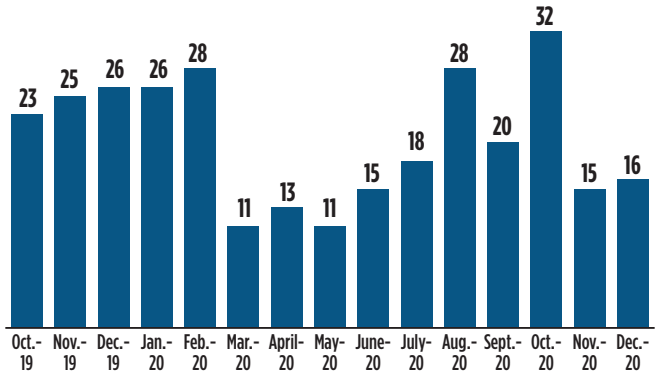

New project announcements, October 2019–December 2020

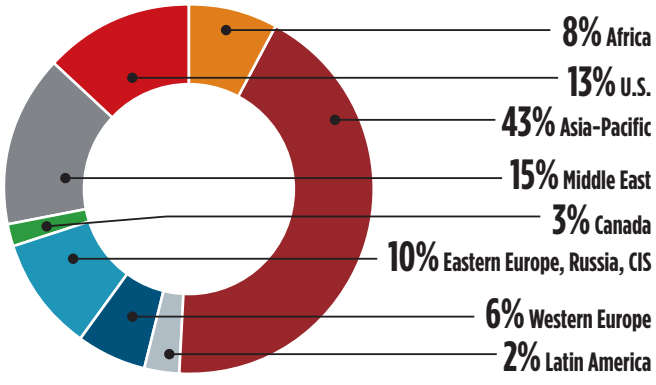

New project market share, by region, 2020

HYDROCARBON PROCESSING CONSTRUCTION BOXSCORE DATABASE

Detailed and up-to-date information for active construction projects in the refining, gas processing and petrochemical industries across the globe | ConstructionBoxscore.com

LEE NICHOLS, EDITOR-IN-CHIEF/ASSOCIATE PUBLISHER
Lee.Nichols@HydrocarbonProcessing.com

HP Construction

AFRICA

TechnipFMC has begun construction on **Assiut National Oil Processing Co.'s** new hydrocracking complex in Egypt. The facility will consists of several new processing units. The capital-intensive investment will enable the Assiut refinery to increase the production of ultra-low-sulfur fuels, such as Euro 5 diesel.

ASIA-PACIFIC

Lummus Technology was awarded a technology licensing contract from **Kingfa Science and Technology Co. Ltd.** for two new propane dehydrogenation (PDH) units. Both units—each with a processing capacity of 600,000 tpy—will be built in the Qingzhi Industrial Park, Ningbo City, Zhejiang Province, China.

Kaijin Blue Sky Energy Co. Ltd. has selected **LyondellBasell's** processing technology for a new 600,000-tpy polypropylene (PP) plant. The facility will be built in Wenzhou, Zhejiang Province, China. The PP plant will use LyondellBasell's Spheripol and Spherizone technologies.

W. R. Grace will supply its UNIPOL PP process technology to **PT Pertamina Rosneft Pengolahan dan Petrokimia's** PP plant in Tuban, Indonesia. The plant will consist of two PP production lines, each with a production capacity of 580,000 tpy.

Shandong Yulong Petrochemical Co. let a Master Licensor service contract to **Lummus Technology** for multiple units at the company's mega-integrated complex. The facility, located in Shandong Province, China, consists of two mixed-feed crackers, an ethylbenzene/styrene monomer plant and two PP lines.

Ceylon Petroleum Corp. (CPC) has been given approval by the Sri Lankan government to pursue plans to expand the 40,000-bpd Sapugaskanda refinery. CPC has begun a new feasibility study to increase the refinery's capacity by 100,000 bpd.

Honeywell UOP was awarded a contract by **Oriental Energy Co. Ltd.** to supply its C3 Oleflex technology for on-purpose propylene production. The PDH plant is being built at Oriental Energy's facility in Maoming, Guangdong Province, China. The unit is scheduled to begin producing on-purpose propylene in 2022.

EUROPE

Skovgard Invest, supported by **Vestas** and **Haldor Topsoe,** is planning to build the world's first commercial-scale green ammonia plant. The facility will be in Western Jutland, Denmark, and produce more than 5,000 tpy of green ammonia from renewable power. The production is forecast to prevent 8,200 tpy of CO_2 from being emitted into the atmosphere. Production is scheduled to begin in 2022.

Clariant is building a new cellulosic-ethanol production plant in Podari, Romania. The plant, based on the company's sunliquid technology, will process approximately 250,000 tpy of straw to produce 50,000 tpy of sunliquid cellulosic ethanol. The plant's carbon-neutral biofuel can be blended into conventional fuel. Construction is scheduled to be completed by the end of 2021.

Naftna Industrija Srbije commissioned Stage 2 of the Pancevo refinery's modernization program. Stage 2 consisted of the construction of a deep conversion complex to boost production of Euro-5 gasoline and diesel. The more than $360-MM project included several new processing units, including a new delayed coking unit utilizing proprietary technology from **Chevron Lummus Global.**

Repsol selected **Axens'** Vegan technology for a new biofuels plant to be built in Spain. The 250,000-tpy plant will be built at Repsol's Cartagena refinery. Once completed, the biofuels plant will produce biodiesel, biojet fuel, bionaphtha and biopropane.

LATIN AMERICA

In mid-November 2020, **TechnipFMC** was given a Notice to Proceed with construction work on **IEnova's** Costa Azul LNG project in Baja California, Mexico. At a cost of approximately $2 B, Phase 1 includes the construction of a 3.25-MMtpy liquefaction plant. TechnipFMC expects to complete Phase 1 activities in late 2024. Phase 2, if implemented, would include expanding the facility by 12 MMtpy, including the construction of two additional liquefaction lines and storage.

MIDDLE EAST

In late November, Iraq's oil minister announced plans to invite international companies to bid on the completion of the Fao refinery. The 300,000-bpd refinery will include an integrated petrochemical plant.

U.S.

Mitsubishi Chemical Corp. is considering building a $1-B, 350,000-tpy methyl methacrylate plant in Geismar, Louisiana. The plant would be located on a 67-acre greenfield site the company acquired from Lion Elastomers. Mitsubishi Chemical Corp. plans to take FID by mid-2022.

Bayport Polymers, a JV between **Borealis** and **Total,** plans to start up its 1-MMtpy ethane cracker in Port Arthur, Texas, by the end of 1Q 2021. The company has pushed back the startup of its 625,000-tpy HDPE plant, being built in Bayport, Texas, to 1Q 2022.

Grön Fuels announced plans to potentially develop a $9.2-B renewable fuel complex in Louisiana. The project—to be completed over several phases—will be located on the west bank of the Mississippi River near Port Allen. Phase 1 includes the construction of processing units to produce 60,000 bpd of low-carbon renewable diesel. Phase 1, scheduled to be completed by 2024, investments are expected to eclipse $1.25 B. HP

HEINZ P. BLOCH, RELIABILITY/EQUIPMENT EDITOR
Heinz.Bloch@HydrocarbonProcessing.com

Viewing every maintenance intervention as an upgrade opportunity

When a long-time maintenance supervisor was promoted to the head of his refinery's reliability department, he wanted to make "Precision Maintenance is Our Passion" his banner and headline. I have always reserved passion for other things because passion for the job often leads to neglect of one's family. My recommendation was "Every Job as an Opportunity to Upgrade," or a similar wording.

He then asked for a few examples of upgrading, but took the position that his facility had several large oil mist lubrication units and that little more could probably be done. Fortunately, he agreed that reliability professionals rarely see perfection and can often provide details that support my suggested heading. He encouraged me to explain further, asking only that everything be plausible to his workforce, readily implementable, and pay back the required monetary outlay within no more than 6 mos.

Following are some of the practical examples I gave him:

1. Pre-purchase a small, portable oil mist unit and place it in the storeroom. Be prepared to install it near pumps or blowers experiencing frequent bearing distress.
2. Any pump that fails more than twice in a rolling 18-mos period should have its oil ring(s) and constant level lubricator assembly removed and discarded. Thereafter, pump bearing housings should be connected to one of several already-existing oil mist headers at this refinery.
3. The breather vents on oil mist-lubricated bearing housings should be plugged.
4. Only the best available bearing housing protector seals should be installed, and oil mist should be directed into the space between an advanced-style bearing housing protector seal and the adjacent bearing. As shown in FIG. 1, the oil mist will then flow through the bearing and exit at the bottom drain.[1,2] From there, the condensed oil flows back into the small oil mist unit or into a collecting pot to be reclaimed.
5. Electric motors should have their bearings connected to the existing plant-wide oil mist systems at this facility (per FIG. 1).

In the years since 1990, *Hydrocarbon Processing* has published a few dozen similar ways of turning every maintenance intervention into a cost-effective upgrade. This publication has described similar upgrades relating to mechanical seals, seal flush strategies, small steam turbine packing glands, and many more. The various upgrades can be found in the referenced books.

For his part, and because he now finds himself in the enviable position of heading an entire department, our reliability department head could restore the long-lost art of reading technical books. He might consider mandating that the best-in-class practices described in these books are being compared to, or contrasted against, the "as presently done here" practices at his refinery.

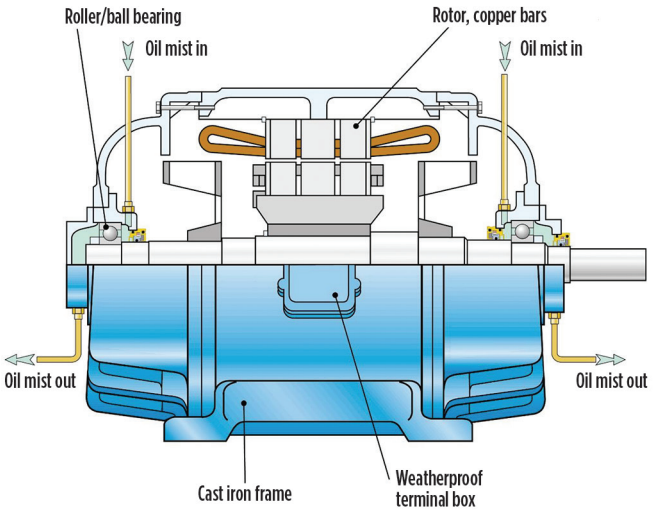

FIG. 1. Oil mist path through electric motor bearings equipped with three modern, single-face magnetic seals. Source: AESSEAL Inc.

Productive meetings could be held to demonstrate that the addition of oil mist to electric motors in an installation where oil mist is presently supplying lubricant only to pump bearings will have a 3-mos payback. Upgrading below-average seal flush systems has also resulted in paybacks of less than 6 mos, as did the routine retrofitting and upgrading to cartridge-style steam turbine packing glands. These and many other opportunities present themselves today, decades after we began making them public. HP

LITERATURE CITED

[1] Bloch, H. P., D. Ehlert and F. Geitner, *Optimized Equipment Lubrication, Oil Mist Technology, and Storage Preservation,* Reliabilityweb.com, Fort Myers, Florida, January 2020.
[2] Bloch, H. P., *Petrochemical Machinery Insights,* Elsevier Publishing, Cambridge, Massachusetts, 2017.

HEINZ P. BLOCH resides in Montgomery, Texas. His professional career commenced in 1962 and included long-term assignments as Exxon Chemical's Regional Machinery Specialist for the U.S. He has authored or coauthored more than 770 publications, among them 23 comprehensive books on practical machinery management, failure analysis, failure avoidance, compressors, steam turbines, pumps, oil mist lubrication and optimized lubrication for industry. Mr. Bloch holds BS and MS degrees (cum laude) in mechanical engineering from the Newark College of Engineering (NCE) and is one of 10 inaugural inductees into NCE's Hall of Fame, which honors its most distinguished alumni.

C. BREWER
Sphera, Denver, Colorado

Do companies have the right tools to make proactive safety decisions?

A process safety management/operational risk management survey conducted by Sphera in 2020 polled respondents on the following items:

- Safety culture
- The reality of risk across hazardous industries
- The methods organizations use for identifying, understanding and communicating risk
- Priorities and company plans for digital transformation.

The industry breakdown included oil and gas (36%), chemicals and petrochemicals (19%) and manufacturing (17%), as well as other industries like oilfield services, utilities, metals and mining. Participation was offered globally, and feedback was received across all regions.

Some of the key statistics include 88% of participants indicating that safety is part of corporate value structures, supported by upper management; 78% of respondents continuously monitoring safety performance; and 60% of participants striving to reduce operational and major accident hazard risk exposure. The survey suggested additional drivers for improving safety performance, including continuous process improvement, operational excellence, regulatory compliance, and satisfying corporate and board priorities, among others.

Risk awareness can pay for itself. Despite good intentions, 49% of survey respondents said most organizations are unaware of their major accident hazard risk vulnerability, and only 37% are confidently and proactively managing process safety risk exposure. For the last 5 yr, the percentage of companies that proactively manage safety have been surveyed; year on year, the result is somewhere in the 36%–40% range.

This statistic gives reason for pause. Earlier this year, Marsh published its 100 largest hydrocarbon loss report. It is striking that over the past 2 yr, the industry faced its largest losses on record—$4.5 B, which is 10% of the combined 50-yr total. Aging infrastructure and high utilization in the downstream sector were largely to blame (FIG. 1). Over those 2 yr, the oil and gas industry was recovering from its previous oil price downturn, which may very well repeat itself again 2 yr from now. It begets the question: Do companies actually have the right tools to proactively manage infrequent, high-consequence events?

FIG. 1. Aging infrastructure and high utilization in the downstream sector are largely to blame for the $4.5 B of hydrocarbon losses reported over the past 2 yr.

Sphera asked companies how they identify risks. Audits and inspections, hazard and operability studies (HAZOPs), "what-if" studies and process hazards analyses (PHAs) are the most common means. Around 46% of participants suggested that they have deployed technology systems to support their risk assessments. However, they also highlighted concerns about the frequency and effectiveness of those studies. Half of the companies said they review risk every 1 yr–6 yr, with only 8% reporting that they review risk daily or weekly. Approximately 53% indicated that they are assessing only a portion of their facilities, while half are concerned with the consistency and quality of their assessment and audit practices. On average, companies reported that they are able to complete only 68% of their average safety-critical maintenance and asset integrity inspections every year. Data is siloed, systems are static and information is dated and incomplete.

Also, only 51% of respondents said they thought it was practical to set 100% of their planned maintenance and inspections to active, because limited resources (72%), conflicting priorities (71%) and limited budget (49%) were getting in the way—the same three challenges seen in every survey for the last 5 yr running. Also, average scheduled maintenance and inspections achieved has hovered at the 70% level for the last 3 yr. These results reinforce the thinking that perhaps the right tools are *not* available to make proactive safety decisions.

Lacking and lagging insights are perhaps the reason the majority of industry leaders told us there are gaps between well-engineered process safety approaches and the reality on assets. They also agreed that risk changes between periodic process

safety review periods due to a loss of experienced personnel, lack of operational risk visibility, conflicts between procedures and work practices, and poor process execution and management of change. The factors with the most impact on those elements, however, are organizational culture, senior leadership and human factors.

Shoring up safety with real-time technologies. Companies know they are operating without the right insights—they need something more comprehensive. They also understand the value of technology and how it makes their companies and teams safer. In fact, 2020 witnessed an 11% growth in this trend over last year. Survey participants also told us that they are using technology to remotely monitor facility and operational performance, to improve work prioritization and planning, and to monitor asset health.

Some of the technology solutions companies are using today are helping them understand process safety lessons learned, changes in operating procedures and changes in equipment health and performance. Organizations also shared that they are making big investments to implement remote sensors and equipment-related risk identification tools. In fact, equipment sensors (59%) and condition monitoring (50%) are the most commonly implemented systems, with 23% deploying new equipment performance solutions at the regional level to monitor when an answer requires service.

Companies understand that they are presently operating with piecemeal data. With that understanding, it is interesting to note that 39% of companies are working their digital strategies to integrate environment, health, safety and sustainability (EHS&S) and operational risk management (ORM) solutions at the enterprise level. Integration goals are in service of creating new, data-driven business processes across functions, understanding where to make safety improvements and map dynamic risk pathways. Such dynamic risk pathways are new. Sphera's subject matter experts have shared more about this trend.

Industry is now looking for real-time condition monitoring solutions to bring operating and asset conditions together. The creation and ongoing validation of PHAs, HAZOPs and other risk studies are time-consuming and expensive, and it can be difficult to capture ongoing and evolving information. Operators know that when well-designed and well-specified processes and equipment enter service, things begin to change. Over time, assets age; but there are also daily interventions on the plant. Things change—whether because of new management-of-change (MOC) procedures being put into place or because of existing MOCs being extended.

Impairments, startups, shutdowns and permitted maintenance activities introduce hazards and risk to the assets. This is an interesting statistic because process safety leaders see technology as the digital leap needed to overcome their siloed, lagging situations. They are now moving in a direction to simulate and visualize, in real time, the health status of risk pathways that pertain to specific scenarios captured through bowtie risk visualization diagrams and PHAs. This idea would essentially bring live data from historian distributed control systems (DCSs), maintenance systems, inspection/MOC and control of work databases to understand the operational, maintenance and verification conditions and status of safety-critical equipment in real time.

One area where technology is rapidly taking off is fog/edge computing, which enables the gathering of more data that sits closer to the asset. Industry leaders expect sixfold growth in this area. Another area is digital twin technology, which promises to support safer operations, plantwide productivity and performance, and safer, more efficient shutdowns and turnarounds. Digital twin technology is anticipated to post threefold growth.

Looking at the results of this year's survey, one of the industry trends … is that complex systems migrate toward states of high risk, but operators often do not realize it until something bad happens.

How to know what you don't know. Looking at the results of this year's survey, one of the industry trends that is visible between the data presented here and the data coming from others like Marsh, is that complex systems migrate toward states of high risk, but operators often do not realize it until something bad happens. For some companies, it is not that process safety is simply "out of sight, out of mind." These companies have done their risk studies. They have noted their lagging indicators and lessons learned. What they do not have is a joined-up, real-time view of asset and operating conditions. They know the risk this poses, and they know that no single, siloed system provides good safety indicators. Here is seen the big leap from 51% reviewing risk every 1 yr–6 yr, to 52% wanting access to the nuanced state of process safety barriers in real time and wanting the ability to simulate operating conditions based on certain risk scenarios.

The stakes are simply too high to ignore the financial and reputational savings offered by advanced asset safety monitoring. The oil and gas industry, in particular, needs this level of resilience due to the critical nature of its assets. A recent article published in the *Houston Chronicle* described Total's perspective: The combination of the coronavirus pandemic and the oil crash are accelerating digital transformation to help companies boost efficiency, cut costs and make money at lower commodity prices. We hope they also find value in improving safety.

Going back a couple of years to our 2018 survey, we asked the industry what they thought the safety impact would be following the low oil price. Of the total respondents, 72% said process safety risk increases. As we saw with the Marsh data and expectations about future years, meeting those projections will require a dramatic digital transformation today. HP

COURTNEY BREWER is Sphera's Product Marketing Manager for operational risk management. She is responsible for developing and delivering the global go-to-market and product marketing strategy.

D. H. PURO
ProSight, New York, New York

Escaping the "cyclone market" in downstream energy

To say that the downstream energy sector is facing a time of unprecedented challenge would be the understatement of the decade. What began with a market shift coupled with the oil and gas crisis has morphed into a pandemic-driven economic standstill with fewer planes flying, fewer cars driving and overall energy consumption plummeting.

As if those issues were not enough of a concern for the industry, refining and petrochemicals are feeling the squeeze from insurance companies, which—facing their own challenges—are beginning to offer less capacity (coverage limits) while increasing rates on the coverage they *do* offer, and perhaps even reducing the breadth of coverage. We call this a "hardening market" in insurance terms, and this unprecedented market is one of the hardest in recent memory.

Having underwritten downstream energy risks for the better part of two decades, I could sit here and tell you *why* insurance carriers are pulling back on capacity in the refining and petrochemicals sectors or pushing rate increases (due to things like reinsurance costs and underperforming coverage lines), but I also know that the reasons why probably do not matter to insureds who need affordable coverage to keep their operations afloat. Insurance customers in this sector need solutions. These insurance market challenges have created a significant problem—one I have dubbed the "cyclone" market.

The challenges facing the refining and petrochemicals sectors are daunting enough on their own. When these challenges are combined with the oil and gas crisis, the COVID-19 pandemic, and reduced insurance limits/coverages at significantly higher prices, a self-sustaining whirlwind starts to form around companies—a seemingly inescapable cyclone that sucks them in and closes around them. Worse, this cyclone market is not going away anytime soon—not for at least another 12 mos–18 mos. Fortunately, this is not where the story ends.

A way out of the cyclone market. The good news is that refining and petrochemicals companies can emerge from this cyclone with both adequate *and* affordable insurance coverage. Navigating this path may be different than what energy companies have done historically to obtain insurance, but these unique circumstances require unique action. For insureds to successfully navigate this cyclone market will require a new level of engagement between the insurance buyer(s) and their insurance partners (their broker and carrier), as well as creativity and innovation by all parties to find the right insurance solution.

An active engagement approach will lead to the creativity and innovation needed to craft an insurance policy customized to each company's specific needs. It is critical that each company plays an active role in its insurance purchase process. Companies must come to the table alongside their brokers to meet with prospective carriers. There is power in these face-to-face (even if virtual) engagements—not only do they show brokers and carriers that companies are invested in their decisions, but they also give companies the opportunity to ensure that their needs are met.

An interactive dialogue with a broker and carrier gives a company a more prominent seat at the table during these negotiations, while further strengthening a long-term partnership. It also serves as a strategic blueprint to help craft the right insurance plan for each company. Fortunately, a number of options are available for downstream energy companies to consider, with a range of limit profiles at reasonable premiums.

Tailored approaches to insurance for the downstream. One plan option is to analyze exactly how much risk a company is comfortable taking on vs. transferring to the insurance carrier—e.g., utilizing deductibles or self-insured retentions (SIRs). Not paying for what is not needed is a great way to lower premium costs to a more affordable level.

Another "outside-the-box" option to consider is a captive. A "captive" is a company or organization that insures itself (usually by partnering with an existing insurance company) to stabilize its rates. While forming a captive is not an option for every refining or petrochemicals operation, it does decrease volatility in insurance rates compared to what is available on the open market. A captive could be an attractive long-term solution to navigating out of the cyclone market.

Finally, a simple, yet often overlooked, solution is to evaluate all of the terms and conditions in a company's insurance policy to understand exactly what and how the company is covered and the premium commensurate with those coverage grants. This process can be tedious, but taking this step with a broker and carrier can bring a much clearer understanding of how a policy works and what can be added or removed to make it a better fit for a company's specific needs and requirements.

By increasing engagement with the insurance supply chain and exploring creative ways to craft insurance coverage, refineries and petrochemicals companies can take critical steps to navigate the cyclone market. While this does not solve every challenge facing the industry, it is an important step to get energy customers back on solid footing. HP

DAWN H. PURO is Program Executive for ProSight's Energy niches: Petrosure, Downstream Energy Contractors, and Propane and Fuel Oil Delivery. She brings with her more than 20 yr of property and casualty expertise in energy, product liability, transportation, public entity, construction, healthcare, product recall and crisis management. She has been featured as a panelist, speaker and moderator at various industry conferences including PLRB and Advisen Insights. Ms. Puro graduated from Fairleigh Dickinson University with a BA degree and received further executive leadership training from Harvard University and Columbia University's Graduate School of Business.

A. J. S. Rathore, Indorama Eleme Petrochemicals & Fertilizers Ltd., Port Harcourt, Rivers, Nigeria

Use the correct lube oil grade to avoid equipment failures

Lubrication is imperative to the performance of rotating equipment. Each year, millions of bearings fail due to poor lubrication, the most common cause of bearing failure. An estimated 36% of bearings suffer lubrication failure—studies have shown that actual lubrication cost is just 1%–3% of the total maintenance budget, while 40% of maintenance cost is linked to poor lubrication.

Poor lubrication includes:

- Inappropriate lubricant
- Improper quantity
- Inadequate relubrication intervals
- Contamination.

The primary functions of lubricant are to reduce friction and wear, heat dissipation, protection against corrosion, and provide a sealing effect by creating an oil film between mating surfaces. However, depending on the operating temperature and the process, a lubricant is expected to provide other properties that are as equally important and aid in extending the life of the equipment.

Many different varieties and formulations of grease and lube oils are available in the market—every lubricant cannot perform every job, and each lubricant must be selected specifically for the equipment. Key parameters to be considered include load, speed, environmental conditions and operating temperature, which determine the viscosity, additives, non-reactivity to metals being lubricated and other properties. Choosing the right lubricant is critical for an application and should not be replicated, as every application is different.

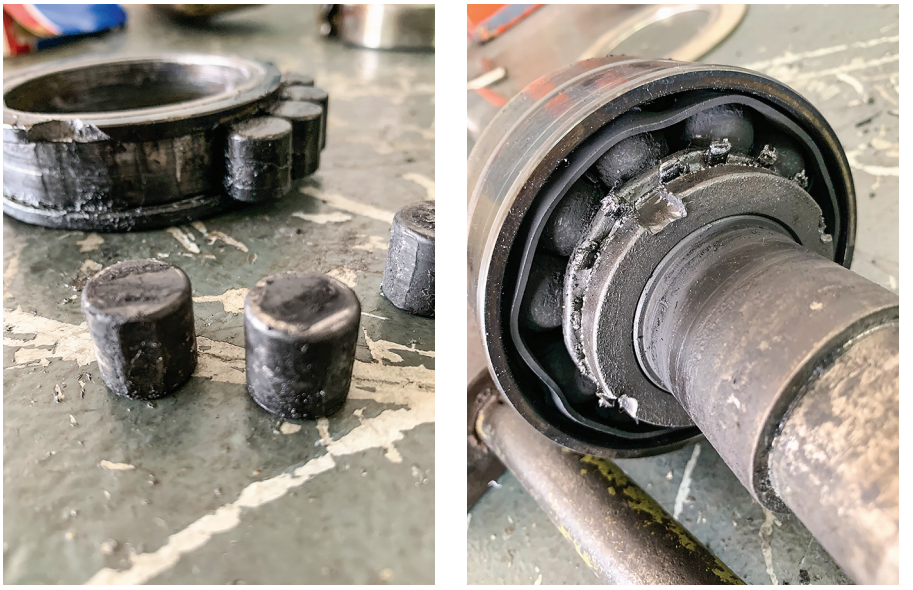

FIG. 1. Failed bearings that are not properly lubricated can result in the complete seizure of the pump as well as secondary damages.

Case study. This case study is about single-stage centrifugal OH1 pump responsible for pumping high-temperature thermic fluid used as a heating medium in the process. The pump is directly coupled to a 75-kW motor, which gives the pump a speed of 2,975 rpm. A pair of 7311 angular contact ball bearings are mounted in back-to-back arrangement, with thrust bearings and a cylindrical roller bearing N212 as the radial bearing. The lube oil used for the bearings was Mobil SHC 626, which is synthetic oil with an ISO viscosity grade of VG 68 and a viscosity index of 165. The operating temperature measured on the bearing housing was 70°C (158°F) and the discharge pressure generated by the pump was 10 kg/cm^2.

The pump experienced frequent bearing failures: five failures in 3 yr made it a serious reliability concern. Every failure was similar and resulted in complete seizure of the pump. This was negatively affecting spares consumption, maintenance costs and, most importantly, plant reliability figures. The measured vibration velocity was always below 2.5 mm/sec, eliminating unbalance, looseness, misalignment or any such low-order issues as probable causes. Conversely, high-frequency indicators, such as acceleration and enveloping, were always in the alarming zone with symptoms of lubrication starvation, even for a newly overhauled pump. No oil leakage from the pump was detected and the oil quality was always properly maintained without any contamination. Frequent oil flushing was carried out, but no positive results were realized.

Observations. When examining the failed bearings—like those in FIG. 1—it appeared that the bearings were not getting properly lubricated. Every failure was similar and resulted in the complete seizure of the pump bearings as well as secondary damages. Process parameters were verified to address any operational deviation, but the pump was found to be operating within the integrity operating window. Vibration analysis suggested lubrication starvation with high values of acceleration and enveloping even after a complete overhaul of the pump. Oil

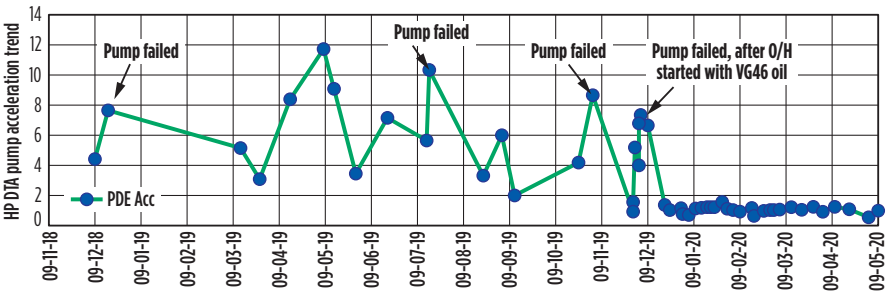

FIG. 2. Trends of acceleration enveloping before and after lube oil change.

flushing/oil replenishment was done as and when required, but no substantial results were achieved.

Action taken.

- It was decided to ensure that the lube oil used for the bearings was the correct lubricant. The viscosity required to lubricate the bearings used in the pump was calculated.
- The calculation of viscosity is a stepwise procedure that includes the calculation of rated viscosity initially, for which bearing mean diameter (dm) is required.
- The dm is the sum of the bearing bore (d) and its outer diameter (OD) divided by 2. For 7,311, the mean diameter is 87.5 mm $[OD = 120, d = 55, dm = 0.5 (OD + d)]$.
- Referring to the standard chart between the rated viscosity and dm for the above calculated value and 3,000 rpm, the rated viscosity for the pump bearings was calculated to be 10 mm^2/sec.
- After determining the rated viscosity, the ISO viscosity grade was calculated to be 27 mm^2/sec using the standard chart between operating temperature and viscosity.
- Considering the kappa value to be > 1, the required lube oil viscosity as per ISO 3448 (with an operating temperature of 70°C) was ISO VG 32. This means that the required lube oil viscosity to effectively lubricate the bearings of this pump is ISO VG 32.
- It was decided to move one step down from the presently used VG 68 to VG 46 to get closer to the calculated value. After this overhaul, the pump was operated.

FIG. 2 shows the trend of vibration data showing the pump behavior before and after changing the lube oil. It is clearly evident that a significant reduction in pump vibration values occurred, and the pump, which always started with higher values after overhauling, is running with low values even after 5 mos of operation.

Takeaway. The higher-viscosity grade synthetic oil being used was not lubricating the bearings properly. High-viscosity oils and lubricants will prevent metal-to-metal contact, but will generate unnecessary heat and loss of power as the rolling elements are forced to work through the oil film. The oil used was almost double the rated viscosity for the bearings and had a high-viscosity index, which also effects the thickness of the hydrodynamic film.

In hydrodynamic lubrication, the coefficient of friction increases with higher viscosity of the lube oil due to internal lubricant friction, which can affect the lubricating film when the load and rpm are constant. A common myth is that if the bearings are failing and the operating temperature is high, a higher-viscosity oil must be used. Sometimes, this may provide a positive result, but changing lube oil without a thorough investigation should never be done, as it can become a cause of the failure. The rated viscosity plays a vital role and can be easily calculated using bearing mean diameter, operating temperature and rpm. HP

AKHIL JEET SINGH RATHORE works as a Mechanical Engineer for Indorama Eleme Petrochemicals & fertilizers Ltd. in Nigeria. He has more than 12 yr of vibration analysis experience in the cement, automobile, petrochemicals, refining and fertilizer industries. Mr. Rathore previously worked with SKF India for 5 yr as a reliability engineer. He holds Mobius Vibration Analysis CAT-II, BINDT CAT-I, SKF India VA Level-II, SKF Nigeria MCSA CAT-I, ASNT UT-II certificates.

A. ANWER AND N. QURESHI
Contributing Authors, Abu Dhabi, UAE

Address damage caused by galvanic corrosion

At petrochemical and refining facilities, it is common for U-clamps over piping runs to become corroded, sometimes to the extent where they are completely thinned out. Localized thinning of supports can also happen, which may remain unnoticed. Fasteners lose their coating and a thin layer of rust appears that can potentially turn into something more significant that requires action.

These forms of galvanic corrosion can be observed externally with visual aids only. Slowly, these damages lead to the implementation of refurbishment projects to eliminate this form of corrosion. While notable cases exist where galvanic corrosion happens within process equipment, the focus here is the monitoring and elimination of those areas where galvanic corrosion happens externally and is often noticeable with visual aids only.

Galvanic corrosion can start where dissimilar metals are in contact without any precautions taken. One of the metals must be a noble-type; the other must be an active metal. While this contact can sometimes be avoided during the design stage, it is not always possible and designers may have many places onsite where a noble metal is in contact with an active metal. Another required element for galvanic corrosion is the presence of an electrolyte. Because this article is focused on the external areas that are vulnerable to galvanic corrosion, atmospheric conditions play an important role in defining the electrolyte present in the galvanic triangle: electrolyte, noble metal and active metal. Any missing element eliminates the chances of galvanic corrosion.

Vulnerable areas. Galvanic corrosion can become evident in numerous places, and some are more critical to plant integrity than others. Supports over or under austenitic stainless-steel piping are critical areas that should be inspected closely for any signs of damage by galvanic corrosion. Vessel internals constructed from dissimilar materials can cause serious damages. In heat exchangers in which the baffles or tube sheet are of different material than the tube, galvanic corrosion can aggressively attack the active metal.

Areas that are less critical but still experience unnoticed and unreported galvanic corrosion include instrument tubing supported through U-bolts over the length. Instrument tubing is normally of austenitic stainless-steel metallurgy and the installed U-bolts are of plain carbon steel material. Also, non-pressure parts can be attached together without considering galvanic corrosion damages. This is sometimes done inadvertently when a superior material is used just in case the required is unavailable, and that better material becomes the noble and the other active. A classic case is when austenitic stainless-steel nuts and bolts are placed over carbon steel flanges, leading to the inevitable and noticeable galvanic corrosion.

Knowledge of active and noble materials is important, and information tables are available where the significance of galvanic corrosion is shown when any two materials come in contact. Based upon this significance, galvanic corrosion should be monitored across the site. This galvanic series is useful during the design stage as well, especially when selecting piping support materials for different piping networks.

Prevention. Prevention of galvanic corrosion is normally done by applying coating systems. Essentially, coating should be applied over the noble metal if austenitic stainless steel is in contact with carbon steel—the austenitic stainless steel must be coated, but what normally is found onsite is that the coating has been applied on carbon steel material, which is the active metal. Installation of structural steel supports like U-bolts over austenitic stainless-steel piping with rubber pads or other foam material in between is a common practice that is incorrect. Over time, these rubber pads degrade, and close inspection of piping at all levels to ensure that these insulating consumable pads still exist is rare.

To preventively address damages by galvanic corrosion, a 5-yr survey is recommended across the site to identify those areas where this damage already exists or can potentially exist and to take remedial action. This survey should essentially remove all existing and potential threats due to galvanic corrosion found externally. At the same time, there must be a record of equipment in which dissimilar materials have been installed as internals. That record can be kept as a list and for all such equipment, a check for galvanic corrosion should be made part of the written scheme of inspection.

For those areas where galvanic corrosion is seen or can potentially exist, corrective action must be taken.

To be identified, galvanic corrosion does not demand state-of-the-art inspection techniques. Visual aids can easily identify problematic areas and corrective actions can be taken accordingly based upon the situation. Once galvanic corrosion is eliminated at sites, major replacement or refurbishment costs can be significantly lowered, especially for those locations where operating assets are installed in a marine environment. HP

ASHFAQ ANWER is an Inspection Professional with more than 15 yr of experience in ammonia-urea complexes, petrochemical units, and the oil and gas industry. He has extensive expertise in material selection, corrosion mapping and control, fitness-for-service studies, defining inspection framework and implementing inspection plans for old and new units.

NABEEL QURESHI is an Inspection and Corrosion Specialist with more than 13 yr of experience in deploying advanced inspection methodologies, corrosion monitoring and static equipment repair and integrity assurance.

M. HALVACI, E. A. SUBAIE and N. A. FUDHAIL, Saudi Aramco, Dhahran, Saudi Arabia; and C. PIERRE and E. ROUSSEAU, Axens, Rueil-Malmaison, France

Ras Tanura: The creation of a clean-fuels complex

The primary objective of the Ras Tanura Refinery Clean Fuels Project is to enable the Ras Tanura refinery—the largest refinery in Saudi Arabia—to produce transportation fuels that will be compliant with future specifications. The project targets the ability to produce gasoline and diesel products to Euro 5 specifications, as well as to maximize refinery gasoline production, especially through the utilization of Khuff gas condensate naphtha. The scope of the project is to install new process units that provide flexibility for maximizing fuels production in the near term, while being able to transition to petrochemical production in the future.

The Ras Tanura refinery is a major gasoline producer in the Middle East. It can produce up to 170,000 bpd of gasoline, primarily using reformate from its three reforming units. It operates one continuous catalyst regeneration (CCR) reforming unit and two fixed-bed semi-regenerative reformers. Due to the use of the fixed-bed reformers, the reformate pool tends to have high levels of benzene. Mitigation measures to reduce these levels (e.g., cut point adjustments) are insufficient to adhere to upcoming clean fuels specifications. This is especially problematic when trying to maximize gasoline production.

The refinery's naphtha supply also exceeds the current reformer capacity. Under the previous specifications, the relatively low sulfur content of the Khuff naphtha allowed for direct inclusion into the gasoline pool. This naphtha inclusion provided for a means to dilute the benzene and aromatics of the reformate pool. The lower sulfur levels mandated by the new specifications no longer allow this practice to continue. In the future, even these lower sulfur naphtha streams must also be desulfurized to be included in the gasoline pool.

At the early stages of project development, it was decided to replace the two fixed-bed reforming units with a new, larger CCR reforming unit. The new CCR reformer was to be designed primarily to process Khuff condensate naphtha. Additionally, the project was to maximize the octane (through isomerization) of the large, light-naphtha stream that was also available.

The selected approach was to install a world-scale naphtha reforming complex consisting of a naphtha hydrotreating unit, a CCR reforming unit and an isomerization plant. The near-term objective was for the reformer to produce a low-benzene reformate stream. With the availability of other relatively high-octane streams, including the new isomerate, it would be possible to operate the reformer at a relatively low severity for total aromatics control in the gasoline pool. The reforming unit was to also have the ability to maximize aromatics—particularly mixed xylenes—in the future.

Clean fuels complex. Saudi Aramco is building a world-scale clean fuels complex at the Ras Tanura refinery. The process units' capacities are to be some of the largest in the world. For example, the complex will include a 140,000-bpd naphtha hydrotreating unit, a 90,000-bpd CCR reforming unit[a] (**FIG. 1**) and a 65,000-bpd C_5–C_6 isomerization unit. The CCR reforming unit will initially be configured for refinery gasoline production but could also be reconfigured for aromatics production for use in petrochemical production. A simplified blockflow diagram of the CCR reforming unit is shown in **FIG. 2.**

FIG. 1. View of the CCR reforming unit under construction at the Ras Tanura refinery.

The Ras Tanura refinery's CCR reforming unit will be one of the world's largest reformers that operates at an ultra-low pressure. The installation of such a high-capacity unit was a technical challenge. However, the unit offers the following benefits:

Saudi Aramco will startup one of the world's largest gasoline producing facilities. This will allow the Ras Tanura refinery to significantly increase gasoline production and be compliant with future gasoline specifications.

- A side-by-side reactor arrangement for ease of construction and maintenance, a low structure for better access and safety, and flexibility in reactor design to optimize unit performance at a minimum cost
- A continuous catalyst circulation system that exhibits the industry's lowest catalyst attrition rate for high on-stream performance—and features a non-pulsing lift system for a smooth operation
- The latest regenerator design, featuring two distinct burning zones and a protective "dry-burn loop" for significantly reduced catalyst aging, with minimum loss of chlorides. The optimized oxychlorination section results in a further reduction in chloride consumption.

The C_5–C_6 isomerization process[b] employed a chlorinated alumina process, characterized by using active and selective chlorinated-alumina catalyst. It has demonstrated a high activity, which enhances equilibrated reactions involved in the isomerization process.

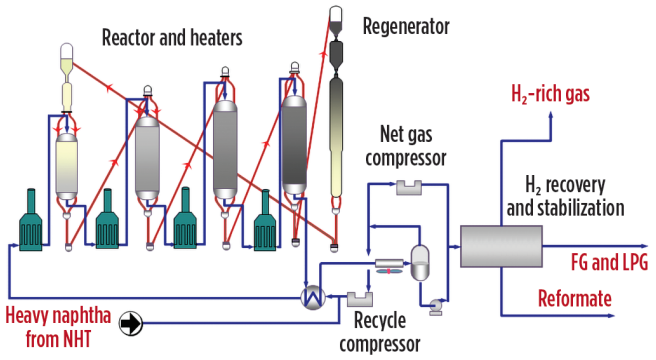

FIG. 2. A simplified blockflow diagram of the CCR reforming unit.

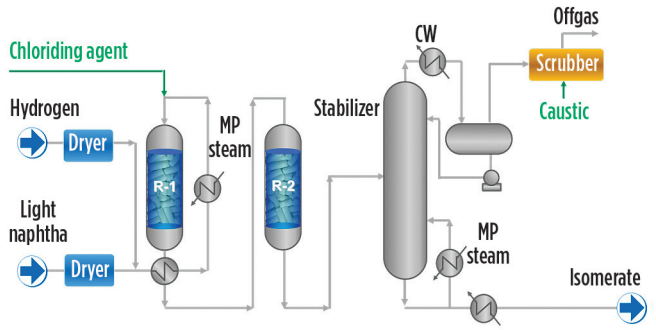

FIG. 3. Simplified once-through isomerization[b] blockflow diagram.

As depicted in **FIG. 3,** the reactor system consists of two reactors in a series, with special valve arrangements—allowing each reactor to be operated in the lead or tail position. Hydrogen utilization is optimized in this once-through scheme, requiring neither a recycle compressor nor a separator drum.

A robust, reliable and simple-to-operate management system of catalyst contaminants was implemented, as well. This includes the removal of water through specific dryers, along with the purification of hydrogen makeup to remove carbon monoxide (CO) and carbon dioxide (CO_2). This arrangement has proven efficient, with the simple catalyst protection helping to maintain long run performances and achieve extended catalyst life.

Project achievements. The primary goal of the Ras Tanura Clean Fuels project is to make the Ras Tanura refinery a premier producer of Euro 5 gasoline in Saudi Arabia, as well as in the Middle East. With this new complex, the capacity for refinery gasoline production could reach 240,000 bpd—enabling the refinery to maximize the value of its naphtha streams. HP

NOTES

[a] Axens' Octanizing™ CCR reforming technology using Axens' CR 600 catalyst series
[b] Axens' C_5–C_6 isomerization technology using Axens' ATIS-2L catalyst

MIKE HALVACI is a Facilities Planning Consultant in the Facilities Planning Department of Saudi Aramco. He has more than 30 yr of experience in refinery operations, economics and project development. He joined Saudi Aramco in 2000 and has been involved in the development of numerous refinery projects within the Saudi Aramco system. Mr. Halvaci earned Bch and MS degrees in chemical engineering from the University of Tulsa.

EMAD AL SUBAIE is a Work Director in the Facilities Planning Department of Saudi Aramco. He has 14 yr of experience in refining and project development. He started his career in 2007 as a process engineer in the Yanbu refinery, where he worked in several operations and engineering units. He earned a Bch degree in chemical engineering from Soongsil University in South Korea.

NOAMAN AL FUDHAIL is a Work Director with the Facilities Planning Department of Saudi Aramco. He has more than 23 yr of experience in refinery operations, engineering and project development. He joined Saudi Aramco in 1997 as a process engineer in the Ras Tanura refinery, where he advanced his technical and leadership skills during his 14-yr tenure. He earned a Bch degree in chemical engineering from the University of Washington.

CHRISTOPHE PIERRE is a Technology Team Manager in Axens' Gasoline and Petrochemicals business line. He joined Axens in 2002 as a process engineer in the Engineering Department, and later became a project manager for reforming and gasoline projects. He joined the technology group in 2007 and oversaw reforming and isomerization technologies related to gasoline pool problematics. Mr. Pierre earned an engineering degree from the École Nationale Supérieure des Industries Chimiques, along with a post-graduate engineering degree from the IFP School in Rueil-Malmaison, France.

EMILIE ROUSSEAU is the Sales Development Manager for Process Licensing at Axens. She has more than 14 yr of experience in the hydrocarbon processing industry. Ms. Rousseau joined Axens in 2009 as a strategic marketing engineer, moving to process licensing in 2018. She earned a chemical engineering degree from the École Nationale Supérieure des Ingénieurs en Arts Chimiques et Technologiques in Toulouse, France; an MS degree in chemical engineering from Imperial College of London; and an MS degree in energy economics and corporate management from the IFP School in Rueil-Malmaison, France.

P. HOBBINS, Placid Refining Co., Port Allen, Louisiana;
H. BLAIR, Johnson Matthey, Arvada, Colorado; and
T. HOCHHEISER, Johnson Matthey, Orange County, California

FCC NO_x reduction methods: Complying with regulations without capital investment

As fluid catalytic cracking (FCC) nitrogen oxides (NO_x) emissions regulations become increasingly strict, refiners are driven to find the most economic compliance option. Multiple capital and non-capital project options are available to mitigate NO_x emissions. Selective catalytic reduction, selective non-catalytic reduction, a proprietary NO_x removal technology[a] and regenerator hardware modifications are discussed in this article for capital project opportunities. A carbon monoxide (CO) promoter, optimization of oxygen (O_2) and CO, feed nitrogen reduction, flue gas ammonia injection and NO_x additives are also covered for non-capital project options. These solutions are discussed, including their NO_x reduction potential, and how they can be integrated into existing regenerator or flue gas systems.

The successful NO_x reduction strategy at Placid Refining Co. is also described. This strategy includes the utilization of an additive for NO_x reduction, combined with a non-platinum CO promoter. In addition, process variables are optimized to reliably control both NO_x and CO emissions.

FCC NO_x emissions regulations have been gradually tightening. In many countries, NO_x emissions regulations have existed for decades, while others are just beginning to implement NO_x limits. The range of NO_x limits is substantial. For example, new FCC units (FCCUs) in India are limited to 260 parts per million (ppm), while many FCCUs in the U.S. have limits in the range of 25 ppm–75 ppm. Based on proposed legislation, Southern California anticipates NO_x regulations reaching as low as 2 ppm. A possibility exists for regulations on hydrogen cyanide (HCN) emissions that would come into force sometime within the next several years.

With more stringent emissions limits, refiners must determine how to comply in the most efficient way possible. The following work examines several methods of NO_x control that utilize both capital investment and non-capital strategies. FCC NO_x chemistry is also discussed, along with a case study from Placid Refining Co.'s refinery in Port Allen, Louisiana.

NO_x chemistry. In most FCCUs, 5 wt%–9 wt% of the feed is converted to coke. Coke comprises carbon, hydrogen and contaminants, including nitrogen. Typically, 40%–50% of feed nitrogen is converted to coke. In the regenerator, the nitrogen in coke reacts to form reduced nitrogen species [HCN and ammonia (NH_3)], some of which is oxidized to N_2 and NO_x (**FIG. 1**). The amount of nitrogen that is converted to NO_x is highly dependent on regenerator operation.

Many variables impact the formation of NO_x in the regenerator. The type of feedstock will influence the amount of NO_x formed. Processing heavier feeds (e.g., coker gasoil, residue or deasphalted oil) can increase regenerator NO_x formation. Alternatively, hydrotreating FCCU feed reduces the amount of feed nitrogen, leading to lower NO_x in the regenerator. Regenerator operating conditions impact NO_x formation, as well. In full-burn regenerators, higher excess oxygen leads to increased NO_x formation. Operators can minimize oxygen to minimize NO_x formation; however, low amounts of O_2 will increase CO emissions. Therefore, a balance must be achieved.

In partial-burn regenerators, there are three contributors to CO boiler NO_x emissions: NO_x formed in the regenerator, NO_x formed in the CO boiler from regenerator flue gases HCN and NH_3, and NO_x formed in the CO boiler from air N_2. In the regenerator, HCN and NH_3 oxidize to form N_2 and NO_x species, but this reaction is limited by oxygen availability. Consequently, reduced nitrogen species are present in the regenerator flue gas. In the CO boiler, these reduced nitrogen species are readily converted to NO_x. The third source of NO_x is from thermal oxidation of N_2 in the CO boiler burners. Thermal NO_x can be minimized with lower flame temperatures and by optimizing air, fuel gas and flue gas mixing.

Regenerator design also has a major bearing on NO_x formation. Well-mixed or counter-current regenerators help limit

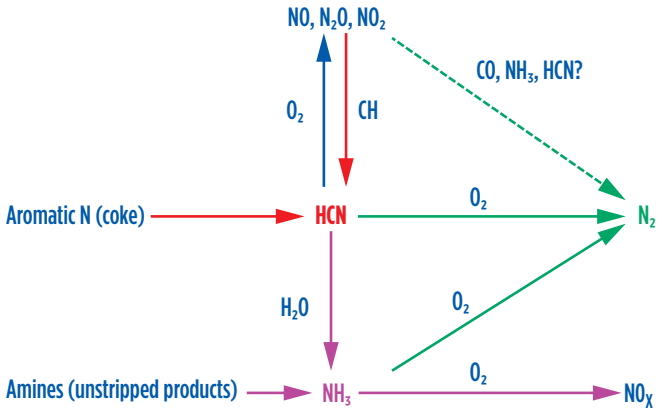

FIG. 1. Regenerator nitrogen reaction pathways.

NO_x formation due to consistent catalyst and air mixing. This avoids pockets with high or low oxygen content. Additional factors that impact NO_x formation are the use of CO promoters and the use of antimony (Sb). Most U.S. refiners have switched from platinum-based promoters to palladium-based, but platinum is still widely used across the rest of the world. Platinum catalyzes the formation of NO_x and will continue to contribute to NO_x while present in equilibrium catalysts (Ecat). Palladium promoters also generate NO_x but to a lower extent than platinum. In addition, the NO_x-generating half-life of palladium is lower than platinum. Sb is often used for nickel (Ni) passivation, but this can also increase NO_x.

Placid Refining was able to effectively use a NO_x reduction additive to reduce FCCU NO_x emissions by 32%. This enabled emissions limit compliance without having to invest in a sizeable project.

NO_x reduction options. Multiple strategies are available to decrease FCCU NO_x emissions. These strategies can be divided into two main categories: capital investment projects and non-capital solutions. Most solutions involve some level of ongoing operating expense.

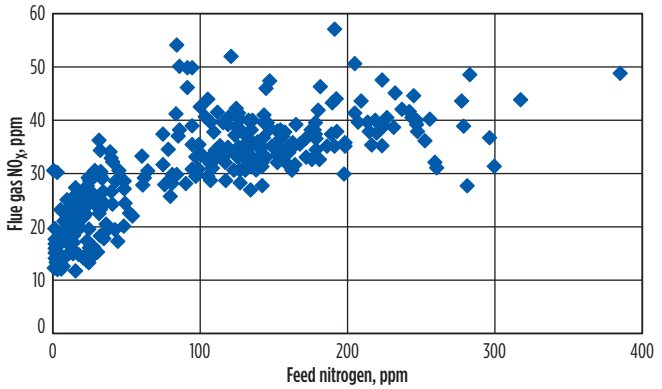

FIG. 2. Impact of feed nitrogen on flue gas NO_x.

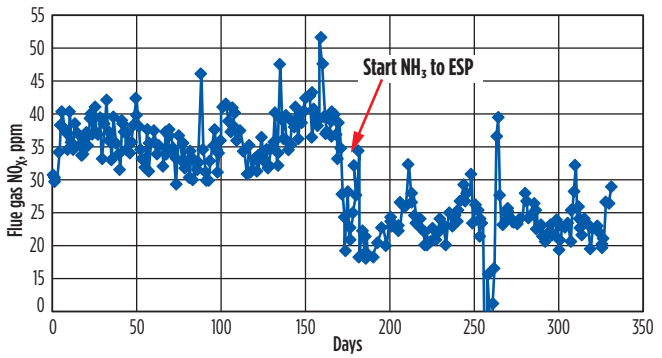

FIG. 3. NO_x reduction from ESP NH_3 injection.

Capital project options. The following are capital project options to reduce FCCU NO_x emissions.

Regenerator hardware. Upgraded regenerator air grids, advanced spent catalyst distribution systems and well-mixed regenerator designs are becoming more common to reduce NO_x emissions and optimize regenerator performance. The hardware improvements not only improve NO_x control, but also provide other benefits, such as lower CO, lower afterburn and lower regenerated catalyst coke levels. Multiple licensors offer enhanced regenerator designs. These designs can be implemented either through revamps or through the installation of new regenerators. The various designs have different levels of achievable NO_x reduction.

Selective catalytic reduction (SCR). SCR is a process that involves the injection of NH_3 into the FCCU flue gas followed by reaction across a catalyst bed. The reaction occurs between 287°C–399°C (550°F–750°F) and produces N_2 and water vapor. The main reaction (1) as the majority of FCC NO_x is NO_x. The cost of the system is primarily driven by the SCR reactor, which must be incorporated in the flue gas system. In some FCCUs, feed-forward control is utilized. Flue gas NO_x is measured upstream of the SCR unit and is used to control the NH_3 injection rate slightly above the molar equivalent ratio. Feedback control measures NO_x downstream of the SCR and adjusts NH_3 injection accordingly. The process has operating costs for NH_3 and catalyst changeouts and can achieve up to 95% NO_x reduction.

The reduction chemistry is detailed below:

$$4\,NO + 4\,NH_3 + O_2 \rightarrow 4\,N_2 + 6\,H_2O \quad (1)$$

$$2\,NO_2 + 4\,NH_3 + O_2 \rightarrow 3\,N_2 + 6\,H_2O \quad (2)$$

$$NO + NO_2 + 2\,NH_3 \rightarrow 2\,N_2 + 3\,H_2O \quad (3).$$

Selective non-catalytic reduction (SNCR). SNCR is like SCR in that it uses NH_3 to react with NO_x to form N_2 and water. The process is completed at a higher temperature than SCR, allowing it to be accomplished without a catalyst. The temperature must be maintained between 926°C–1,093°C (1,700°F–2,000°F) for the reaction to take place; therefore, the SNCR system is incorporated with the CO boiler. Urea may be used instead of NH_3 due to the higher temperature of SNCR. The process includes an injection system with air, which is designed to produce effective mixing. Precautions include NH_3 slip at high injection and NO_x breakthrough at low injection. SNCR can remove up to 50% NO_x and is generally a lower capital investment than other NO_x projects.

Proprietary NO_x emissions reduction technology[a]. This proprietary process is a system that combines an ozone generator with a wet gas scrubber to remove NO_x. The ozone generator converts supplied oxygen to ozone. The ozone selectively oxidizes insoluble NO_x into soluble nitrogen species that can be removed in the wet gas scrubber. The process can remove up to 95% NO_x, with low flue gas pressure drop. The associated operating costs include oxygen, power supply and caustic.

These four different capital project options—which can achieve different levels of NO_x removal—have both benefits and precautions. The choice depends significantly on the existing flue gas system and how the different solutions could be integrated into the existing system.

Non-capital investment options. The following are non-capital investment project options to reduce FCCU NO_x emissions:

CO promoter optimization. All CO promoters contribute to NO_x formation. To reduce NO_x, the CO promoter addition rate should be minimized and, if feasible, stopped. If a CO promoter is required, utilizing a non-platinum rather than a CO promoter is a common first step to lower NO_x. Non-platinum CO promoters typically utilize palladium to catalyze CO oxidation, although other metals can be used.

O_2/CO optimization. The most prominent operating variable to control NO_x is excess oxygen in a full-burn regenerator. Lower excess oxygen contributes to lower flue gas NO_x. In partial-burn operations, NO_x emissions are measured at the CO boiler outlet. Lower flue gas CO results in lower CO boiler NO_x. NO_x increases in deep partial burns because the amount of HCN and NH_3 in the regenerator flue gas increases. These reduced nitrogen species are converted to NO_x in the CO boiler. Usually, the lowest NO_x formation can be achieved when operating at the crossover point between full burn and partial burn.

Feed nitrogen reduction. Minor changes in feed nitrogen do not typically have a noticeable impact on NO_x formation. However, major changes in feed nitrogen have shown an impact on NO_x. FIG. 2 is from an FCCU that was able to decrease its feed nitrogen by an order of magnitude by adjusting gasoil hydrotreater severity. This action allowed the operator to significantly reduce NO_x formation. Another method that could significantly decrease feed nitrogen is by changing the feed source, such as removing residue or coker gasoil from the FCCU feed stream or changing the crude slate.

Flue gas NH_3 injection. Some refiners have successfully reduced NO_x through NH_3 injection into the flue gas system. This is done at a low temperature and without a NO_x reduction catalyst system. The injection point is often upstream of the electrostatic precipitator (ESP), as NH_3 also improves ESP performance. FIG. 3 shows an FCCU that began injecting NH_3 upstream of the ESP and was able to achieve a 35% reduction in flue gas NO_x emissions.

NO_x reduction additive. NO_x reduction additives can be used to reduce both regenerator flue gas NO_x and HCN. These additives are injected into the regenerator through an additive addition system. The additives are designed to catalyze the oxidation of HCN to N_2 (FIG. 4). The additives are used at 1 wt%–2 wt% concentration in Ecat and can reduce NO_x by up to 40%. Refiners can also use NO_x reduction additives in combination with other technologies to optimize operating costs.

Case study from the Placid Refining Co. refinery. The Placid Refining Co. refinery was able to effectively manage its flue gas NO_x emissions by using a strategic FCC additive regimen and process variable optimization. NO_x emissions were first decreased by changing the combustion promoter from a platinum-based promoter to a palladium-based one. Emissions were further reduced with an NO_x reduction additive specifically designed to catalyze the conversion of HCN and NH_3 to N_2.

Placid Refining operates a 25,000-bpd FCCU. The facility's crude slate is typically composed of Light Louisiana Sweet and Gulf Coast Sour crudes. The refinery's FCCU feed comprises 70%–80% gasoil and 20%–30% deasphalted oil. The feed basic nitrogen averages 440 ppm, with a typical API gravity of 20.9.

In 2010, Placid Refining began initial steps in overall NO_x control by changing from a platinum-based CO promoter to a proprietary non-platinum promoter[c]. Removing the platinum promoter from the FCCU typically results in a 60%–70% reduction in NO_x emissions.

In 2015, Placid Refining started analyzing the benefits of a capital project vs. a non-capital project solution to further reduce NO_x emissions. This was in preparation for a new environmental regulation limiting NO_x to a 45-ppm rolling average limit. The proprietary non-platinum additive was trialed to determine if capital investment could be avoided.

Placid Refining conducted a two-phase trial: 1 wt% concentration followed by 2 wt%. During each phase of the trial, noticeable reductions were observed in the level of NO_x emissions. The trial was successful and proved that Placid Refining would be able to meet its emissions regulations without capital investment. The proprietary non-platinum additive was stopped after the trial and reintroduced once the NO_x regulation went into

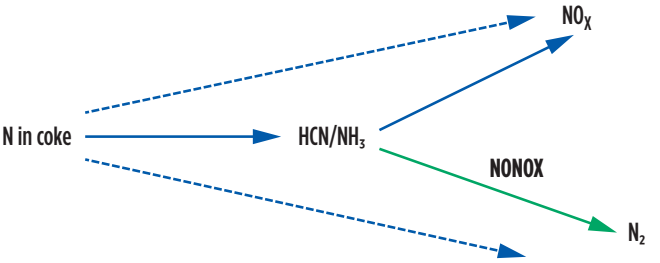

FIG. 4. NO_x reduction additive[b] mechanism.

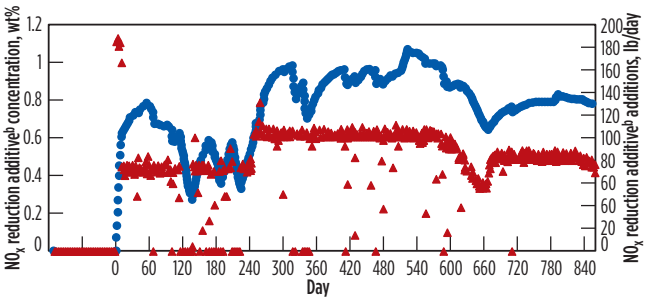

FIG. 5. Proprietary non-platinum additive[c] addition rate and concentration.

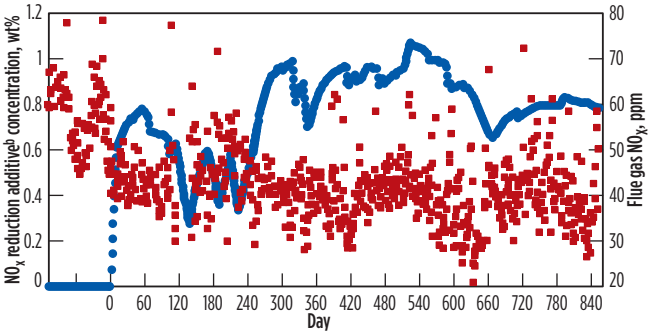

FIG. 6. Proprietary NO_x reduction additive[c] reduced NO_x emissions.

effect. The following data is from when the proprietary NO_x reduction additive was reintroduced to the FCCU.

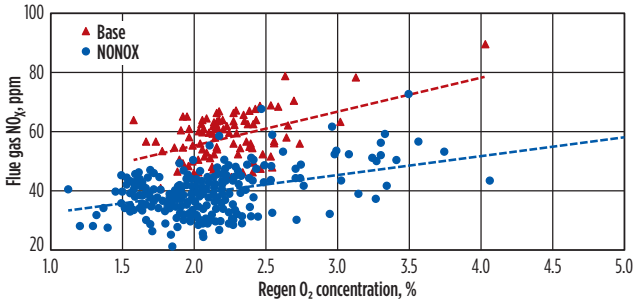

FIG. 7. The proprietary NO_x reduction additive reduced NO_x emissions by 32%.

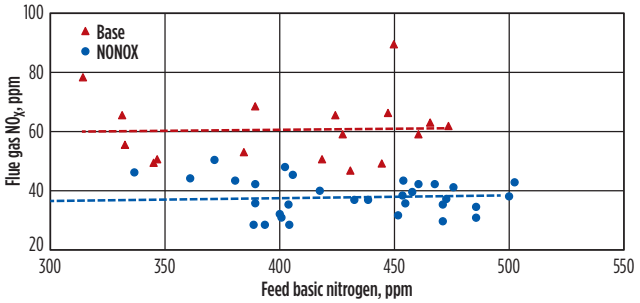

FIG. 8. Feed nitrogen did not have an impact on NO_x.

Placid Refining started with a 10-d baseload and has maintained an average of 0.8 wt% concentration since reintroduction. As the proprietary NO_x reduction additive concentration increased, a reduction in NO_x emissions was achieved (**FIGS. 5** and **6**).

Placid Refining optimizes process variables to ensure that the refinery is minimizing NO_x while optimizing FCCU operation. Sb is used for Ni passivation, and Placid Refining closely monitor the Sb injection rate and Ecat Sb/Ni to ensure that the unit was not producing excess NO_x. Steps have also been taken to minimize excess oxygen to a CO limit. A base period prior to the proprietary NO_x reduction additive's use was compared against operation with the additive included. The proprietary NO_x reduction additive use showed a clear reduction in NO_x emissions at similar excess oxygen levels (**FIG. 7**). Placid Refining was able to achieve and maintain an NO_x reduction of 32% relative to base emissions.

For additional insight, NO_x emissions—as a function of feed nitrogen—were also analyzed. Placid Refining's feed nitrogen does not have an observable impact on NO_x emissions. However, the reduction between the base data and the proprietary NO_x reduction additive time period is transparent (**FIG. 8**).

Takeaway. Many different FCCU NO_x reduction strategies can be employed to successfully meet emissions limits. The different strategies have varying levels of NO_x reduction and can be integrated into different flue gas system designs. Some of the options require capital investment and affiliated operating expenses, while others can be successfully implemented without upfront investment.

Placid Refining was able to effectively use a NO_x reduction additive to reduce FCCU NO_x emissions by 32%. This enabled emissions limit compliance without having to invest in a sizeable project. The refiner continuously optimizes its regenerator excess oxygen level to operate in balance with CO limits. In addition, Sb is used to successfully passivate Ni without creating excess NO_x. HP

NOTES

[a] Linde's LoTOx process
[b] Johnson Matthey's NONOX additive
[c] Johnson Matthey's COP-NP non-platinum CO promoter

PATRICK HOBBINS is a Process Engineer for Placid Refining in Port Allen, Louisiana. He is responsible for technical support for the FCCU and alkylation unit, as well as gasoline blending. He has previously worked on all units of the refinery and has provided engineering support for major revamps of the DHT and treater units. Mr. Hobbins earned a BS degree in chemical engineering from Louisiana State University and has 15 yr of experience in the refining and petrochemical industries.

HEATHER BLAIR is an FCC Technical Engineer for Johnson Matthey. She is responsible for analysis, recommendations and customer interface in the FCC additives business. She started her career with HollyFrontier in Cheyenne, Wyoming, as a Product Blending Engineer. She has 10 yr of experience in the refining industry. Ms. Blair earned BS and MS degrees in chemical engineering from the University of Wyoming.

TODD HOCHHEISER is Manager of FCC Technical Service for Johnson Matthey. He is responsible for the engineering team that provides technical assistance on the use of additives and catalyst addition systems. Mr. Hochheiser earned his Bch degree in chemical engineering from the University of Delaware and an MBA from the University of California Irvine. Prior to joining Johnson Matthey, he held engineering, operations, and planning and economics positions with Valero Energy and ExxonMobil.

A. A. KISS, University of Manchester, Manchester, UK;
V. N. MALETA, Maleta Cyclic Distillation LLC, Tallinn, Estonia;
and **A. SHEVCHENKO** and **O. BEDRYK,** National University of Food Technologies, Kiev, Ukraine

Cyclic distillation: A novel enhanced technology for processing hydrocarbons and derivatives

Distillation is the most widespread separation method in history.[1] Despite its simplicity and flexibility, distillation remains a very energy-inefficient process. Novel distillation concepts based on process intensification (PI) principles can deliver major advantages in terms of significantly lower energy use and reduced capital costs while improving ecological efficiency.

The PI concept has been around since the mid-20th century, but has received more attention in the last two decades. The objective of PI is to design substantially smaller plants while improving their operational safety, environmental performance and energy efficiency. The Rapid Advancement in Process Intensification Deployment (RAPID) Institute, supported by the U.S. Department of Energy, has placed a spotlight on PI in the U.S. RAPID aims to target and promote major advances in energy efficiency and productivity in the process industries.[2]

With respect to PI, distillation has enjoyed a number of major enhancements based on process intensification—e.g., HiGee distillation, dividing-wall column, heat-integrated distillation, membrane distillation and reactive distillation.[3] Among these advanced technologies, cyclic distillation stands out as a new challenger in fluid separations due to a different way of contacting the liquid and vapor phases.[4] In contrast to classic operation, cyclic distillation uses separate phase movement (SPM) that can be achieved with specific internals and a periodic operation mode.[5] Cyclic distillation can also bring new life to old distillation columns by replacing classic internals with new ones and using a cyclic operation mode. One operating cycle consists of two key parts: a vapor flow period (when the thrust of rising vapor prevents liquid down flow) followed by a liquid flow period (when the liquid flows down the column, dropping by gravity, first to a lock chamber and then moving to the tray below). **FIG. 1** illustrates this operating cycle.[6]

From the outside, a cyclic distillation column looks like a regular tower. However, the cross-section view inside a cyclic distillation column shows the absence of downcomers and the presence of different internals (**FIG. 1,** left) that allow an efficient separate-phase movement in practical operation. Recent articles and a mini-review of cyclic distillation provide more details about the history of cyclic distillation, working principle, design and control methods, benefits and limitations.[7–10]

Theoretical background. The theory of the cyclic distillation processes has been developed over several decades of engineering. The best established design algorithms for cyclic distillation columns include analytical and numerical methods of increased complexity and usability, developed from 1977–2014.[11] **FIG. 2** illustrates the modeling of a classic theoretical stage and the operating lines in case of classic vs. cyclic distillation—where L and G are the liquid and gas (vapor) flowrates,

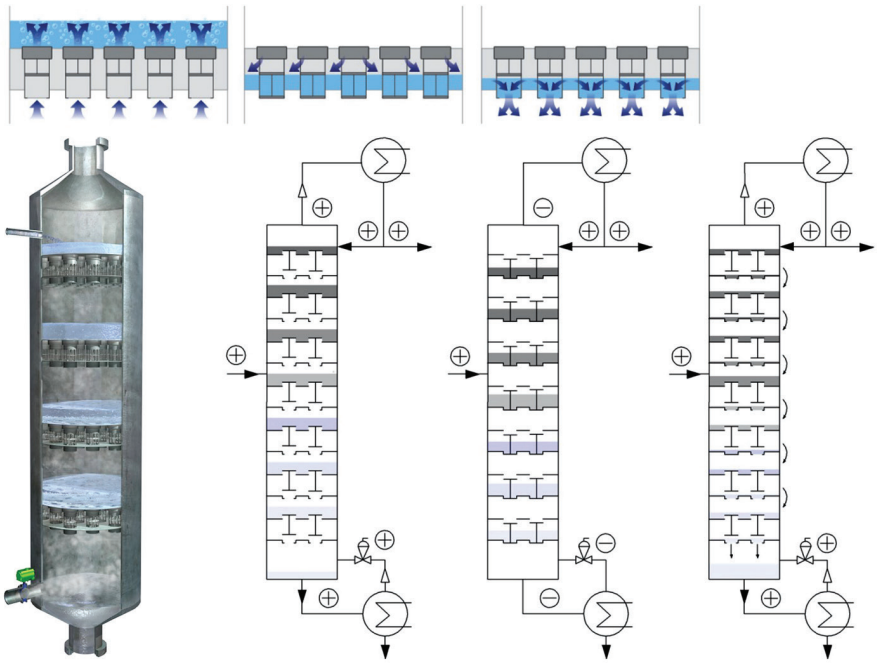

FIG. 1. Cross-section of a cyclic distillation column (left). Schematics illustrating the operation principle of the cyclic distillation system (right): vapor flow period, followed by first and second half-liquid overflow (tray–sluice–tray below).

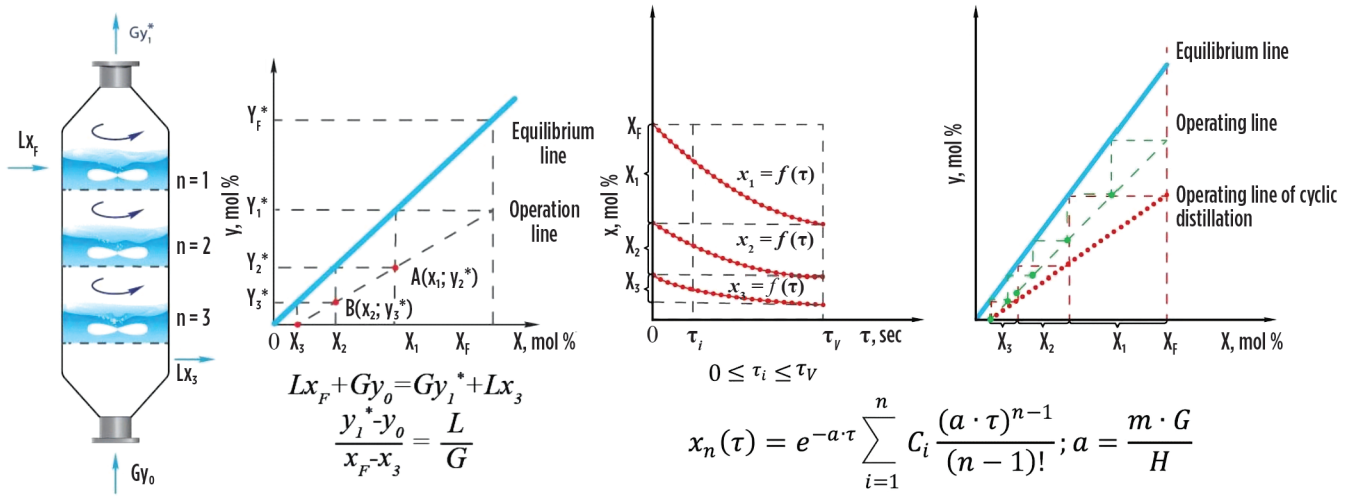

FIG. 2. Conventional theoretical stage and operating lines (left); operating lines for cyclic mode (right).

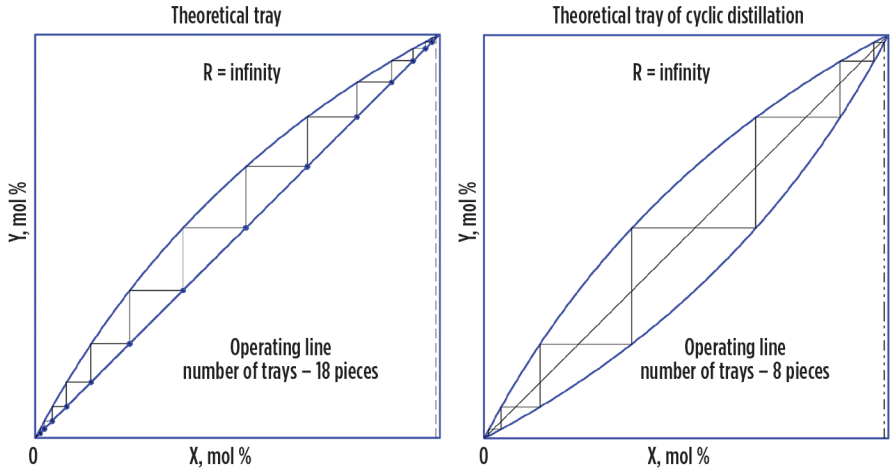

FIG. 3. Operating lines for the separation of a binary mixture in case of classic (left) and cyclic distillation (right).

H is the liquid holdup on the tray (mol), τ is the vapor period duration (sec), and x and y are the liquid and vapor composition, respectively.[4]

FIG. 3 shows an example of the operating lines for binary separations in the case of classic distillation vs. cyclic distillation. The operating lines are at the basis of designing distillation columns, and a distinction stems from the different theoretical-stage concepts. This difference is demonstrated by the effectiveness of the minimum number of theoretical plates required for the separation at total/infinite reflux. The operating lines provide the number of stages, which is much lower in the case of cyclic distillation, due to the larger driving force of the process. A visual clue of this advantage is the operating line that is actually a mirror image of the equilibrium line relative to the diagonal.

Recent studies proposed iterative numerical solutions of the cyclic distillation simulation model with simultaneous tray drainage. An iterative procedure has been proposed[8] to calculate the tray holdups and compositions at the end of vapor flow and liquid flow periods, respectively.

A method was developed[12] for organizing cyclic modes in a sectioned apparatus, with the operation of one of the sections in the liquid flow mode and the other sections in the vapor flow mode. A driving force was proposed[11] based on a design adapted from classic continuous distillation to cyclic distillation. Recently, both mass and energy transfer were considered in a new model[10] that is able to describe binary and multiple-component systems with both ideal and nonideal liquid phases, as well as account for multiple feed locations and side draws.

An integrated process design and control approach was proposed[9] based on the application of simple graphic design methods known from conventional distillation columns. This approach has shown that operating a cyclic distillation column at the largest driving force results in an optimal design in terms of controllability and operability, which is less sensitive to disturbances in the feed and has the inherent ability to efficiently reject disturbances.

Techno-economic advantages. The cyclic mode of operation leads to major economic advantages, reported both theoretically and experimentally:

- 20%–50% lower investment cost (due to lower column height, smaller column diameter, smaller area of the heat exchangers, less steel construction and less space used)
- 20%–35% lower hot utility usage (due to high mass transfer efficiency and reduction of the reflux rate)
- 20%–35% lower cold utility usage (due to lower reflux rate)
- Improvement of product quality (due to high mass transfer efficiency and higher concentration of key product)
- Increase of product yield (due to high mass transfer efficiency and more concentrated impurities or other fractions)
- Enhanced process sustainability (due to less GHG emissions due to lower energy usage).

The technological advantages of cyclic distillation include the following:

- Mass transfer efficiency of one cyclic distillation tray is equal to

three classic distillation trays
- Reduction of the residence time of liquid in the column, and the uniform arrangement of liquid on the tray
- Ability to control the amount of liquid on the tray and the reaction time (in the case of reactive distillation)
- Any geometric configuration of the trays, which allows the possibility to build dividing-wall columns with trays
- The separation efficiency does not depend on the column diameter, which allows easy industrial scale-up
- Placement of any type of packing between the trays further increases the mass transfer efficiency
- The pressure drop in the column does not depend on the liquid load in the column since the amount of liquid on the trays is constant and only the frequency of cycles is changed (range: 1 m^3/m^2hr–30 m^3/m^2hr liquid load)
- The vapor velocity in the column typically ranges from 0.2 m/sec–20 m/sec, as it depends on the pressure in the column
- The operation remains stable and efficient in case of changed concentrations of the key components.

However, cyclic distillation is also characterized by important limitations when considering the technology for various applications. It is difficult to apply to vacuum systems due to the pressure drop on the trays, and the performance enhancement critically depends on the separation of the vapor and liquid periods.

Industrial equipment. Industrial interest in cyclic distillation has been renewed due to the availability of design and control methods and the introductions of special trays that allow better control of phase movement. Due to these developments, during the past decade, cyclic distillation has become accepted as a proven technology and emerged as a challenger of the status quo in distillation. Along with the scientific research carried out at several universities in the EU, cyclic distillation has sparked the interest of large companies,[13] software vendors and technology providers.[14]

Although all simulation studies predicted enhanced separation performance, when applying conventional internals in practice, the fluid dynamic limitations restrained the industrial breakthrough of cyclic distillation technology. However, this barrier has been removed with the development of new internals.[4] Also, the cyclic operation uses reliable stop valves (butterfly valves with pneumatic drive) from leading manufacturers, which can withstand up to 20 MM cycles (e.g., the first industrial columns operated well for more than 10 yr).

The present leader offering cyclic distillation technology has developed novel engineering solutions for more efficient contact devices (e.g. trays with lock chambers allowing the liquid to follow the path of tray to lock chamber to the tray below), as shown in **FIG. 4,** and a full column in **FIG. 5.**[6] Practical implementation at pilot and large scale has showed the following benefits achieved in operation:
- High tray efficiencies (140%–200% Murphree efficiency) translates into reduced equipment cost
- Higher throughput and equipment productivity than conventional distillation
- Reduced energy requirements (20%–35% savings) translate into lower operating costs
- Increased product quality due to higher separation efficiency.

FIG. 4. Trays suited with sluice chambers, especially designed for cyclic distillation columns (left). Top view of an installed cyclic distillation tray column with a diameter of 1.7 m (right).

FIG. 5. Cyclic distillation (dividing-wall) column prepared for transportation to a chemical site.

Industrial applications. So far, cyclic distillation has been used mostly in the food industry, but the application range is expanding to other areas with potential use, such as oil refining, chemicals, petrochemicals, pharmaceutics, biofuels, etc.

Ethanol separation and purification. Ethanol is an essential chemical that can be produced by fermentation of sugars by yeasts, or via petrochemical processes. It is used in the food industry, for medical applications, as a chemical solvent, in manufacturing processes and also as a renewable fuel (bioethanol). **FIG. 6** shows the flowsheet of a typical ethanol production plant.[15] An ethanol production plant consists of a beer column pre-concentrating ethanol (C1), a hydro-selection column (C2), a rectification column (C3), a column for end-cleaning, which produces high-purity ethanol (C4), a column for concentrating impurities (C5), a fusel column (C6) and a methanol column (C7). The light (head), intermediate and heavy

(end) impurities are removed by distillation columns C2, C5 and C7.

The main goals in the purification of ethanol are to obtain a product with a minimum impurities content and to maximize product yield. In addition, energy savings can be achieved by operating the columns at different pressures; for example, the vapor from the beer column is used to heat the hydro-selection and the methanol columns. All these distillation columns can be replaced with cyclic distillation units. However, for the production of food-grade ethanol, column C3 remains due to insufficient knowledge about the actual distribution of impurities in this multi-feed, multi-product column in cyclic operation mode.

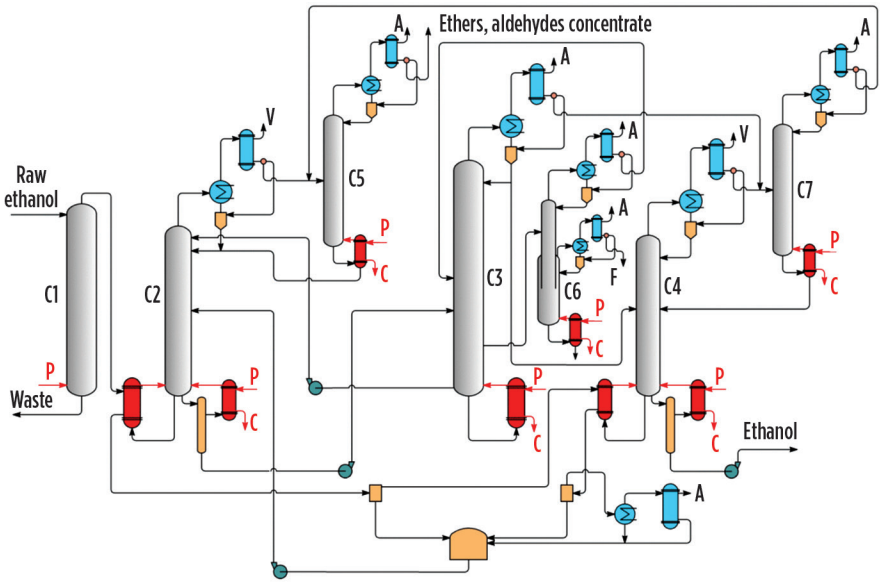

FIG. 6. Flowsheet of an ethanol production plant.

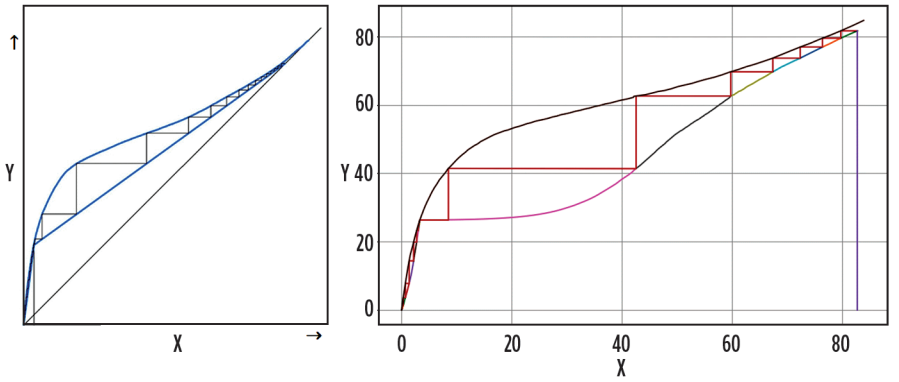

FIG. 7. XY diagrams for ethanol-water separation for classic (left) and cyclic (right) distillation.

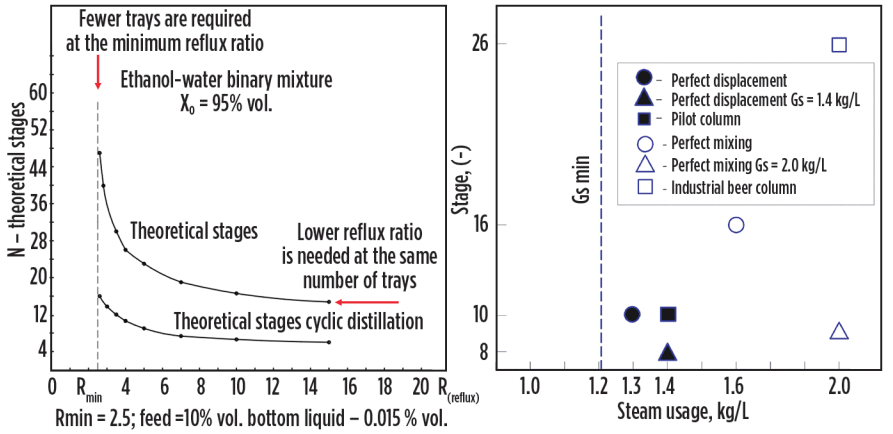

FIG. 8. Ethanol-water separation efficiency in a cyclic distillation column (perfect displacement mode) vs. classic distillation (perfect mixing mode).

FIG. 7 illustrates the difference in the shape of the XY diagrams for the ethanol-water mixture for classic distillation and cyclic distillation. The operating lines for cyclic distillation allow a much lower number of theoretical stages due to the larger driving force of the process.

FIG. 8 (left) illustrates the separation efficiency in a cyclic distillation column (perfect displacement model) vs. classic distillation (perfect mixing mode) for an ethanol-water mixture.[14] At minimum reflux ratio operation, fewer trays are required for cyclic distillation as compared to classic distillation. Similarly, a lower reflux ratio is needed for a cyclic distillation operation as compared to classic distillation, for the same number of trays used. **FIG. 8** (right) shows the difference between the cyclic operation in a pilot column working in parallel to an existing industrial column, thereby performing the same separation task.[14] Note the large steam usage (per liter of ethanol product), which translates into 30% energy savings in the case of cyclic distillation.

FIG. 9 illustrates the quantitative effect of applying the cyclic operation mode to ethanol-water mixtures. The optimal reflux ratio (corresponding to the minimum annualized cost) shifts to the left (lower values), thereby allowing 25% lower energy use as compared to classic distillation. The reflux ratio and the number of trays can be used to achieve various targets—e.g., at reflux ratio 4, the energy savings are 0% but 2.5 times fewer trays are required; at reflux ratio 3.5, the energy savings are 10% and 2.3 times fewer trays are required; and at reflux ratio 2.6, the steam savings are 30% and require 1.5 times fewer trays as compared to classic distillation.

Other industrial applications. Cyclic distillation also offers new opportunities by applying the same principles of the cyclic operation mode to other intensified processes, such as catalytic distillation (CD)[16] or even dividing-wall column (DWC). **FIG. 10** illustrates cyclic distillation DWCs with a coaxial parti-

tion for multi-component separations.[6]

An interesting phenomenon that also occurs in a DWC is the evaporation of superheated liquid when the steam supply to the column is shut off. This results in added process efficiency, especially when obtaining highly pure substances, as volatiles are the first to evaporate. During the vapor period, the liquid gathers much energy; however, when the vapor flow is stopped, the pressure drops and the superheated liquid boils throughout the DWC.

Modern cyclic distillation technology works in stripping columns, rectification columns and tray DWCs with a diameter range of 400 mm–1,700 mm. Cyclic distillation technology has been used in the production of ethanol for biofuels and food, in the recovery of methanol from water and/or acetone, in the distillation of various chemicals (ethers, propylene, propanol, hexane, formalin, aniline, cyclohexane, butyl acetate, ethylbenzene, methyl acetate, BTX), in isopropyl alcohol dehydration, in industrial solvents distillation (white spirit), in the cleaning of raw coal benzole, and in the fractionation of kerosene, with several implementations in Ukraine, Belarus and Saudi Arabia.

For example, since 2006, one company has built and installed commercial-scale plants with cyclic distillation columns of 5–42 trays and column diameters of 0.4 m–1.7 m. In 2014, the same company built an industrial-scale DWC using cyclic operation (42 trays, 1.5 m/1.7 m diameter, and a capacity of 25 m^3/hr) for a plant processing kerosene and white spirit.

Promising industrial use. Some promising areas for using cyclic distillation include the production of high-purity substances, such as:

1. Organic synthesis (e.g., ethyl acetate, methyl acetate) in reactive distillation systems, which offers the ability to control the reaction on a tray, along with the added bonus of avoiding erosion of the solid catalyst due to fluid overflow.
2. Ecological applications (e.g., recovery of solvents and refrigerants and CO_2 absorption processes). A pilot industrial unit was built in Finland by Eco Scandic Oy. An additional pilot unit is planned to conduct research on the development of new technologies. Typically, refrigerants are collected for regeneration by their type and not as mixtures; however, in practice there are no ideal conditions. Mixtures of different types of refrigerants may be present in one tank; fractionation is required to separate and purify them for further reuse. Eco Scandic Oy invested in building a distillation unit for the fractionation of refrigerants (as illustrated in FIG. 11). This is a great prospect for countries with hot climates and heavy use of refrigerants, as it can significantly reduce the environmental burden. In addition, this unit can be used for research purposes, since the unit was designed for pressures up to 30 bar and deep vacuum.
3. Separations of close boiling components (such as isomers of hydrocarbons or isotopes of water).

FIG. 12 illustrates the first use of cyclic distillation DWCs for fractionating kerosene.[6]

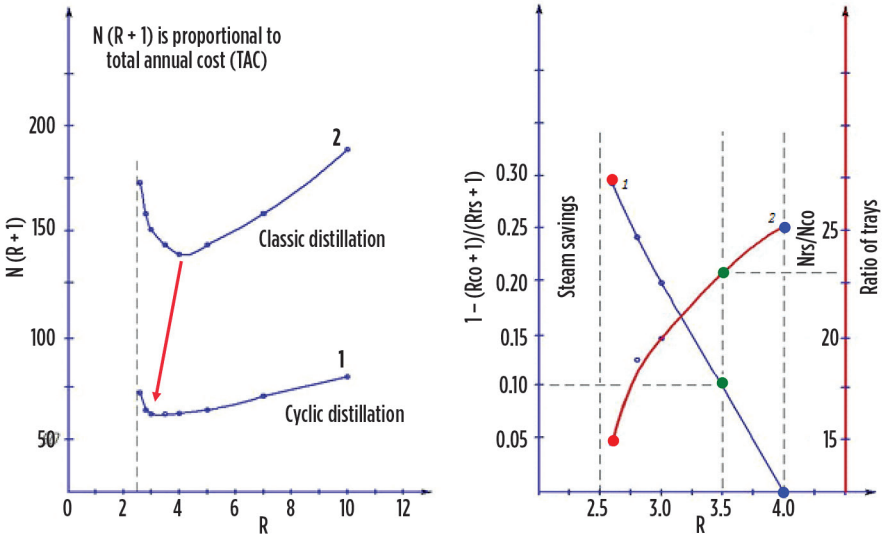

FIG. 9. Quantitative effect of applying cyclic distillation instead of classic distillation to ethanol-water mixtures.

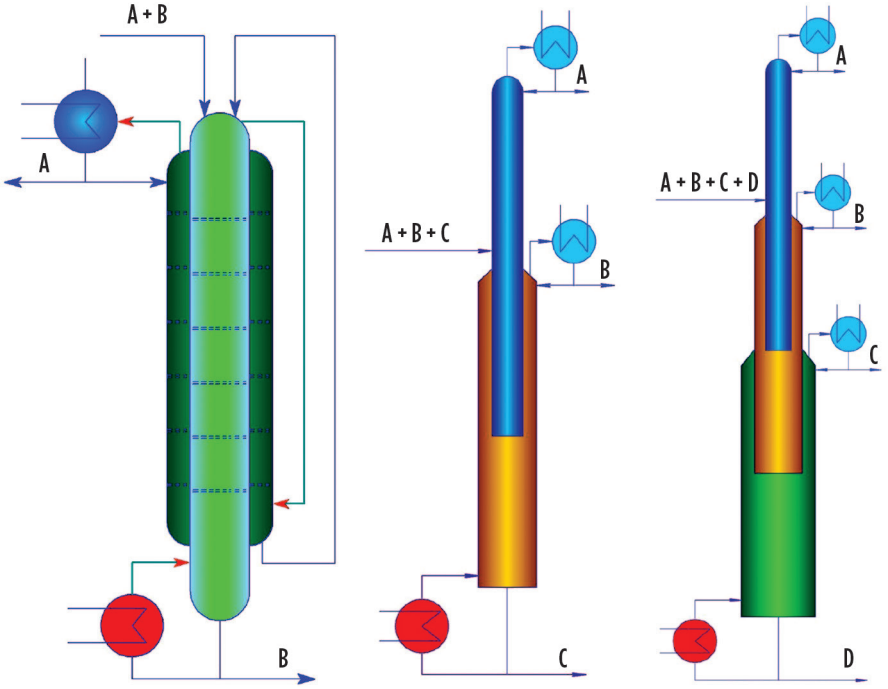

FIG. 10. Cyclic distillation (dividing-wall) columns with coaxial partition—any geometric shape is possible.

The main areas of use for cyclic distillation technology in petroleum refining include high-quality fractionation of gas, high-quality narrow fractions during vacuum/atmospheric distillation of petroleum, second refining of all types of petroleum cracking, combining reaction and distillation processes (catalytic distillation), obtaining isomers of high added value 1,2,3-trimethylbenzene, mesitylene, durene, isodurol and others. However, a potential limitation of the process is crude oil processing, as liquid load on the tray does not exceed 30 m^3/m^2hr.

Takeaway. Cyclic distillation can significantly improve fluid separations for processing hydrocarbons and their derivatives, providing key benefits such as lower energy requirements (by 20%–35%), reduced capital costs (by 20%–50%), increased column throughput and better separation performance (with up to three times higher efficiency than classic distillation trays). The separate phase movement also provides more degrees of freedom that contribute to good process control and simple operation.

Yet, similar to the history of other process intensification technologies (e.g., DWC), the chemical industry and hydrocarbon processing industry seem to be reluctant in adopting new technologies due to various perceived issues: difficult process control, unavailability of adequate models in process simulators or reliability of moving parts to sustain the cyclic operation. For this reason, it is absolutely crucial for industrial champions to lead by example and implement cyclic distillation while addressing the perceived and real issues associated with the technology. HP

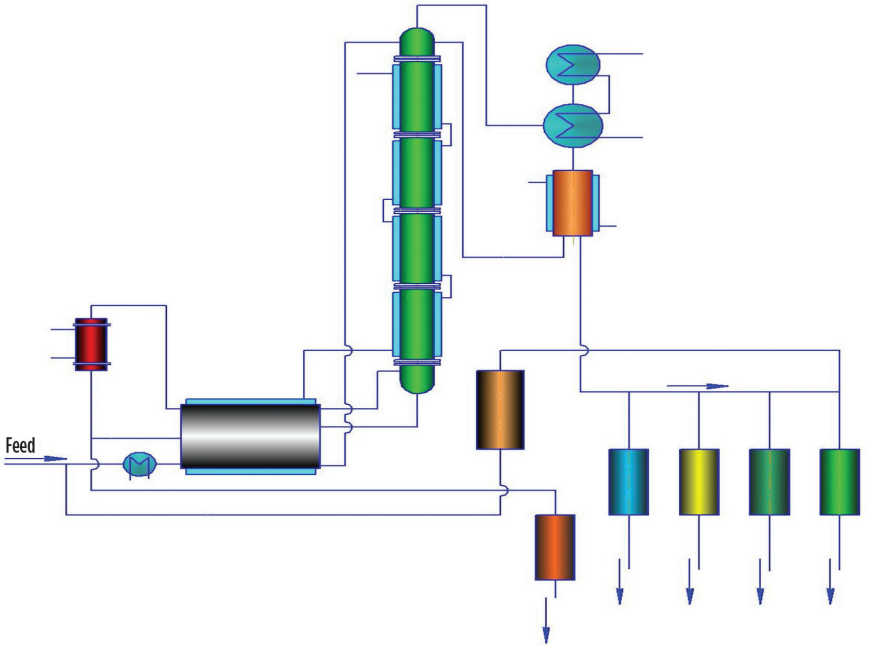

FIG. 11. Cyclic distillation column for refrigerants fractionation.

FIG. 12. Cyclic distillation column as part of a plant producing ethanol in the food industry (left), and two cyclic distillation dividing-wall columns installed for fractionation of kerosene (right).

ACKNOWLEDGMENTS

A. A. Kiss gratefully acknowledges the Royal Society Wolfson Research Merit Award.

LITERATURE CITED

Complete Literature Cited available online at www.HydrocarbonProcessing.com.

ANTON (TONY) A. KISS is a Professor and Chair in chemical engineering at the University of Manchester, a Royal Society Wolfson Research Merit Award holder, a Fellow of IChemE, a Senior Member of AIChE, and a Research Fellow of Royal Society. He has more than 20 yr of academic and industrial experience in a senior role, working for over a decade at AkzoNobel Chemicals. His main research areas cover process systems engineering, process intensification and separation technology. For his pioneering research work, he has received the prestigious prize Hoogewerff Jongerenprijs (The Netherlands), AkzoNobel Innovation Excellence Award (for most successful industrial innovation) and CHEMCON Distinguished Speaker Award for Innovators and Science Leaders (IIChE, New Delhi, India).

VLADIMIR N. MALETA is an entrepreneur who successfully developed and implemented new cyclic distillation technology in industry. He holds an MSc degree in mechanical engineering from the Kiev Institute of Food Industry and a PhD in engineering from the National University of Food Technologies in Ukraine. He started his own company (Maleta Cyclic Distillation LLC) and began implementing scientific developments in the Industry.

ALEKSANDR SHEVCHENKO is the Vice Rector for research and also the Head of the department of processes and apparatus of food production at the National University of Food Technologies in Kiev, Ukraine. His main research areas include developing technologies and equipment for long-term storage of food products, and energy-saving technologies for the beverage industry.

OLESJA BEDRYK holds an MS degree in technology of health and prophylactic products from the National University of Food Technology in Ukraine, and is a PhD student in the department of processes and apparatus of food production.

F. KETELAARS, DNV GL Oil and Gas, Houston, Texas

Hydrocarbons face toughest challenge yet

Over the next 30 yr, the globe's energy ecosystem—where fossil fuels dominate and renewables play catch-up—will evolve exponentially, as efforts intensify to curb carbon emissions and mitigate the detrimental impact of climate change.

In 2018, 81% of the world's energy was supplied by fossil fuels. By 2050, oil and gas will account for 54% of the world's primary energy supply, while non-fossil fuels will comprise 46%.

In DNV GL's latest energy outlook[1], the company forecasts a decarbonizing world in which energy demand plateaus, renewables grow significantly, natural gas becomes the world's largest energy source and oil demand never reaches the levels it saw in 2019.

Although the study predicts that, mid-century, there will still be demand for hydrocarbons, their role in the energy mix depend on how quickly diversification and significant carbon reductions can be achieved.

Changing energy demand. The outlook forecasts a single likely future of the world's energy system, not a range of scenarios. Slower growth in productivity and global population, along with continuous increases in energy efficiency, particularly in transport, will cause global energy demand to plateau by 2050—unlike the past 15 yr, where it increased by approximately 30%.

COVID-19 has played its part, as well. Before the pandemic, the author's company forecast total global energy demand in 2050 to be 456 exajoules (EJ). However, updated modeling shows that the pandemic will reduce energy demand by 8% to 2050—and this is nearly the exact level seen in 2018.

Oil demand will likely never fully recover from market shocks brought on by the COVID-19 pandemic. The outlook forecasts that global crude oil demand will decrease 13% in 2020, reaching a level not seen since the early 2000s. It will rebound somewhat to 2023, before gradually declining to half of its 2018 level by 2050 (FIG. 1).

However, while oil demand will decline rapidly in some regions, it will continue to increase in others. Therefore, continued investments in oil and gas will be needed to maintain production at the levels required to meet global demand, even in a declining market.

The decrease in oil demand will be led by the transportation sector. The decline will first be due to the electrification of passenger vehicles—followed by natural gas, decarbonized and green gas, and biofuels that are increasingly supplying the energy for ships, larger road vehicles and aviation. The Middle East, North Africa, Northeast Eurasia and North America will account for 90% of oil supply in 2050 and will be the only net exporting regions. This will be caused by a shift from producing "more oil" to "cheapest oil," and will put increasing pressure on unconventional onshore and offshore oil production to 2050.

As the least carbon-intensive fossil fuel, natural gas will play a prominent role in the energy transition, taking its place as the world's largest energy source as of the mid-2020s. Global gas demand will peak in the mid-2030s.

Multiple energy transitions. The outlook anticipates that rapid electrification of energy, along with growth in renewables, will significantly reduce emissions in the coming decades. Without greater efforts to remove and adapt to carbon-free operations, the world will miss the 2°C limit for global warming under the Paris Agreement. The analysis warns that the current 1.5°C carbon budget will be exhausted in 2028, with the 2°C budget exhausted in 2051. Extrapolating the emission trends, this points to a 2.3°C warming of the planet by 2100.

There will not be just one energy transition to 2050 but several transitions. These include transitions from fossil fuels to renewables, from coal and oil to natural gas and from fossil fuels to decarbonized gas.

Carbon emissions are expected to remain high until the mid-2030s, falling approximately 15% to 2035 before dropping 40% to 2050. The scaling of decarbonized natural gas, along with the enhanced use of green gas (which is produced using renewable sources), will be key contributors.

The growing awareness of the urgency and magnitude of the climate change challenge is increasing pressure on the oil and gas industry to decarbonize. Several major players have already set net-zero carbon targets and are shifting from being "big oil"

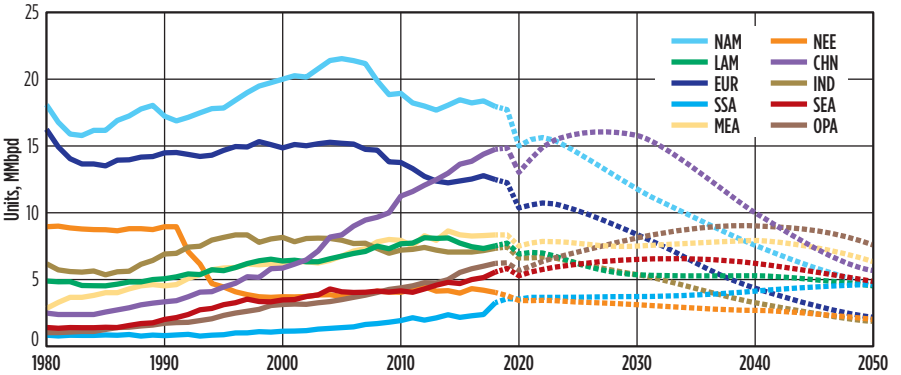

FIG. 1. Oil demand forecast, by region, to 2050.

to "big energy" companies with a broader and more diverse portfolio. Any delay in this transition may challenge the industry's license to operate in some regions. Therefore, longer-term success is dependent on proactively driving this transition rather than being a major carbon contributor. Key solutions include electrifying offshore platforms and oil and gas assets, reducing flaring and venting, increasing efforts to detect and stem methane leaks and obtaining efficiency gains through the digitalization of the oil and gas value chain.

A cleaner, greener energy mix. As the demand for natural gas declines from the mid-2030s, this outlook points to three pertinent predictions:

1. The amount of natural gas used for power generation will start to decrease as renewables scale significantly and electricity is increasingly used to replace natural gas in sectors where it is feasible to do so.
2. Natural gas will become partially decarbonized through gas reforming, with carbon capture and storage (CCS) to produce blue hydrogen, resulting in rapid growth toward 2050.
3. Hydrogen produced from renewables (i.e., green hydrogen) will join decarbonized gas in replacing some of the final demand for natural gas, largely in hard-to-abate sectors such as steel, cement, aluminum and glassmaking processes.

The outlook forecasts that 13% of natural gas will be decarbonized in 2050. This follows rapid growth in hydrogen production from natural gas, and of natural gas with CCS in power and industry sectors over the next 30 yr.

In terms of lowering the emissions of natural gas consumption, the forecast asserts that hydrogen—produced from fossil fuels with CCS and from renewables via electrolysis—will supply 23% of end-user demand for gas. Around half of this hydrogen will be produced from fossil fuels in 2050—with approximately 70% coming from natural gas. The other half will be produced from electricity derived from predominantly renewable sources. Both the decarbonization of natural gas through CCS and the use of hydrogen as a vector to reduce emissions from natural gas consumption will be led by Europe, China and North America, and by Pacific countries that are members of the Organization for Economic Co-operation and Development (OECD).

The transition to decarbonized and green gas, with related scaling of CCS and hydrogen, will not be quick enough to meet the goals set in the Paris Agreement, as neither CCS nor hydrogen processes will begin to scale for at least 15 yr. Although the technology is available and viable, the policy framework is only now just taking shape in selected regions. Governments must quickly incentivize industry to adopt these solutions to climate change (such as through a competitive carbon price), so that the cost-learning curve will become financially viable.

Proactive partnerships and policies are vital. Forming partnerships among government, industry and associations will be crucial in scaling innovation and new technologies for decarbonization. Public energy strategies are key, not just in setting out the path for the world and the oil and gas industry to reduce and remove carbon, but also in deciding how fast the world will reach that destination.

The outlook points to policies in Europe, China and North America to create the impetus for scaling hydrogen and other low-carbon fuels globally and to propel recognition that scaling CCS will be essential to meet climate targets. Such policies are influenced by the available energy resources and by societal pressures, which include rising concerns over climate change and calls for cleaner energy.

Some of these policies will affect demand for existing oil and gas products and will drive companies to reduce their carbon footprint—while other policies may completely transform the oil and gas industry. Ultimately, these policies could transform the oil and gas industry into being the decarbonizer of hydrocarbons and the supplier of CCS. The mid-2030s is estimated to be the point at which these policies will begin to act as a catalyst for this transformation.

All regions are balancing decarbonization with the need to ensure an increasing supply of secure and affordable energy. In Europe, net-zero targets have launched the region's energy transition, and these efforts are now being extended to hard-to-abate sectors. The European Union (EU) is also considering a CO_2 border tax that would extend a price on carbon to include imported products. Greater China's emissions reduction trajectory is also vital to the global energy transition. From 2030, the region will account for more than half of the world's net emissions reductions.

A patchwork of policy targets and incentives at state and federal levels in North America will drive decarbonization through increases in renewables and electrification, and, additionally, by lowering the carbon intensity of fuels. Policies in the Indian Subcontinent, Southeast Asia and Sub-Saharan Africa regions will largely focus on the transition from coal to natural gas, and on growth in renewables and electrification, thus ensuring the regions' increased energy independence and their ability to meet growing pressure to curb local pollution.

Urgent action required. Pressure is mounting on the oil and gas sector to address the climate change crisis. However, while the move to greener gas will help to significantly reduce emissions, the forecast doubts that this will have much of an impact on meeting the tough goals set out in the Paris Agreement.

Ultimately, realizing a brighter, greener future for the energy mix requires quicker transformation of the industry. Although leaders, innovators and regulatory bodies are making some headway in putting this energy transition at the top of their agendas, climate change and their ambitions to reduce it are outpacing action. The benefits of the energy transition are clear and achievable, with hydrogen and CCS complementing renewable electricity, advanced battery technology and alternative low-carbon fuels. HP

LITERATURE CITED

[1] DNV GL, "ENERGY TRANSITION OUTLOOK 2020—Oil and Gas Report: A Global and Regional Forecast to 2050," October 2020, https://eto.dnvgl.com/2020/oil-gas/

FRANK KETELAARS is the Director for Oil and Gas Operations for DNV GL in the Americas region. His responsibilities include oil and gas operations in the U.S., Canada, Mexico, Brazil, and Trinidad and Tobago. His experience covers verification and advisory work for offshore and onshore operations, with a focus on safety and regulatory compliance, integrity management and performance improvement. Mr. Ketelaars earned an MSc degree in electrical engineering from the Delft University of Technology in the Netherlands.

K. K. MANDAL, Nayara Energy Ltd.,
Vadinar, Gujarat, India

Search for advanced technique of desalter control–TON control for interface level

While it may seem like a simple vessel, the desalter is a critical section in a crude distillation unit. Its purpose is to remove salt and impurities from the crude oil. Improving desalter performance will increase reliability of the downstream equipment, as well as secondary units. Most crude available in today's market is heavy and tough in nature, so the removal of salt and impurities from crude oil, the reduction of oil carryover and brine pose significant challenges.

Several articles are available that offer valuable suggestions and best practices about desalter operations, as well as operational variables, including chemical treatment/dosing. However, very little literature is available on interface level control, how it can help to improve desalter performance with respect to oil carryover along with brine, and the maximization of wash water flow for the reduction of salt. Advance process control (APC) systems are available for almost all process units and working well for quality prediction and process parameter correction.[1] This is not very effective for desalter interface level control, as well as crude blend change (i.e., crude switch over).

The desalter is a closed vessel operating with pressurized condition at a temperature of 140°C–145°C (284°F–293°F) and an operating pressure of 10 kg/cm^2–15 kg/cm^2. Crude enters the desalter vessel after preheating and mixing with wash water (approximately 4%–7%). This water-mixed crude oil is settled and gravity separated in the vessel with a residence time of about 15 min–20 min. One mixing valve is provided after the wash water injection to improve the mixing of the water with crude oil, and a 0.25 kg/cm^2–1 kg/cm^2 differential pressure is maintained. An electric field is used to encourage water separation inside the desalter vessel. Interface level indication for monitoring and control was provided through an interface level measurement instrument and a control valve. The desalter can be a single-stage or two-stage type—some refineries are also installing three-stage desalters. Details of single-stage desalter arrangement are given in FIG. 1.

Analysis on desalter operation. For desalter performance analysis, interface level indications, control valve openings, brine flow and wash water flow trends were considered for 1st and 2nd stage for 8 hr of operation. Typical level trends of a desalter interface level, control valve opening and flow indication trend are shown for better understanding (FIG. 2). As seen from the trend, the interface level and flow are both fluctuating steadily for both stages with steady wash water flow. Interface level fluctuation is seen more in the 1st stage compared to the 2nd stage.

Interface level control and interface control are discussed here to understand water balance/material balance of the desalter system. Water balance is basically water input along with crude oil and can be estimated based on basic sediment and water (BS&W) and wash water, and water output will be water content along with post desalter crude oil and brine flow. Theoretically, some increase in brine flow is seen as extra water content in crude oil will come out along with the brine. The desired operational requirement is that brine flow should remain steady; in turn, crude flow from the ex-desalter will remain steady.

Desalter interface level control arrangement. The desalter interface level control valve operates based on the interface level indication in LC control mode [normal distributed control system (DCS)/proportional integral derivative (PID) control]. This control system operates on input and feedback, so

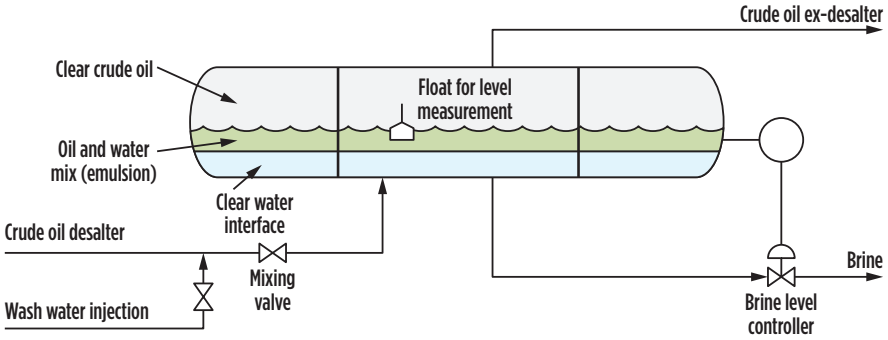

FIG. 1. Typical single-stage desalter configuration with mixing valve and water injection.

a continuous fluctuation can be noticed in any level control system. The desalter is a large vessel; for a small variation in level, the flow variation is large.

As seen in FIG. 2, both the trend level and flow are fluctuating steadily, although the level fluctuation is low and the flow fluctuation level is very high, indicating that the brine flow can be low or high. It is also observed that during very high brine flow, oil carryover along with brine increases, and during low brine flow watercarry over along with crude increases.

In the present scenario, crude quality is getting worse due to challenges in the market for low-cost, high-TAN, high-sulfur crude. The TON control is ideal for achieving maximum efficiency in desalter performance and is beneficial in any interface level and surge vessel level control for steady downstream flow.

Another problem faced during crude blend changeover is a sudden increase or decrease in interface level due to a change in density of the crude oil, or a change in water content along with the crude. Due to the abnormal behavior of the interface level indication and C/V opening variation, large water carryover along with post desalter crude oil is sometimes observed, resulting in post-desalter PSV popping and water carryover to the overhead section, which leads to a total disturbance in the fractionator column. Similar behavior can also be noticed during the processing of slop oil in the crude unit.

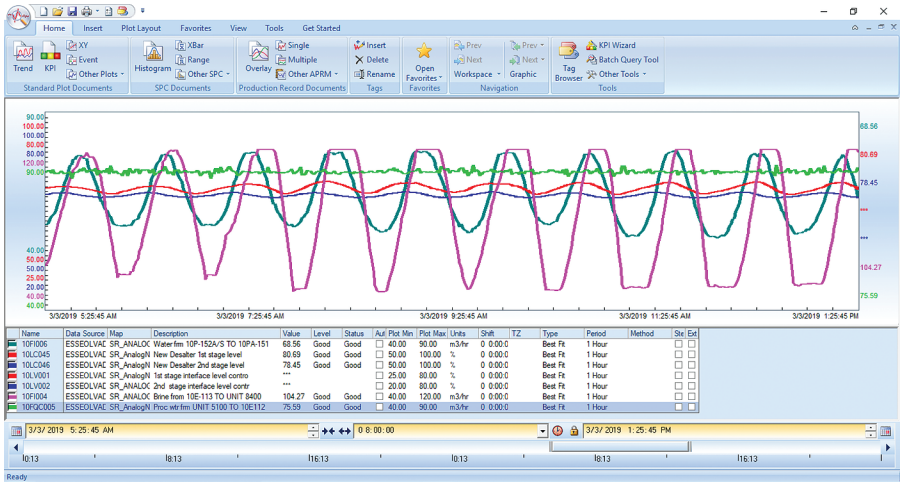

FIG. 2. Desalter 1st- and 2nd-stage interface level and brine flow trend with wash water flow in normal operation.

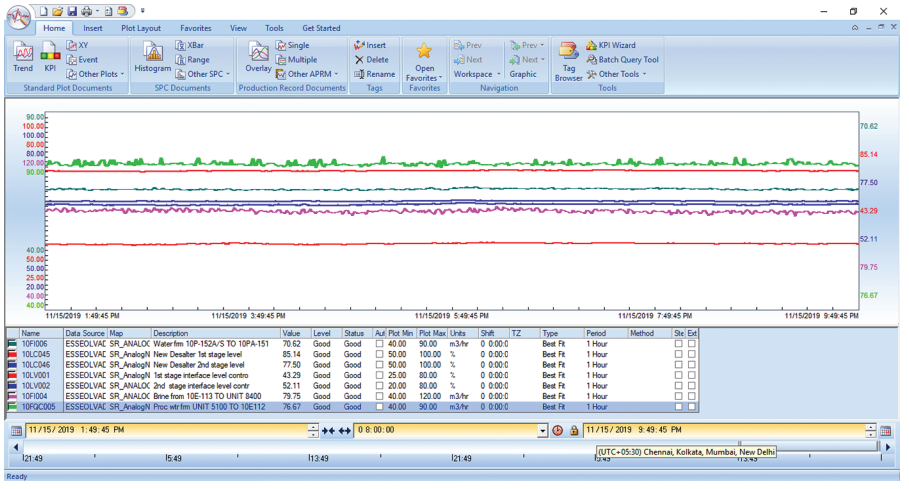

FIG. 3. Desalter 1st- and 2nd-stage interface level and brine flow trend with process water flow after implementation of TON control.

Reduction in brine flow fluctuation. To avoid flow fluctuation of brine and the interface level control valve, the minimum opening (manipulated value) must be locked so that minimum brine flow will be restricted closer to the theoretical brine generation. The theoretical brine generation will be:

process water flow + differential BS&W % in crude (crude inlet-outlet BS&W) × crude flow to desalter + % of water content in slop oil × slop oil flow.

It is observed that BS&W in crude oil and water content in slop oil remains almost steady until the tank/blend is changed. This idea was working with reduced brine flow fluctuations, but required a lot of attention by the panel officer, particularly during crude changeover and slop oil tank change. This idea was accepted by the operating crew members but was unpopular in the long run due to the attention it required.

Use of APC. To avoid human interference, assistance was provided by the existing crude unit APC. Here, brine flow was fixed based on the previously mentioned brine estimation and the wash water flow was kept as a variable parameter in APC mode, which will manipulate the

wash water flow and maintain a 1st-stage interface level. Initially, APC became very popular with the desalter operators. As process water flow was being adjusted with the change of crude blend and change of slop oil processing tank and flow, the idea of wash water manipulation became a discussion point as process water flow was reduced or increased due to changes in the water content in crude oil or slop oil. However, with the performance of the desalter interface level with wash water flow control in APC mode, the brine flow remains absolutely steady, with a slight variation in wash water flow.

Implementation of target opening non-linear (TON) control. Avoid operating parameter adjustment by operators, such as the manipulation of level control valve opening locking based on brine flow estimation, or by APC for wash water flow adjustment. Both options were working better than normal but were not accepted by operation crew members. A new idea was identified and subsequently implemented for interface level control: TON control, which works based on level differences (set level and actual level) with a correlation:[2]

The calculated output to the interface level control valve = (Actual level – set level) × *M* + target output.

The configuration of control logic can be selected as: 1) for normal DCS mode, or 2) for TON control mode. This modification can be carried out in the DCS with the help of an instrumentation engineer. Apart from the selection of DCS or TON, three fields exist in the DCS: target output, level setpoint and factor *M*. The target output of the interface level control is basically the control valve opening at which the estimated brine flow is achieved. The level setpoint is the desired interface level to be maintained—the actual level indication value will be taken from the DCS. *M* is a factor to be set once as a system requirement; usually it will vary from 1–2.5.

Performance and benefit achieved. The performance trend after the implementation of TON control, the interface level and flow trend are shown in **FIG. 3.** It can be seen during 8 hr of operation that the interface level, control valve opening and brine flow are steady. With this steady brine flow, the following benefits were achieved:

- No water carryover along with the crude, and no water surge during blend changeover
- Steady brine flow, resulting in reductions in oil carryover along with the brine
- With little to no interface level control valve fluctuation, crude flow ex desalter remained steady
- Steady desalter current and no desalter transformer tripping due to high current, even during blend change.

Crude unit blend/crude changeover is a common process and is done every 2 d–3 d. During each blend changeover, the desalter gets disturbed due to changes in API, BS&W and free water content (bottom portion crude tank). It is observed during blend changeover that brine flow varies abnormally, resulting in water carryover along with crude during low brine flow; oil carry will be high during high brine flow. In the case of TON control, the brine flow variation will be very low and post desalter crude flow and brine flow will remains almost steady, resulting in no disturbance during blend changeover. Only minor variations in the interface level, control valve opening and brine flow were noticed during the blend changeover period. TON control also works well during abnormal water content in crude oil/crude oil tank, as shown in **FIG. 4.** Here, only one action was taken by the operator: the reduction of process water, as brine flow was increasing at a faster rate due to very high water content in the crude oil.

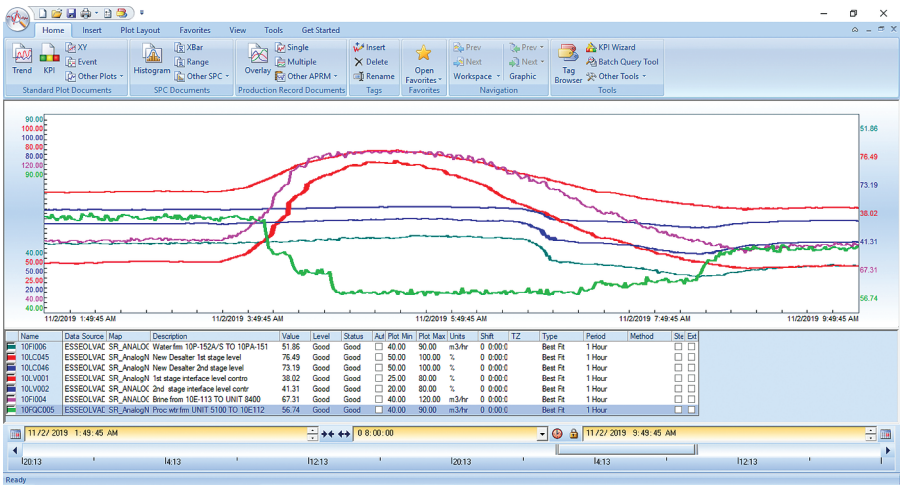

FIG. 4. Desalter 1st- and 2nd-stage interface level, valve opening and brine flow trend with wash water flow during blend changeover with TON control with abnormal water contentment along with crude oil.

Takeaway. With the challenges presented by a market for low-cost, high-TAN, high-sulfur crude, the desalter must operate with maximum efficiency. TON control is a viable solution for efficient interface level control and improved desalter performance. The cost for this modification is minimal and it can be performed easily within the DCS. This modification has been implemented in three sets of two-stage desalters of Nayara Energy Ltd. at Vadinar, Gujarat, with varying crude flow capacities of 350 m^3/hr–1,500 m^3/hr, and all are working exceptionally well on a continuous basis. HP

LITERATURE CITED

[1] Mandal, K. K., "New level control techniques," *Hydrocarbon Processing*, October 2004.
[2] Mandal, K., "Improve desalter control," *Hydrocarbon Processing*, February 2005.

KISHORE KUMAR MANDAL is a Technical Consultant for Nayara Energy Ltd., in Vadinar, India, after retirement from Indian Oil Corp. as General Manager (TS) of the Panipat Refinery, Panipat, India. He has worked on different refinery units, including atmospheric vacuum distillation, FCC, DHDT and hydrocracker units. Mr. Mandal has carried out assignments in commissioning, operations, technical services and projects. He has worked for Indian Oil Corp. for 36 yr. Mr. Mandal obtained his B.Tech (honors) degree in chemical engineering from IIT, Kharagpur, India.

J. COLANNINO, Contributing Editor,
San Diego, California

Optimize processes with a spreadsheet

Hydrocarbon processing industry (HPI)/continuous process improvement (CPI) processes are often characterized by complicated kinetics and simultaneous heat and mass transfer. Often, a significant amount of simulation science has gone into setting operating conditions with process control loops tuned for best results. However, natural feedstocks have inherent variability and even ambient conditions, such as temperature, humidity and barometric pressure, can affect product results. Moreover, start-of-run to end-of-run conditions often require process adjustments. Once initial process conditions have been set, can one hope to wring out additional improvement?

The answer is almost always, "Yes," but operators know that they must always produce on-spec product. One method of achieving process improvement under these constraints is known as evolutionary operation (EVOP)[1,2], which makes small adjustments to known process variables to keep the process in-spec, while gathering information to move toward their optimal combination. These principles have wide applicability to virtually any process, including optimizing pollution control equipment or the production of chemical or hydrocarbon products. This article will show how to enable EVOP using a spreadsheet program, such as Excel.

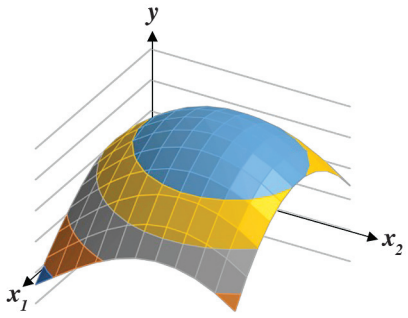

FIG. 1. Hypothetical response surface in two factors. Although depicted here for illustration, this function is not usually known, but can only be observed after contamination with random error (see **FIG. 2**).

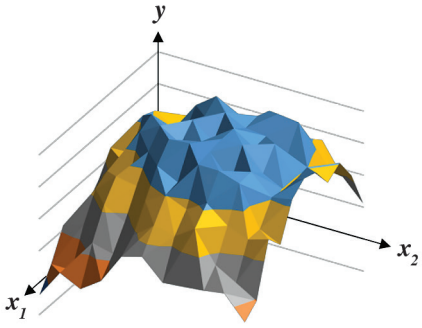

FIG. 2. Observed response surface in two factors, $y(x_1, x_2)$. This is the function of **FIG. 1** after contamination with significant random process noise (i.e., random error).

The use of approximating functions.

FIG. 1 shows a generic response surface derived from a highly non-linear expression as a function of two factors for illustrative purposes. However, in principle, any number of responses of interest and as many factors are possible. Multiple response factors may be assessed individually or combined in a weighted model to create a single process score, which then functions as the response surface to be optimized.

Nonlinear equations—or even systems of them—are typical for many processes. Rather than attempt to elucidate the true function, statistical experimental design (SED) fits a mathematical approximating function ($\hat{y}$), such as Eq. 1:

$$\hat{y} = c_0 + c_1x_1 + c_2x_2 + c_{11}x_1^2 + c_{12}x_1x_2 + c_{22}x_2^2 \quad (1)$$

Here, c_0–c_{22} are regressed coefficients. The observed responses we measure (y) will then be given by Eq. 2:

$$y = \hat{y} + \varepsilon \quad (2)$$

where ε is the error between Eq. 1 and the observed response. The error (ε) cumulates all other variation from the sources that we cannot control (or that we may not even know about), but which nonetheless affect the response in some way. Despite this, the regression can recover a good approximation to the true function. **FIG. 2** depicts actual observations, including random error. Despite significant noise, the regressed approximating function (**FIG. 3**) is nearly indistinguishable from the true function of **FIG. 1**. Considering how contaminated the original data were, the approximation is remarkable.

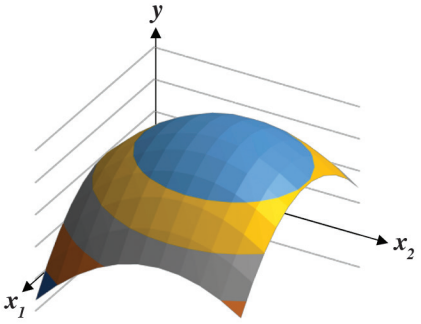

FIG. 3. Regressed response surface in two factors, $\hat{y}(x_1, x_2)$. This is the empirical surface fitted by Eq. 1 to the data comprising **FIG. 2.** The fitted surface is a good approximation to the true surface (**FIG. 1**), despite significant process noise.

The method of steepest ascent.

The genius of EVOP is that we do not need a full picture of the response surface to

move toward its optimum. We only need to know the local landscape and to perturb the process by baby steps. In such a case, a linear model such as Eq. 3 is adequate:

$$y = c_0 + c_1x_1 + c_2x_2 + \varepsilon \quad (3)$$

where c_0–c_2 are regressed coefficients. If we are ascending the response surface, we expect the partial derivatives to decrease if the surface flattens to a maximum. Thus, the direction of steepest ascent is always given by the negative of the partial derivatives, which for Eq. 3 becomes Eq. 4:

$$-\frac{\partial y}{\partial x_1} = -c_1 \text{ and } -\frac{\partial y}{\partial x_2} = -c_2 \quad (4)$$

These define a direction vector – $(c_1 \quad c_2)$, which we normalize to a unit vector via Eq. 5:

$$\left\| c_1^* \quad c_2^* \right\| = -\frac{(c_1 \quad c_2)}{\sqrt{c_1^2 + c_2^2}} \quad (5)$$

This gives us our step size and direction for the next point in our path of steepest ascent (FIG. 4). We interrogate the factor space at this new design center, calculate a new $\|c_1^* \quad c_2^*\|$ vector, and reiterate to make incremental progress to our goal[3,4] (FIG. 5). With small steps, a real danger exists that the difference in response will be small and overwhelmed by process noise. Replicate measurements subject to all of the normal process uncertainty (so-called *genuine replicates*) will increase the information-to-noise ratio, average out the process noise and allow statistical tests for each coefficient.

Deriving a steepest ascent. We shall construct our steepest ascent by reiterating the following sequence:

1. Decide on an acceptable step size for each factor
2. Generate candidate coordinates in factor space
3. Collect response data for each coordinate
4. Test for significance.

If the coefficients are statistically significant, we calculate the path of steepest ascent and go on to collect additional data at a new design center. If not, we run more replicates to increase the information-to-noise ratio. Consider an example here.

Example: Calculation of steepest ascent. Suppose an important process yield responds to temperature and pressure, that the standard operating parameters (SOP) are 300°C and 500 kPa, and that incremental variations of each factor are limited to no more than ±5°C and ±10 kPa. To these, we apply the transforms (Eq. 6):

$$x_1 = \frac{T[°C] - 300[°C]}{5[°C]}, \qquad x_2 = \frac{P[kPa] - 5[kPa]}{10[kPa]} \quad (6)$$

These do nothing more than scale 300 ±5 (°C) and 500 ±10 (kPa) to dimensionless unit ranges of ±1. Scaling process parameters to a dimensionless unit range simplifies some statistical calculations, but otherwise has no effect on the analysis.

These transforms define a unit square in x_1-by-x_2 factor space (FIG. 6). The design center (0,0) is shown in FIG. 6 as p_1 and represents the current SOP. We now must decide on where to collect new data.

Logical design candidates include points at the extremes of our permissible ranges (indicated as points s_1 to s_4 in FIG. 6). Such designs are known as *factorial designs*. For example, in three dimensions, x_1 by x_2 by x_3 would define a unit cube. In higher dimensions, the space is known as a unit *hypercube*. The number of required design points (n_d) in a factorial design is given by $n_d = 2^{nf}$, where n_f is the number of factors.

Therefore, for the two factors we consider in this example (x_1 and x_2), $n_d = 2^2 = 4$ design points (s_1 to s_4 in FIG. 6) plus any center points (e.g., p_1) we choose to run. Factorial designs are convenient and often used. However, if we have numerous factors, we may quickly exceed our resources. For example, a factorial design in five factors requires 32 points, not including replicates or center points. To overcome this limitation, one may use other designs (e.g., *fractional-factorial* or *simplex designs*)[5]. However, for the limited number of factors here, a factorial design is sufficient and we shall proceed on this basis.

Since our step size is deliberately small and our process is noisy, we must repeat some points to better estimate the true response value. We can replicate the entire design multiple times, but in this case, we will just replicate the center

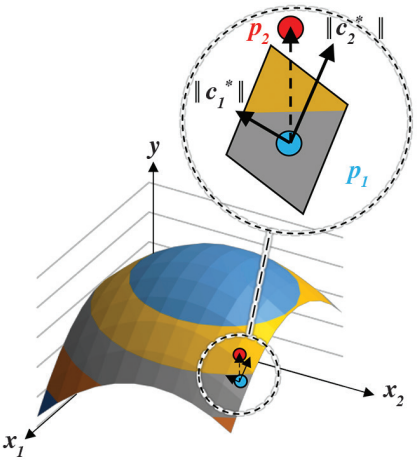

FIG. 4. Method of steepest ascent. Only the local landscape of the response surface is needed (large, dotted circle) to determine the vectors of Eq. 5 and the direction of steepest ascent (p_1 to p_2).

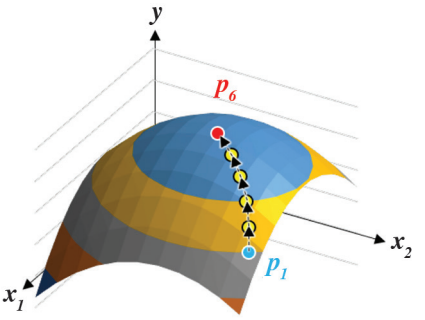

FIG. 5. Steps on a path of steepest ascent. Applying the FIG. 4 process in seriatim constructs a path of steepest ascent bit by bit (e.g., from p_1 to p_6).

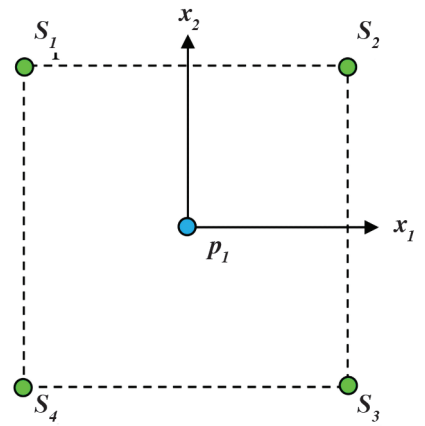

FIG. 6. Factor space. Unit extensions in x_1 by x_2 factor space define a unit square.

point; since the center point of the design represents the current SOP, operators will have no discomfort returning to this point multiple times in the investigation. TABLE 1 gives such a design with sample data. The points s_1 through s_4 are run in random order interspersed with repeated interrogations of p_1 to ensure that the replicates are genuine.

In TABLE 1, the response varies for each center-point replicate due to process noise. If the noise is excessive, it may indicate that we have not taken account of all factors, that our step size is too small, or that other issues with equipment or operation should be corrected. Statistical tests (described presently) will assess this formally.

Our task is to construct an empirical model to correlate the data over the factor ranges. In general, factorial designs support models of the form (Eq. 7):

$$\hat{y} = \alpha_0 + \sum_{k=1}^{n_f} \alpha_k x_k + \sum_{j<k}^{n_f-1} \sum_{k=1}^{n_f} \alpha_{jk} x_j x_k \quad (7)$$

Here, a_0 to a_{jk} are coefficients to be determined, n_f is the number of factors under consideration, and j and k are indices for the summation operator. In our case, $n_f = 2$ and our model reduces to (Eq. 8):

$$\hat{y} = c_0 + c_1 x_1 + c_2 x_2 + c_{12} x_1 x_2 \quad (8)$$

The term $c_{12}x_1x_2$ accounts for interactions (synergy or moderation) between the factors, if they exist. For the small steps taken in EVOP, interactions are unlikely. We test for them, nonetheless.

The method of least squares. According to Eq. 8 and TABLE 1, nine observations must be accounted for (Eq. 9):

$$\begin{aligned} y_1 \quad & c_0 + c_1 x_{1,1} + c_2 x_{2,1} + c_{12} x_{1,1} x_{2,1} + \varepsilon_1 \\ y_2 \quad & c_0 + c_1 x_{1,2} + c_2 x_{2,2} + c_{12} x_{1,2} x_{2,2} + \varepsilon_2 \\ \vdots \quad & \qquad\qquad \vdots \\ y_9 \quad & c_0 + c_1 x_{1,9} + c_2 x_{2,9} + c_{12} x_{1,9} x_{2,9} + \varepsilon_9 \end{aligned} \quad (9)$$

where the second subscript indicates the associated run number of each observation. The same system of equations may be put in matrix form as shown in Eq. 10:

$$\begin{pmatrix} y_1 \\ y_2 \\ \vdots \\ y_9 \end{pmatrix} = \begin{pmatrix} 1 & x_{1,1} & x_{2,1} & x_{1,1}x_{2,1} \\ 1 & x_{1,2} & x_{2,2} & x_{1,2}x_{2,2} \\ \vdots & \vdots & \vdots & \vdots \\ 1 & x_{1,9} & x_{2,9} & x_{1,9}x_{2,9} \end{pmatrix} \begin{pmatrix} c_0 \\ c_1 \\ c_2 \\ c_{12} \end{pmatrix} + \begin{pmatrix} \varepsilon_0 \\ \varepsilon_1 \\ \vdots \\ \varepsilon_9 \end{pmatrix} \quad (10)$$

or more simply (Eq. 11):

$$\mathbf{y} = \boldsymbol{X}\boldsymbol{c} + \boldsymbol{\varepsilon} \quad (11)$$

Here, the bolded lower-case letters refer to the respective column vectors of Eq. 10, and X refers to the matrix of factors that has both rows and columns (i.e., Eqs. 9, 10 and 11 are all equivalent expressions). The values for the coefficients ($\mathbf{c}$) must now be determined. If we presume that the errors of Eq. 9 are normally distributed, the best method for fitting the coefficients is to minimize the sum of the squared errors (ε). For equations of the form (Eq. 11), least squares reduces to the following matrix equation (Eq. 12):

$$X^T y = (X^T X) c \quad (12)$$

where T indicates the transpose operator (which swaps the rows and columns of $\boldsymbol{X}$).

Excel implements the transpose with the function = TRANSPOSE ($\mathbf{y}$) where $\mathbf{y}$ is the column vector holding the responses in Excel and X is the matrix in Eq. 10. In fact, $\boldsymbol{X}^T\boldsymbol{X}$ is an n_c-by-n_c square matrix, where n_c is the number of coefficients. For Eq. 9, which has four coefficients, $\boldsymbol{X}$ is a 4-by-4 matrix. To find $\mathbf{c}$, we need only pre-multiply by the inverse of $\boldsymbol{X}^T\boldsymbol{X}$, denoted as $(\boldsymbol{X}^T\boldsymbol{X})^{-1}$. This is implemented in Excel using = MINVERSE (M) where M is a square matrix. This provides Eq. 13:

$$\mathbf{c} = (\boldsymbol{X}^T\boldsymbol{X})^{-1}(\boldsymbol{X}^T\boldsymbol{y}) \quad (13)$$

We may now calculate $\hat{\boldsymbol{y}} = \boldsymbol{X}\boldsymbol{\alpha}$ using the Excel formula = MMULT (X,c). FIG. 7 shows the spreadsheet and all of the calculations up to this point, along with a calculation legend that details every formula.

The columns $\mathbf{y}_r$ and $\bar{\mathbf{y}}$ will become important when statistical significance is

TABLE 1. The run number gives the sequential order in which the points were run; the next column shows the label of the point (see FIG. 6); the x_1 and x_2 columns hold the factor coordinates for each point; the y column holds the response in the form of a yield index (higher is better)

Run	Point	x_1	x_2	y	Run	Point	x_1	x_2	y
1	p_1	0	0	165	6	s_2	1	1	144
2	s_3	1	–1	118	7	p_1	0	0	152
3	p_1	0	0	162	8	s_1	–1	1	203
4	s_4	–1	–1	172	9	p_1	0	0	161
5	p_1	0	0	161					

	A	B	C	D	E	F	G	H	I	J	K	L	M	N
1	Run	y	ŷ	y_r	$\bar{y}$	0	1	2	12	XTX				XTy
2	1	165	160	160	160	1	0	0	0	9	0	0	0	1438
3	2	118	119	118	160	1	1	-1	-1	0	4	0	0	113
4	3	162	160	160	160	1	0	0	0	0	0	4	0	-57
5	4	144	145	144	160	1	1	1	1	0	0	0	4	-5
6	5	161	160	160	160	1	0	0	0	$(X^TX)^{-1}$				c
7	6	203	204	203	160	1	-1	1	-1	0.111	0	0	0	159.8
8	7	152	160	160	160	1	0	0	0	0	0.25	0	0	-28.3
9	8	172	173	172	160	1	-1	-1	1	0	0	0.25	0	14.3
10	9	161	160	160	160	1	0	0	0	0	0	0	0.25	-1.3
11	CALCULATION LEGEND													
12	X^TX: = MMULT(TRANSPOSE(F2:I10),F2:I10)									X^Ty: = MMULT(TRANSPOSE(F2:I10),B2:B10)				
13	$(X^TX)^{-1}$: = MINVERSE(J2:M5)									c = $(X^TX)^{-1}X^Ty$: = MMULT(S7:V10,W2:W5)				
14	ŷ = Xa: = MMULT(F2:I10,W7:W10)					y_r: = AVERAGE(B2,B4,B6,B8,B10)				$\bar{y}$: = AVERAGE (B2 .B10)				

FIG. 7. Spreadsheet sample: the spreadsheet shows the values and results of the Excel calculations

TABLE 2. General analysis of variance (ANOVA): the table provides a convenient consolidation of statistical properties for the data set

Term	SS	DF	MS	F	p
M	4,011	3	1,337	69.05	0.0002
R	97	5	19	s:	4.4
T	4,108	8		R^2:	0.9764

assessed: $\mathbf{y_r}$ holds the averages for replicate observations. In the case of a single observation, the value of the replicate mean and the observation are identical. In the case of multiple interrogations of the same point in factor space, the replicate mean is their average. The column labeled $\bar{\mathbf{y}}$ holds the grand mean—the average of all measured responses. The columns labeled *0, 1, 2* and *12* hold the data of the $\boldsymbol{X}$ matrix in Eq. 10.

Tests for statistical significance. To test for statistical significance, begin by constructing a general analysis of variance (ANOVA) table (**TABLE 2**). For now, note that the sum of squares for the model (M) is SSM = 4,011, and that of the residual error (R) is SSR = 97. SSM + SSR give a total (T), SST = 4,108. We divide SSM and SSR by their respective degrees of freedom (DFM = 3, DFR = 5) to arrive at their mean squares (MSM = 1337, MSR = 19). The ratio of MSM/MSR = F = 69.05 shows that the variance of the model is nearly 70 times that of the residual error. Because p = 0.0002, we have a 0.02% chance that our model does not contain statistically significant coefficients; conversely, we have 99.98% confidence that our model is statistically significant. Generally, anything above 95% confidence will be sufficient (i.e., $p \le 0.05$). **FIG. 8** shows the updated spreadsheet with all the statistical tests in place and how each calculation was derived. In addition to the General ANOVA of **TABLE 2,** and a more detailed one is shown in **FIG. 8** along with standard errors (SE) for each coefficient. The degrees of freedom are found by Eqs. 13, 14 and 15:

$$\text{DFM} = n_c - 1 \quad (13)$$

$$\text{DFR} = n - n_c \quad (14)$$

$$\text{DFT} = n - 1 \quad (15)$$

Here, n_c is the number of coefficients of the model being fit, and n is the number of observations used to fit the coefficients.

In the detailed ANOVA (J11 to O18 in **FIG. 8**), the general ANOVA has been expanded. For example, SSM is parsed to reveal each individual component comprising its sum ($SSc_1 + SSc_2 + SSc_{12}$ = SSM) and SSR has been parsed into components for bias (B, a.k.a. *lack of fit*) and pure error (B). The coefficient c_0 is not included in the detailed ANOVA because SSM is the squared difference from the mean ($\bar{\mathbf{y}}$) and not the mean itself, and c0 is equivalent to the mean, i.e., $c_0 = \bar{y}$.

SSB and SSE are calculated using Eqs. 16–19:

$$\mathbf{SSB} = \mathbf{y_r}^T\mathbf{y_r} - \hat{\mathbf{y}}^T\hat{\mathbf{y}} \quad (16)$$

$$\mathbf{SSE} = \mathbf{y}^T\mathbf{y} - \mathbf{y_r}^T\mathbf{y_r} \quad (17)$$

and

$$\text{DFB} = n_u - n_c \quad (18)$$

$$\text{DFE} = n - n_u \quad (19)$$

Here, n_u corresponds to the number of unique design points, which in this case is 5 (p_1, and s_1–s_4). For factorial designs of this sort, the sum of squares for each component of the model is given Eq. 20:

$$\mathbf{SSc_k} = \mathbf{c_k} \times \mathbf{X}^T\mathbf{y}\big|_k \quad (20)$$

where $\mathbf{X}^T\mathbf{y}\big|_k$ indicates the kth element of the $\mathbf{X}^T\mathbf{y}$ vector (see the calculation legend of **FIG. 7**).

In this analysis, c_{12} is obviously not significant because it does not even exceed its standard error. This latter point may also be seen by individual F-tests on the coefficients, all of which are significant with the exception of the interaction term c_{12} (p = 0.635 >> 0.05). Since no significant interaction is indicated, a purely linear model is adequate to correlate the data. The F-tests also show that no significant bias exists (p = 0.786 >> 0.05), thus the linear approximation appears adequate to gauge the next step on the path of steepest ascent. In fact, assessing the bias separately from the error leads to a difference in the estimate of s (±4.4 vs. ±4.9, see cells I17 vs. O17 in **FIG. 8,** respectively). Because there is no significant bias, SSR is the probably the better basis since it has more degrees of freedom with which to estimate s; however, the model coefficients are significant using either value.

	A	B	C	D	E	F	G	H	I	J	K	L	M	N	O	P	Q
1	Run	y	ŷ	y_r	ȳ	0	1	2	12	XTX				XTy			
2	1	165	160	160	160	1	0	0	0	9	0	0	0	1438			
3	2	118	119	118	160	1	1	-1	-1	0	4	0	0	-113			
4	3	162	160	160	160	1	0	0	0	0	0	4	0	57			
5	4	144	145	144	160	1	1	1	1	0	0	0	4	-5			
6	5	161	160	160	160	1	0	0	0	XTX				c	±	SE	
7	6	203	204	203	160	1	-1	1	-1	0	0	0	0	159.8	±	0.7	
8	7	152	160	160	160	1	0	0	0	0	0.25	0	0	-28.3	±	1.0	
9	8	172	173	172	160	1	-1	-1	1	0	0	0.25	0	14.3	±	1.0	
10	9	161	160	160	160	1	0	0	0	0	0	0	0.25	-1.3	±	1.0	
11				General ANOVA						Detailed ANOVA							
12				Term	SS	DF	MS	F	p	Term	SS	DF	MS	F	p		
13				M	4011	3	1337	69.05	2E-04	c_1	3192	1	3192	134.7	3E-04	*	
14										c_2	812	1	812	34.27	0.004	*	
15										c_{12}	6	1	6	0.264	0.635		
16				R	97	5	19			B	2	1	2	0.085	0.786		
17								s:	4.4	E	95	4	24	s	4.9		
18				T	4108	8		R^2:	0.976	T	4108	8		R^2	0.976		
19	CALCULATION LEGEND																
20	$\mathbf{X}^T\mathbf{X}$: =MMULT(TRANSPOSE(F2:I10),F2:I10) $\mathbf{X}^T\mathbf{y}$: =MMULT(TRANSPOSE(F2:I10),B2:B10)																
21	$(\mathbf{X}^T\mathbf{X})^{-1}$: =MINVERSE(J2:M5)						c: =MMULT(S7:V10,W2:W5)			ȳ: =AVERAGE(B2.B10)							
22	ŷ: =MMULT(F2:I10,W7:W10)						$\mathbf{y_r}$: =AVERAGE(B2,B4,B6,B8,B10)										
23	SE_0: =SQRT(L22*J7)				SE_1: =SQRT(L22*K8)			SE_2: =SQRT(L22*L9)				SE_{12}: =SQRT(L22*M10)					
24	SSM = $\hat{\mathbf{y}}^T\hat{\mathbf{y}} - \bar{\mathbf{y}}^T\bar{\mathbf{y}}$: =MMULT(TRANSPOSE(C2:C10),C2:C10)-MMULT(TRANSPOSE(E2:E10),E2:E10)																
25	SSR = $\mathbf{y}^T\mathbf{y} - \hat{\mathbf{y}}^T\hat{\mathbf{y}}$: =MMULT(TRANSPOSE(B2:B10),B2:B10)-MMULT(TRANSPOSE(C2:C10),C2:C10)													$SSc_k = \mathbf{X}^T\mathbf{y}\big\|_k$			
26	SST= $\mathbf{y}^T\mathbf{y} - \bar{\mathbf{y}}^T\bar{\mathbf{y}}$: =MMULT(TRANSPOSE(B2:B10),B2:B10)-MMULT(TRANSPOSE(E2:E10),E2:E10)													SSc_0=N3*N8			
27	SSB = $\mathbf{y_r}^T\mathbf{y_r} - \hat{\mathbf{y}}^T\hat{\mathbf{y}}$: =MMULT(TRANSPOSE(D2:D10),D2:D10)-MMULT(TRANSPOSE(C2:C10),C2:C10)													SSc_1=N4*N9			
28	SSE = $\mathbf{y}^T\mathbf{y} - \mathbf{y_r}^T\mathbf{y_r}$: =MMULT(TRANSPOSE(B2:B10),B2:B10)-MMULT(TRANSPOSE(D2:D10),D2:D10)													SSc_{12}=N5*N10			
29	SST = $\mathbf{y}^T\mathbf{y} - \bar{\mathbf{y}}^T\bar{\mathbf{y}}$: =MMULT(TRANSPOSE(B2:B10),B2:B10)-MMULT(TRANSPOSE(E2:E10),E2:E10)																

FIG. 8. Sample of updated spreadsheet. The updated spreadsheet now includes a more detailed ANOVA and the calculations callout has been expanded to include the new entries.

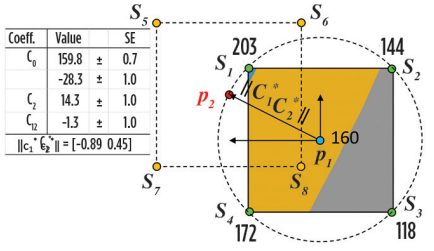

FIG. 9. From p_1 to p_2. The next center of exploration (p_2) on the path of steepest ascent is given in factor space by the coordinates $\|c_1^* \;\; c_2^*\|$ as measured from the old design center (p_1).

Now is the time to calculate the next point on the journey to higher yield. TABLE 2 depicts this process. From the c_1 and c_2 coefficients, the direction of steepest ascent is calculated per Eq. 5, i.e., from p_1 to p_2 in FIG. 9. The step size defines a unit circle in transformed coordinates (dotted circle in FIG. 9). Taking a step along the path of steepest ascent equivalent to an additional +1 units brings us to our new design center, p_2. From there, four supplemental points are added (s_5–s_8) to comprise the next factorial series, which forms the basis for the next iteration. To calculate the actual process settings there, the transforms are inverted in Eqs. 21 and 22:

$$T[°C] = -0.89 \times 5[°C] + 300[°C] = 296°C \quad (21)$$

and

$$P[kPa] = 0.45 \times 10[kPa] + 500[kPa] = 505[kPa]. \quad (22)$$

Therefore, the design center has been moved from p_1 (i.e., 300°C and 500 kPa) to p_2 (i.e., 296°C and 505 kPa). The process yield data is now collected. In this way, additional points along the path of steepest ascent are calculated.

Takeaway. EVOP results in continual process improvement. Although the current method requires only spreadsheet software, EVOP may also be automated as part of a process control strategy. Indeed, EVOP is one of many statistical techniques used to optimize processes and make experimental and research strategies more effective and efficient. Such techniques minimize the time and cost of experimental investigations and are a worthy pursuit for the researcher, process engineer or operator. HP

LITERATURE CITED

[1] Box, G. E. P., "Evolutionary operation: A method for increasing industrial productivity," *Journal of the Royal Statistical Society,* Series C, 1957, online: https://www.gwern.net/docs/statistics/decision/1957-box.pdf

[2] Online: http://asq.org/quality-progress/2015/01/statistics-roundtable/evop-an-underused-technology.html

[3] Colannino, J., *Modeling of combustion systems: A practical approach,* Taylor and Francis, Boca Raton, Florida, 2006.

[4] Box, G. E. P. and N. R. Draper, *Empirical model-building and response surfaces,* John Wiley & Sons, New York, 1987.

[5] Colannino, J., *Modeling of combustion systems: A practical approach,* Chapter 1, "Introduction to Modeling," and "A Linear Algebra Primer,"; and Chapter 3, " Experimental Design and Analysis," Taylor and Francis, Boca Raton, Florida, 2006.

JOSEPH COLANNINO is a registered chemical engineer in the state of California. He has more than 30 yr in the HPI/CPI and specializes in leading process teams to profitable innovation. He has more than 100 patents pending and granted, and many of his innovations are still in revenue-producing service. Mr. Colannino has authored or co-authored several books in combustion, pollution control and experimental design. He was formerly head of research and development for John Zink Co. LLC, and CTO for a Seattle-based startup. Now CEO of Colannino Consultants, he consults in pollution control and teaches industrial courses on process optimization, improving R & D structure and output, and the art of technical presentation and communication. He received his BS degree in chemical engineering from the California Polytechnic University at Pomona and holds an MS degree in knowledge management from the University of Oklahoma with an emphasis in leading research organizations. A spreadsheet containing all the calculations discussed in this article, as well as additional explanatory text, is available from the author by request at colanninoconsultants@gmail.com.

A. V. KARRE, Worley Group Inc, Baton Rouge, Louisiana; and **K. T. VALSARAJ,** Cain Department of Chemical Engineering, Louisiana State University, Baton Rouge, Louisiana

Selection and comparison of thermic fluids in a fired heater

Hot oil, also called thermic fluid, is a heat transfer fluid (HTF) used in oil refineries and chemical plants. HTF transfers heat to the process fluid using sensible heat. Many limitations exist to using steam as a heat source. The steam pressure must be high enough to get the high temperatures required for the process; a steam system also requires water treatment and condensate collection systems; and steam systems are also a common leak point within plants. Conversely, steam is nontoxic and non-flammable, so there is zero negative impact to the environment.

Hot oil can also leak, but it does not require a high-pressure system. By selecting an appropriate HTF, high temperatures can easily be reached. The hot oil process is a closed-loop process. HTFs undergo thermal degradation over time due to the high-temperature process and will often need to be refilled by an external make-up. As shown in **FIG. 1,** a hot oil system consists of a fired heater, circulation pumps, expansion tank, filters, a hot oil cooler, process users and a slop oil system. The respective process equipment is located close to its process user to minimize both the piping and the required hot oil volume. Efficient design of hot oil equipment and the proper selection of the HTF is crucial to the performance of the hot oil system.[1]

Circulating hot oil systems can limit CAPEX, depending on the chosen HTF. These hot oil systems are most advantageous to areas of the plant in which multiple users require process temperatures above what can be achieved with high-pressure steam. In some select cases, a circulating hot oil system can be utilized in which only one fired heater is required vs. installing independent fired heaters for each of the process users.

Many HTFs are available from manufacturers based on various properties, such as temperature range, density, thermal conductivity, heat capacity, vapor pressure, viscosity, corrosivity, flammability, flash point, fire point, thermal expansion, thermal stability, freezing point, flash point and autoignition temperature. The main parameters, such as heat transfer coefficient and line pressure drop, are used to determine the suitability of the hot oil.

A refinery client of the author's company uses a proprietary base oil[a] as the hot oil medium. The base oil degrades rapidly at an operating temperature of 575°F–600°F (302°C–316°C), causing fouling issues in the pumps, pipelines and exchangers. As an example, fouling caused by rapid degradation of hot oil in a heat exchanger is shown in **FIG. 2.** A client refinery condensate fractionation project required a reboiler duty of 48.1 MMBtu/hr. The additional duty for the project required a comparative study of different HTF systems for the service in the naphtha splitter reboiler, as the plant experienced degradation problems with the hot oil. The project team evaluated different hot oils that remain stable and are expected to have a 20-yr life span for operating temperatures ≥ 680°F (≥ 360°C). This study evaluates the hot oils by comparing their heat transfer characteristics, hydraulic benefits, cost benefits and other (vapor pressure, thermal stability, etc.) vital process parameters. The aims of the study are:

1. Investigate thermal and hydraulic performance and suitability of the proprietary oil and ultra-low sulfur diesel (ULSD) hot oils at

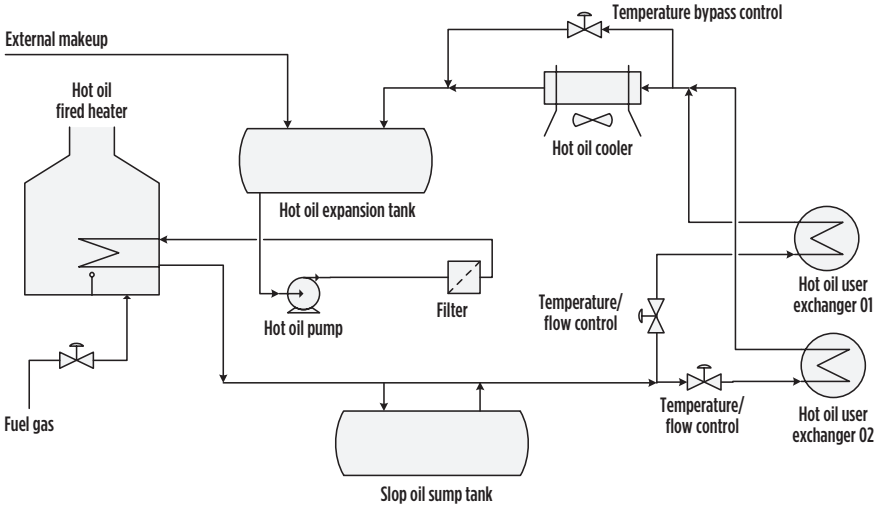

FIG. 1. A hot oil system consists of a fired heater, circulation pumps, expansion tank, filters, a hot oil cooler, process users, and a slop oil system.

an operating temperature above 575°F–600°F (302°C–316°C).
2. Compare different HTFs and recommend an optimal hot oil for operating temperatures above 680°F (360°C).

It is important to note that several operating refineries and chemical plants are still using the same hot oil that was selected 40 yr–50 yr ago. These old plants could be running their hot oil systems inefficiently and experiencing degradation problems, as mentioned here. Any plant or refinery can use this approach to solve a degradation problem and select an optimal HTF suitable and appropriate for their system.

FIG. 2. Examples of fouling caused by rapid degradation of hot oil in a heat exchanger.

METHOD PARAMETERS USED FOR COMPARISON

ULSD and proprietary heat transfer fluids[b,c,d] were selected for comparison in this study because they exhibit the desired properties for the temperature range of 550°F–680°F (288°C–360°C). Note that ULSD has also been observed to break down fairly rapidly above 600°F (316°C) similar to the base oil[a]. The following parameters are estimated for each hot oil fluid, and the description and significance of each parameter are detailed.

Vapor pressure. The vapor pressure is the pressure exerted by a pure component at equilibrium, at any temperature, when both liquid and vapor phases exist.[2] Vapor pressure increases with an increase in temperature. Low vapor pressures are preferred in hot services to avoid any vaporization within the system. A two-phase hot oil system has higher frictional losses and requires more pumping energy, which equates to a higher operating cost. Also, a two-phase system requires additional piping supports, adding to project capital costs. Vapor pressure values for the proprietary heat transfer fluids[b,c,d] are available.[3,4,5] Typically, refinery diesel stream data and a proprietary software[e] simulation are used for estimating ULSD properties.

Fluid properties. Basic fluid properties—such as heat capacity (*Cp*, Btu/lb-°F), thermal conductivity (*k*, Btu/hr-ft-°F), viscosity (*μ*, *cP*) and density (*ρ*, lb/ft^3)—are used to estimate the thermal and hydraulic process parameters. Fluid properties for the proprietary heat transfer fluids[b,c,d] are available.[3,4,5] Typically, refinery diesel stream data and a proprietary software simulation[a] are used for estimating ULSD properties. These fluid properties play an important role in determining the thermal and hydraulic performance of a hot oil.

Absorbed heat duty and mass flowrate. The heat duty (*Q*) is the heat absorbed by the hot oil heater, which is 48.1 MMBtu/hr. Based on the process requirements, the supply temperature from the hot oil heater is 680°F (360°C) and the return temperature is 551°F (288°C). The differential temperature is the difference between the supply and return temperatures (i.e., ΔT = 680°F–550°F = 129°F). The duty and differential temperatures are used to estimate the mass flowrate of a hot oil through the hot oil system. The mass flowrate can then be used to estimate volumetric flowrate of a hot oil. The heat equation (Eq. 1) is:

$$Q = m \times Cp \times \Delta T \quad (1)$$

where *m* is the mass flowrate of the hot oil in lb/hr, *Q* is the heat absorbed, *Cp* is the heat capacity of hot oil in Btu/lb-°F, and ΔT is the differential temperature in °F.

Volumetric flowrates. The hydraulic equation (Eq. 2) is used to convert the mass flowrate into the volumetric flowrate (*VF*), which can then be used to estimate the velocity and the Reynolds (Re)number:

$$VF = (gpm) = \frac{m\left(\frac{lb}{hr}\right)}{500.5 \times SG} \quad (2)$$

where (Eq. 3) *SG* is specific gravity =

$$\frac{\text{density of hot oil } \left(\text{lb/ft}^3\right)}{\text{density of water } \left(62.4 \text{ lb/ft}^3\right)} \quad (3)$$

Velocity, Reynolds number and Prandtl number. The velocity through an 8-in. nominal diameter pipe (7.981-in. inner diameter) is estimated for each hot oil. This diameter is selected based on an approximate 10 ft/sec velocity for liquids. The corresponding Re and Prandtl (Pr) numbers are also calculated.[6] Re and Pr numbers are then used to estimate the heat transfer coefficients, as shown in Eq. 4:

$$V\left(\frac{ft}{\text{sec}}\right) = \frac{VF(gpm)}{\text{Area of tube}} = \quad (4)$$

$$\frac{VF(gpm) \times 1\ USG \times 1 \text{ minute}}{7.48 \text{ ft}^3 \times 60 \text{ sec} \times \frac{3.142}{4} \times (d/12)^2}$$

where *d* is the diameter of the hot oil tube in inches (Eqs. 5 and 6):

$$\text{Re} = \frac{\rho\left(\frac{\text{lb}}{\text{ft}^3}\right) \times V\left(\frac{\text{ft}}{\text{sec}}\right) \times d\left(\frac{\text{inch} \times 1 \text{ ft}}{12 \text{ inch}}\right)}{\mu\left(\frac{cP \times 0.000672 \frac{\text{lb}}{\text{ft-sec}}}{1\ cP}\right)} \quad (5)$$

$$\text{Pr} = \frac{Cp\left(\frac{\text{Btu}}{\text{lb} - \text{F}}\right) \times \mu\left(\frac{cP \times 0.000672 \frac{\text{lb}}{\text{ft-sec}}}{1\ cP}\right)}{k\left(\frac{\text{Btu}}{\text{hr} - \text{ft} - \text{F}}\right)} \quad (6)$$

Nusselt number and heat transfer coefficient. The Nusselt number (Nu) and the heat transfer coefficients (h) are based on the Dittus and Boelter equation.[6] Since *d* and 0.023 are constant for all of the hot oils, Eq. 7 is rearranged to Eq. 8 and is defined as the modified heat transfer coefficient, *H*. The net change in modified heat transfer coefficient (ΔH) is also defined to compare the heat transfer performance of the new hot oils with the proprietary oil.[a] The required heat exchange area decreases as *H* and ΔH increase, because the heat transfer coefficient is inversely proportional to the surface area (Eq. 9):

$$Nu = \frac{h \times d}{k} = 0.023 \times \mathrm{Re}^{0.8} \times \mathrm{Pr}^{0.4} \quad (7)$$

$$\frac{h \times d}{0.023} = k \times \mathrm{Re}^{0.8} \times \mathrm{Pr}^{0.4} = H \quad (8)$$

$$\Delta H = \left(\frac{\text{heat transfer coefficient of hot oil-heat transfer coefficient of 100 N}}{\text{heat transfer coefficient of 100 N}} \right) \times 100 \quad (9)$$

Frictional factor and pressure drop. The friction factor (f) and line pressure drop (ΔP) are estimated per approximations of the Colebrook equation.[7] These parameters are used for estimating the hydraulic horsepower requirement and associated cost, as shown in Eqs. 10 and 11:

$$f = \frac{0.25}{\left[\log \left(\frac{\varepsilon}{3.7 \times d \left(\frac{\text{inch} \times 1\,\text{ft}}{12\,\text{inches}} \right)} + \frac{5.74}{\mathrm{Re}^{0.9}} \right) \right]^2} \quad (10)$$

where ε is the pipe roughness factor of 0.0005 ft:

$$\Delta P\,(Psi) = \frac{f \times L(ft) \times V^2 \left(\frac{\text{ft}}{\text{sec}} \right)^2 \times \rho \left(\frac{\text{lb}}{\text{ft}^3} \right)}{d \left(\frac{\text{inch} \times 1\,\text{ft}}{12\,\text{inch}} \right) \times 2 \times g \left(\frac{\text{ft}}{\text{sec}^2} \right) \times 144} \quad (11)$$

where *g* is acceleration due to gravity (32.17 ft/sec^2). ΔP per 100 ft of pipe (ΔP/100 ft) is estimated by substituting 100 ft for pipe length (L) in Eq. 11. ΔP per 2,000 ft of pipe is also estimated by using 2,000 ft for *L*.

Horsepower. Equivalent hydraulic horsepower (HH) and the actual horsepower (AH) for the calculated line pressure loss are estimated using pump Eqs. 12 and 13:

$$HH(hp) = \frac{VF(gpm) \times \Delta P(Psi)}{1{,}714} \quad (12)$$

Assuming a pump efficiency of 60%:

$$\text{Actual horsepower } (AH, hp) = \frac{HH(hp)}{\text{Pump efficiency}} = \frac{HH(hp)}{0.6} \quad (13)$$

Cost of horsepower. The cost of horsepower is estimated based on the cost of industrial electricity in the client's location, and with the assumption of 8,000 hr of operation. The estimated costs are compared for the different hot oils: 1 hp = 0.7457 kw; cost of industrial electricity in client's location, U.S. = \$0.617/kwh;[8] industrial hours in a year = 8,000 hr (Eq. 14):

$$\text{Cost} = 0.7457 \times 6.17 \times AH \times 8{,}000 \times 0.01 = \text{USD} \quad (14)$$

Cost of thermic fluid. The cost of proprietary heat transfer fluids[b,c,d] products are very high (\$1,600/bbl). The wax-free oil[a] and ULSD are normally less than \$100/bbl (more like \$70 /bbl on average).

RESULTS AND DISCUSSIONS

As seen in **TABLE 1,** the proprietary base oil[a] has the lowest vapor pressure at 680°F, but is not suitable at the operating temperature. The base oil degrades rapidly above 600°F, which causes fouling issues within the pumps and exchangers. ULSD has the highest vapor pressure, which means the system pressures need to be higher to avoid two-phase conditions within the system. The proprietary heat transfer fluid[c] has the lowest vapor pressure at both 680°F and 551°F, second only to the base oil. As shown in **TABLE 1,** the viscosities for all of the hot oils are relatively low when compared to water (1 *cP*). A lower viscosity leads to lower energy requirements for circulation within the system.

TABLES 2 and **3** show the hydraulic performance of different hot oils. The frictional factors for all of the hot oils are close to each other. ULSD requires the lowest mass flowrate. The base oil[a] requires the lowest volumetric flowrate, but is not selected for use due to known fouling issues. One of the proprietary heat transfer fluids[c] requires the lowest volumetric rate. That fluid also is lower in ΔP/100 ft, line pressure losses and hydraulic horsepower requirement compared to the other hot oils. The lowest cost found for that fluid shows that approximately \$13,435/yr is needed, which is about 16% lower than ULSD and about 39% lower than both other heat transfer fluids[b,d]. The lowest pumping cost for the heat transfer fluid[c] is due to the lowest volumetric flowrate compared with other hot oils.

As shown in **TABLE 4,** one thermic fluid[c] has a higher heat transfer coefficient than both ULSD and the base oil[a], but is still slightly lower than the second thermic fluid[b]. The third thermic fluid has a slightly higher heat transfer coefficient than both the first and second fluids[b,c]. The higher the heat transfer coefficient, the lower the required area. The capital cost related to equipment could be lower due to the reduced area requirement, but the operating cost (pumping) would still be much higher for the third thermic fluid[d], as shown in **TABLE 3.** The first and third thermic fluids discussed here[b,d] have higher ΔH values than the second fluid[c], but that fluid has a lower operating cost and lower volumetric rates.

Every hot oil system requires a certain amount of hot oil volume in the system, and frequent refill is required to account for losses and thermal degradation. The aforementioned thermic fluids[b,c,d] are about 23 times more expensive compared with ULSD and the base oil[a], but they provide higher operating temperature required for the process.

Takeaway. Fluid properties and cost data of hot oils can be used to determine their suitability. Properties—temperature range, density, thermal conductivity, heat capacity, vapor pressure, viscosity, etc.—are used to estimate the hydraulic and thermal performance of a hot oil. The pressure drop through a line and the heat transfer coefficient are essential for the selection of a hot oil. The original hot oil[a] was not selected due to its poor fluid properties and degradation at a temperature above 600°F. The low vapor pressure of the termic fluid[c] is needed at a high operating temperature of 680°F to keep the hot oil in the liquid phase. Other hot oils with a higher vapor pressure like the first and third fluids[b,d] and ULSD require a higher system operating pressure, which increases the operating costs of pumping. The

second fluid mentioned here[c] has the lowest line pressure drop and lowest cost per year, which minimizes the operating costs of pumping. Even though the third fluid[d] has the highest heat transfer coefficient, it is not preferred due to the higher pumping related operating cost. The cost of these fluids per barrel is very high compared with the base oil[a] and ULSD. The second thermic fluid[c] was chosen for the project due to its stability at very high temperature and lowest pumping cost compared with the other two fluids discussed here[b,d]. The base oil[a] and ULSD are unsuitable for an operating temperature above 600°F.

Over a 10-yr–20-yr cycle, a hot oil system has exchanger leaks, flange leaks, solids building up in the system, etc., which can amount to substantial volume loss. Also, de-inventorying the system for 10-yr vessel inspections typically results in some fairly high system losses as some will ultimately get pushed to the flare, regardless of how well the plant minimize the losses. Large systems are harder to manage in a refinery system. Due to the sheer volume of the hot oil system, and the fact that the refinery frequently contaminates and purges high volumes of hot oil material (especially during an outage), the price-rendered specialized heat transfer fluids[b,c,d] are infeasible. For this reason, the refinery went with a superheated 450# steam on another new project. If a hot oil system loses appreciable volumes of material, or simply needs a fresh load, it is going to take at least a month for the thermic fluids[b,c,d] to generate and supply the necessary volumes. The refinery still uses hot oil systems such as the base oil[a] and ULSD for operating temperatures below 600°F. Through trial and error in the refinery, the plant noticed that if the existing system is operated near 575°F, virtually no thermal degradation occurs, making the base oil[a] and ULSD thermally stable below 575°F, ideally. Although, the base oil[a] and ULSD are economically very attractive, these can only be used when the system operating temperatures are below 575°F.

This research can be utilized in any revamp, new grassroot refinery or a chemical project where hot oil fluids require comparison. It is vital to look for temperature range of processes, and vapor pressure is a critical parameter in selecting an appropriate hot oil fluid for a system. With the presented calculation approach, defining heat transfer and hydraulics process parameters can be estimated to properly select a hot oil type. Additionally, it is important to note that a single parameter is insufficient; analysis of many parameters provides a bigger picture of the system. Refinery experience with operation of a particular hot oil fluid and the cost of hot oil play critical roles in choosing a hot oil for new projects. HP

TABLE 1. Fluid properties of hot oils at 680°F (360°C) and vapor pressures at 680°F and 551°F (288°C)

Thermic fluids	Density, lb/ft³	Viscosity, *cP*	*Cp*, Btu/lb-°F	*k*, Btu/hr-ft-°F	Vapor pressure, psia at 680°F	Vapor pressure, psia at 551°F
100N[a]	40.19	0.2	0.746	0.02756	37.8	15.16
ULSD	35.13	0.1	0.762	0.02358	133.9	50.85
Dowtherm A[b]	45.94	0.15	0.608	0.0487	90.4	27.51
Dowtherm G[c]	49.1	0.21	0.651	0.05404	**48.8**	**14.35**
Therminol 72[d]	48.1	0.16	0.591	0.0568	68	20

TABLE 2. Estimated mass and volumetric flowrates of different hot oils

Thermic fluids	Absorbed heater duty required, MMBtu/hr	m, lb/hr	VF, gpm
100N[a]	48.1	499,823	1,551
ULSD	48.1	**489,328**	1,737
Dowtherm A[b]	48.1	613,270	1,664
Dowtherm G[c]	48.1	572,762	**1,454**
Therminol 72[d]	48.1	631,911	1,635

TABLE 3. Hydraulic performance of different hot oils

Thermic fluids	F	*ΔP*/100ft	*ΔP* for 2,000 ft	*HH*, hp	*AH*, hp	$/yr
100N[a]	0.0186	**1.2**	**24.01**	**21.7**	**36.2**	**13,312**
ULSD	0.0185	1.31	26.2	26.5	44.2	16,257
Dowtherm A[b]	0.0185	1.57	31.46	30.6	51	18,772
Dowtherm G[c]	0.0186	**1.29**	**25.78**	**21.9**	**36.5**	**13,435**
Therminol 72[d]	0.0185	1.59	31.81	30.4	50.7	18,649

TABLE 4. Thermal performance of different hot oils

Thermic fluids	*V*, ft/sec	*Re*	*Pr*	*H*	*ΔH*%
100N[a]	9.9	1.95E + 06	0.003703	316	-
ULSD	11.1	4.06E + 06	0.002075	386	22
Dowtherm A[b]	10.7	3.24E + 06	0.001258	545	73
Dowtherm G[c]	9.3	2.16E + 06	0.0017	493	56
Therminol 72[d]	10.5	3.13E + 06	0.00112	**589**	**87**

NOTES

[a] Ergon 100-N oil by Ergon North & South America
[b] Dowtherm A Heat Transfer Fluid by Dow
[c] Dowtherm G Heat Transfer Fluid by Dow
[d] Therminol 72c Heat Transfer Fluid by Eastman
[e] ASPEN HYSYS

LITERATURE CITED

Complete Literature Cited available online at www.HydrocarbonProcessing.com

AVINASHKUMAR KARRE is a Process Engineer with Worley Group in Baton Rouge, Louisiana. He has 13 yr of experience in the refining and chemical industries, as well as extensive experience in oil refinery revamp operations, catalysis and water treatment areas.

KALLIAT T. VALSARAJ is the Charles and Hilda Roddey Distinguished Professor of Chemical Engineering at Louisiana State University in Baton Rouge, Louisiana. Dr. Valsaraj received his B.Sc degree from Calicut University, India; an M.Sc degree from the Indian Institute of Technology, Madras; and his PhD from Vanderbilt University in Nashville, Tennessee. He is a fellow of AIChE, AAAS, NAI and RSC.

J. POTH, Integrated Global Services,
Schleiden, Germany

Stop oxidation and scale growth with high-emissivity coating

Oxidation of external tube surfaces is responsible for metal loss at around 0.25 mm/yr, which limits tube life. Scale growth produces an insulating layer that restricts conductive heat transfer to the process fluid and eventually limits production. Moreover, severe scaling also prevents accurate onstream monitoring of tube skin temperatures, using infrared (IR) thermography.

The application of proprietary high-emissivity ceramic coatings[a] stopped oxidation in an aromatics plant. The units are no longer limited and are running at design capacity or above. Payback from the investment was within 6 mos.

Oxidation and scale growth of radiant tubes. Following a detailed root cause analysis, it was recommended to apply the high-emissivity ceramic coatings to the radiant tubes. In addition, the coatings were applied to the refractory surfaces to improve radiant heat transfer efficiency.

The application of high-emissivity ceramic coatings[a] to the refractory and radiant tube surfaces creates a near black body enclosure, which maximizes radiant heat transfer efficiency. In addition, preventing oxidation of radiant tube surfaces eliminates metal loss and extends tube life.

Process and equipment design. The aromatics plant was commissioned in November 2009. It consists of a naphtha reforming unit based on a continuous catalyst regeneration (CCR) system designed to produce an aromatics-rich stream, along with high-purity hydrogen (H_2) as byproduct. The plant typically experiences varied feed composition (higher naphthenic content, etc.) depending upon the quality of imported naphtha.

Low-pressure, high-temperature operation. The high performance of the licensed process is largely owed to low-pressure operation coupled with high temperatures, which, in conventional fixed-bed reactors, would lead to very short cycle lengths (**FIG. 1**).

Continuous regeneration. Continuous regeneration eliminates the need for shutdown for the regeneration of the earlier fixed-bed reformers. It also minimizes the amount of catalyst in the unit, while allowing high aromatics yield and quality. A high temperature [an estimated 545°C (1,013°F)] is required to promote the chemical reactions that improve aromatics production—hence the need for reheating of the feed.

For this purpose, four heaters are provided (one preheater and three inter heaters), with their primary purpose to provide the required heat for reactions in the reactors. The heaters are arbor-type with vertical inverted "U-type" radiant tubes (**FIG. 2**), which are typically used for low-pressure vapor flow units, such as CCR units. The single-pass radiant tubes have a material specification of ASTM 335 Gr P9 (9Cr-1Mo), with a wall thickness outer diameter (OD) of 114.3 mm x 6.02 mm and a corrosion allowance of 1.5 mm. Heaters are designed as per API (2) 530, with a design life of 100,000 hr.

Damage mechanisms. The life of radiant tubes in furnaces is governed by the combination of several possible time-dependent degradation mechanisms and by the tube wall temperatures and loadings. The main degradation mechanisms in reforming service are fireside oxidation, thermal microstructural degradation and creep. Apart from this, carburization and metal dusting have also been reported in many catalytic reforming heater tubes, although these are uncommon due to

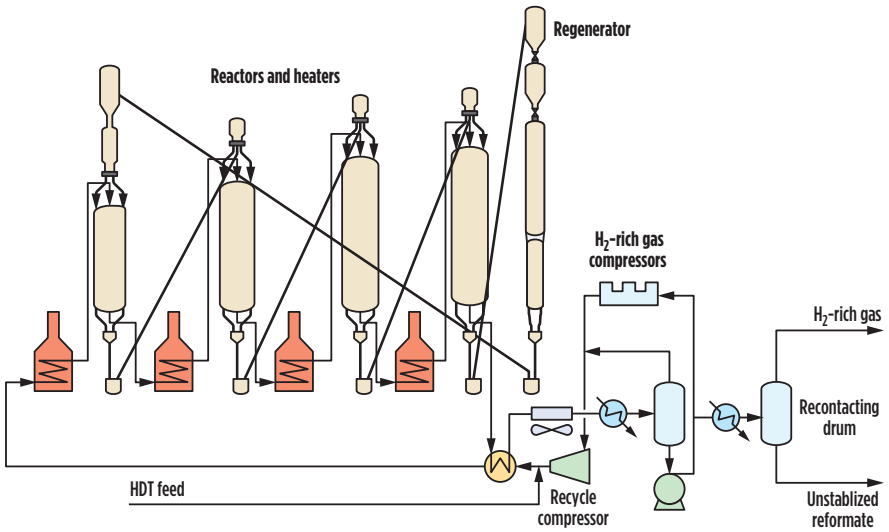

FIG. 1. Unit schematic of a conventional fixed-bed reactor.

sulfide injection that forms a protective layer and prevents carbon diffusion.

Process tube materials. Tube materials in CCR fired heaters are usually 9Cr-1Mo. Tube dimension design and corrosion allowance generally follow the API 530 standard. With time, these Cr-Mo materials experience thermal degradation, and their typical normalized and tempered structure (pearlite or bainite depending upon normalization heat treatment) and ferrite grains will degenerate to ferrite grains with intra- and intergranular carbides. The material's tensile and creep strength reduce during this process.

Damage mechanism in reforming heaters.

- **Oxidation**—Severe scaling due to oxidation is expected in these heaters due to high operating temperatures. Above approximately 500°C (932°F), the 9Cr-1Mo materials tend to oxidize and may scale very rapidly as temperatures increase. The corrosion rate based on material and temperature is approximately 0.25 mm/yr.
- **Carburization**—This is the diffusion of carbon into the metal matrix at high temperatures > 600°C (> 1,112°F), forming a hard and brittle structure. The extent of carburization can be determined by metallography and causes a substantial increase in hardness and loss in ductility. Where the operating temperatures result in high metal temperatures of about 650°C (1,202°F) or higher, carbon at the surface has a higher tendency to diffuse into the metal and thicker carburized layers tend to form. This phenomenon initially strengthens the tube wall, but ultimately leads to crack initiation, through-wall crack propagation and, therefore, enhanced rates of life consumption.
- **Metal dusting**—This catastrophic form of carburization in the 480°C–816°C (896°F–1,501°F) temperature range generally results in rapid metal wastage in the form of erosion at the hotter areas of the tubes or small pits filled with metal oxides and carbides. In mild form, metal dusting results in discrete pitting, but at an extreme can effectively produce a rapid inner wall thinning mechanism.
- **Creep**—Other prominent damage mechanisms include creep, and its susceptibility grows with increasing temperature and reduced thickness. In subject heaters, (to date) only external oxidation has been found, and no internal carburization or metal dusting nor signs of creep damage have been detected.

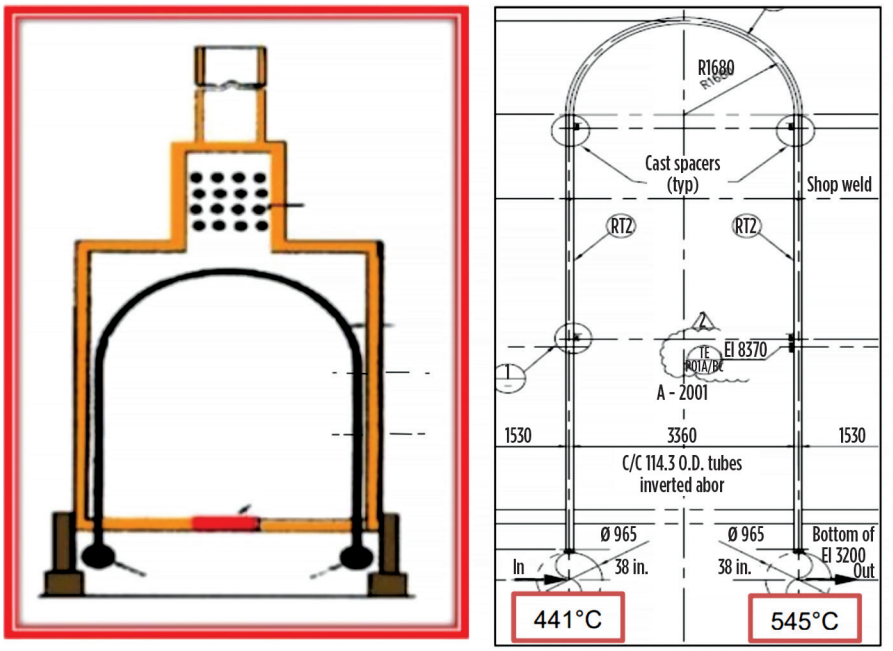

FIG. 2. Arbor-type heaters with vertical inverted "U-type" radiant tubes are typically used for low-pressure vapor flow units, such as CCR units.

FIG. 3. Severe scaling on the external surface of the radiant tubes.

Aromatics plants: Petrochemical unit. The aromatics plant is an important downstream petrochemical unit that produces various aromatic hydrocarbons, such as xylenes, benzene and toluene, which are the basic building blocks for the production of polyester and polymers, resulting in different consumer goods.

The heart of the aromatics plant is a licensed high-performance naphtha reforming unit that operates at the low pressure and high temperatures required to

promote chemical reactions that improve aromatics production.

Fired heaters, arbor-type coil configuration. To achieve the required heat, four fired heaters with an arbor-type coil configuration raise the feed naphtha temperature to approximately 545°C (1,013°F). The radiant tubes of the heaters are of 9Cr-1Mo (ASTM(1) A335 Gr P9) metallurgy with a maximum tube wall temperature of 652°C (1,206°C). The tubes are prone to excessive scaling due to high-temperature oxidation and scale thickness of up to 1 mm–2 mm that were found in the tubes. The problem arising due to scaling affects not only the mechanical integrity of the radiant tubes but also leads to multiple operational constraints.

Oxidation and scale growth. As previously stated, oxidation of external tube surfaces is responsible for metal loss at around 0.25 mm/yr, which limits tube life. Scale growth produces an insulating layer that restricts conductive heat transfer to the process fluid and eventually limits production. Moreover, severe scaling also prevents accurate onstream monitoring of tube skin temperatures using IR thermography.

Root cause analysis and observations. Following a detailed root cause analysis, it was recommended to apply a ceramic coating on the radiant tube and extend it to the refractory in the furnace box to improve operational and thermal efficiency, while maintaining metallurgical integrity and reliability. Observations included:

- Severe scaling on the external surface of the radiant tubes with thick scales (tree bark appearance) was more prevalent in the outlet tubes of the heater (FIG. 3).
- Scaling was due to oxidation, which is common in these heaters considering the high operating and tube wall temperatures.
- Scale thicknesses measured were in the range of average 0.5 mm–1 mm, with some locations as high as 2 mm.
- By appearance, it typically looked like two layers of oxide scales were generated out of the tube metal. Loose scales fell on the furnace floor, whereas some tight adherent scale was still found on the tube surface.
- UT measurements (spot + scanning) were done across many tubes of the four heaters, and a minimum thickness of 4.6 mm was recorded against the original thickness of 6.02 mm.
- An overall review of thickness measurements for all heaters revealed a minimum of 1 mm reduction in most of the radiant tubes.
- The corrosion rate was calculated

Proprietary high-emissivity ceramic coatings stopped oxidation. The units are no longer limited and are running at design capacity or above. Payback from the investment was within 6 mos.

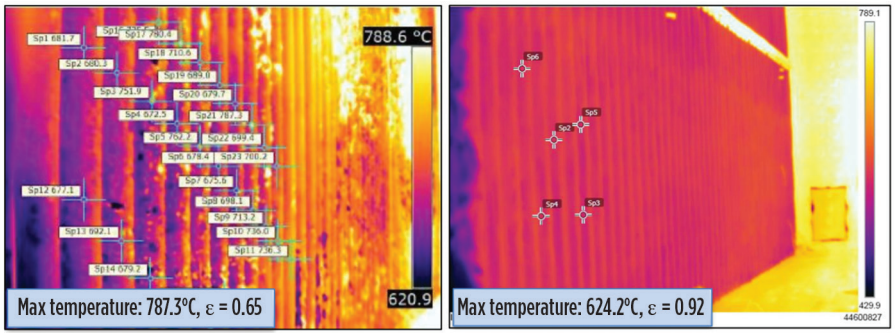

FIG. 4. Before (left) and after (right) the high-emissivity coating[a] application.

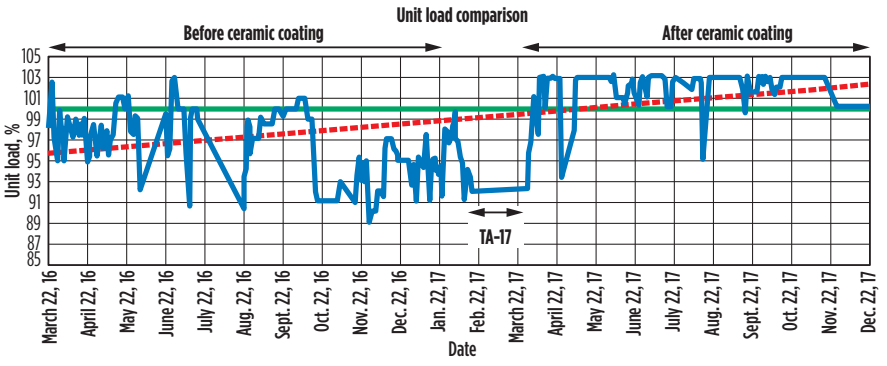

FIG. 5. The unit load prior to ceramic coating was 97%–98%.

TABLE 1. The corrosion rate was calculated to determine the remaining life of the tubes

Heater	Location of minimum thickness	Original thickness, prior to service, mm	Minumum measured thickness, post service, mm	Retirement thickness, mm	Corrosion rate, mm/yr	Remaining life, yr
1	Tube #64	6.02	4.8	3.8	0.24	4
2	Tube #100	6.02	4.8	3.8	0.24	4.2
3	Tube #78	6.02	4.6	3.8	0.28	2.8
4	Tube #47	6.02	4.8	3.8	0.24	4.2

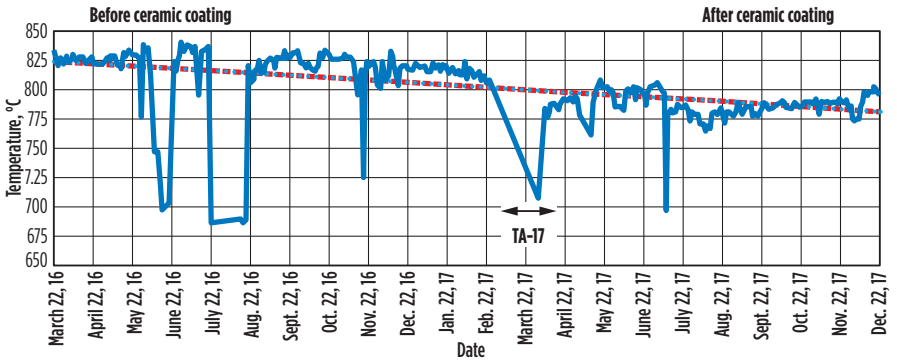

FIG. 6. Bridgewater wall temperature, °C.

based on the lowest thickness recorded and was 0.28 mm/yr.

- Based on the minimum recorded thickness for each heater, the corrosion rate was calculated to determine the remaining life of the tubes (**TABLE 1**). The corrosion rate was based on the operating life of 5 yr (November 2009–August 2014).

Again, preventing oxidation of radiant tube surfaces eliminates metal loss and extends tube life (**FIG. 4**).

Increased throughput. The unit is being operated at higher throughput regardless of feed variations. The unit load prior to ceramic coating was 97%–98%, as shown in **FIG. 5.** Moreover, when processing high-naphthenic feed, the unit load was reduced further to 96%. However, post coating, the unit is being operated at 103%, regardless of feed composition—even with high-naphthenic feed, desired throughput is obtained with the same fuel firing.

Controlled steam generation. With ceramic coating on tubes and refractory, radiant heat loss has been considerably reduced, increasing the efficiency of the radiant heat transfer and reducing bridge wall temperatures by an average of 30°C–50°C (86°F–122°F). Therefore, even when operating at higher loads, the arch temperatures have relatively reduced, avoiding excessive steam generation and high heat loads on the convection steam coils (**FIG. 6**).

Fuel gas savings. With the commissioning of a new refinery, the H_2-rich fuel gas from the aromatics plant is being sent to the off-gas recovery section, and the heaters are being operated entirely on natural gas. The amount of fuel burned in MMBtu/hr post-coating to maintain a 103% load is less than the fuel required to maintain 96%–99% load prior to coating.

Cost savings and ROI. The total project cost was approximately $25 MM, with an expected return on investment (ROI) within 11 mos of operation, with an internal return rate (IRR) of 111%. However, considering all factors and a favorable market, the ROI was achieved within 6 mos of operation.

Advantages. The proprietary ceramic coating[a] eliminates oxide scale formation and increases conductive heat transfer to the process fluid. The high-emissivity coating of the refractory increases radiant heat transfer efficiency, and the increase in radiant section efficiency allows for energy (fuel) savings and/or production increases, while providing uniform heat distribution in the firebox. Foulant adhesion to the tube surface and refractory is limited, and bridge wall temperature and convection section temperatures are lowered. Tube wall temperature can be directly inferred from thermography or infrared measurement. HP

NOTES

[a] IGS's Cetek ceramic technologies

JOHANNES POTH is a Cetek Subject Matter Expert in ceramic science and engineering. He earned an engineering degree in ceramics from the University of Applied Science in Koblenz, Germany. Mr. Poth then joined Fosbel as a Quality and Product Manager, specializing in Cetek high-emissivity ceramic coatings. Over the years, he has been responsible for the development, application and market introduction of Cetek ceramic coatings globally. Mr. Poth joined Integrated Global Services (IGS) in 2017, when the Cetek brand was acquired by IGS, and continues to support fired heater efficiency optimization projects in Europe and around the globe.

W. A. ALHARBI, A. GHAZAL and **D. TURCAN,**
Saudi Aramco, Dhahran, Saudi Arabia

Resolving a chronic water injection pump high vibration through a shaft-lifting technique

This article explores the investigation into the chronic high vibration issues of a particular water injection pump. This pump had been prone to high vibration since 2014 and had been completely overhauled seven times. The vibration level persisted despite multiple corrective actions. This article examines how the root cause was identified and resolved after performing extensive vibration analysis.

Pump problems. A water injection pump (FIG. 1) had experienced high vibration over the last six years, and several attempts to reduce the vibration levels had failed. These attempts included alignment and a complete overhaul of the pump. Pipe strain checks at suction and discharge flanges were also performed. The case was investigated through vibration analysis and a motion amplification system. The goal was to diagnose the vibration by using high-speed camera and video processing software that can amplify motion 50 times. Eventually, these techniques made it possible to detect a bowed shaft and a slightly unbalanced rotor.

Background. This water injection pump—which had been shipped to the site in 2003 and in operation since 2005—has five stages. The pump's specifications include:

- Rated speed: 4,964 rpm
- Rated capacity: 4,861 gpm
- Rated head: 6,451 ft
- Net positive suction head ($NPSH_A$): 324 ft.

A site visit was conducted to run the pump and collect vibration data. Prior to operating the pump, all necessary checks were completed, such as for alignment, coupling, pipe strain and foundation condition. The following details were discovered:

- **Alignment:** Hot alignment was carried out using a dial indicator and was found to be within limits.
- **Coupling:** Coupling was checked and found to be in excellent condition (FIG. 2).
- **Pipe strain:** Suction and discharge flanges were dismantled and checked against any piping strain. Only minor piping strain was found, which was corrected.
- **Foundation:** Minor cracks were found near both pumps and were repaired. The foundation was then inspected and found to be in good condition.
- **Overhaul:** Pump B underwent a complete overhaul at the vendor's facility. The bearing housing bolts were found to be broken (sheared) due to incorrect assembly. As a result, the shaft was not supported by any bearings. Both bolts and bearings were replaced.

FIG. 1. View of the troubled pump from the O/B side. The pump is surrounded by scaffolding to allow access for maintenance personnel.

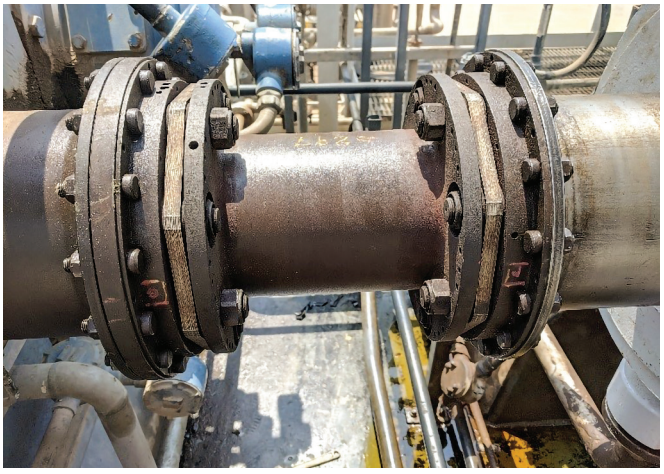

FIG. 2. An inspection showed that the pump's coupling was in excellent condition.

Data collection. The pump trip delay was extended from 30 sec to 60 sec to allow more time for vibration data collection. Using the motion amplification camera, the coupling guard was removed to allow a direct recording of the coupling movement while the machine was running. The following observations were noted:

1. When the pump started, the vibration level was 4.2 mm pk-pk at a speed of 1,650 rpm. Approximately 13 sec later, the machine reached full speed and the vibration level was 4.7 mm pk-pk at the I/B side (FIG. 3).
2. At 11:51:48, the machine reached steady state—the vibration level dropped gradually by 1.5 mm pk-pk and 1 mm pk-pk at the O/B vertical and horizontal, respectively, over the steady-state duration of 45 sec.
3. At 11:52:38, the machine tripped at an overall vibration level of 4.6 mm pk-pk on the I/B side and at 2.9 mm pk-pk on the O/B side (FIG. 3). During shutdown, the vibration trend reached 1.5 mm pk-pk on the pump I/B side, and 0.8 mm pk-pk on the pump O/B side at low speed (600 rpm).

Data analysis. Investigating the bode plots of the I/B and O/B sides showed that, during shutdown, the pump O/B plot dropped following a parabolic shape and then settled around 0.8 mm pk-pk at low speed (500 rpm). Similarly, the pump I/B plot dropped following a parabolic shape and then settled around 0.2 mm pk-pk at low speed (500 rpm). This observation indicated the existence of high runout at pump O/B, and a more dominant effect of unbalance on pump I/B. In addition, investigating the orbit plots at pump startup, steady state and shutdown revealed the following:

- At startup, the orbital shape of pump I/B was round, and the waveform was sinusoidal, indicating 1X frequency with a runout of 3 mm pk-pk. Similarly, at pump O/B, the orbital shape was round, and the waveform was almost sinusoidal, with slightly clipped peaks and an overall runout of 2 mm pk-pk (FIG. 4). During steady state, the orbital shape was slightly preloaded, and the time waveform remained sinusoidal. During shutdown, the orbital shape remained preloaded and the waveform showed rattles, indicating a runout.
- Recording the coupling by using the motion amplification technology while the machine was at full speed revealed high vertical motion on the coupling on the pump side of 11 mm pk-pk (FIG. 5).

The combination of these observations and data showed that the pump experienced two main forcing frequencies:

1. 1X runout, sinusoidal in nature—most likely due to a bent shaft or coupling misalignment
2. 1X unbalance, which could have been due to an imbalance of the rotor and/or coupling.

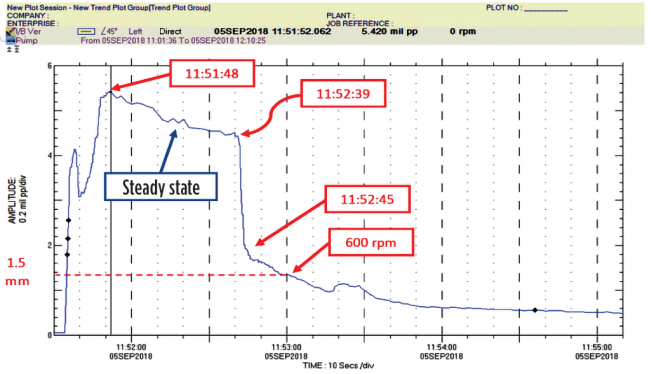

FIG. 3. The trend plot of the pump was extracted from the I/B side.

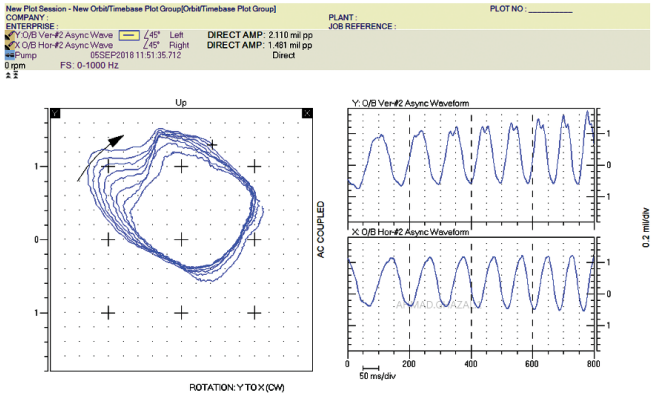

FIG. 4. Orbital shape during pump startup.

Root cause 1: Bent shaft (rotor sag). Typically, when an overhaul is conducted, the pump is dismantled for inspection. Upon assembly, the impeller is shrink fitted on the shaft.

In this case, a hypothesis was made that, if the fitting procedure was not conducted properly, a residual force would be exerted on the fitting area. In turn, this force would start to act during pump shipment to and from the maintenance shop. In this scenario, the fitting residual force would act downward on the shaft opposing the upward normal force transmitted from the truck suspension. This would eventually cause a rotor sag of 1 mm–2 mm, even if shaft straightening was conducted at the shop. When the pump was restarted, the vibration trend—due to shaft sag—would start with high runout on both sides. When the pump reached full speed, the rotor would start to rub on both sides, which explained the preload effect observed on both orbit plots at steady state.

In addition, an interesting observation was made on the vibration trend (FIG. 3). The vibration amplitude started to drop from 5.2 mm pk-pk to 4.5 mm pk-pk after 21 sec from startup. The machine runout at cost down (0.2 mm pk-pk) was also found to be less than the runout during startup (0.8 mm pk-pk). This result indicated that the runout was not static in nature like a normal mechanical runout and was affected by dynamic forces. This observation supported the hypothesis that the shaft started with a sag, and, when ramped up to full speed—due to the centrifugal forces—the shaft would begin to straighten up, leading to less shaft sag. The vibration level of 4.5 mm pk-pk was still higher than the danger limit of 2.8 mm pk-pk, leading to the emergency shutdown system sending a shutdown signal after the trip delay passed. As a result, it was expected that, should the pump continue to operate for a longer time, the vibration would drop below 2.8 mm pk-pk.

Root cause 2: Rotor imbalance. On the latest overhaul, a visual inspection showed elements removed from the shaft

to be used in rotor balancing. This observation supported the hypothesis that the balancing procedure was not done properly. As a result, a residual imbalance remained in the rotor, which was displayed when ramped up to full speed. From this analysis, it was clear that the imbalance effect at full speed was dominated by the bowed shaft and, therefore, would not contribute much to the overall vibration.

Solution. A conclusion was made that the high vibration of the pump was mainly due to shaft sag and rotor/coupling imbalance. A decision was made to conduct field balancing on the pump's coupling and to raise the bearing housing at both sides by 2 mm. The pump was then left to run long enough to straighten up under the influence of the centrifugal forces.

Recommendations. Based on this previous analysis, the following recommendations were provided:

1. If the overall vibration plots indicate that the rotor is behaving as if it is not well-positioned in the pump casing, then personnel should check whether the bearing clearance is about 6 mm pk-pk. This action might be challenging, considering that it is a multi-lobe bearing.
2. Do a lift and drop test of the rotor in the bearing, with an emphasis on the I/B side.
3. Depending on the results of Step 1, lift the bearing housing so that the shaft rises 2 mm pk-pk to 3 mm pk-pk in the stuffing box in a vertical upward direction (compared to the actual position).
4. After completing the lift, check whether the rotor is still capable of freely rotating.
5. If the lift and drop test show an anomaly, or if it is impossible to adjust the rotor so that it is freely rotating, the pump might need to be reopened.
6. After completing all of these steps, restart the pump and measure the vibration.

After implementing these recommendations, the pump was retested. The vibration level dropped from 4.5 mm pk-pk to 1.8 mm pk-pk at full speed. This proved that the sag shaft was causing a rub at full speed—and, consequently, a vibration of 4.5 mm pk-pk.

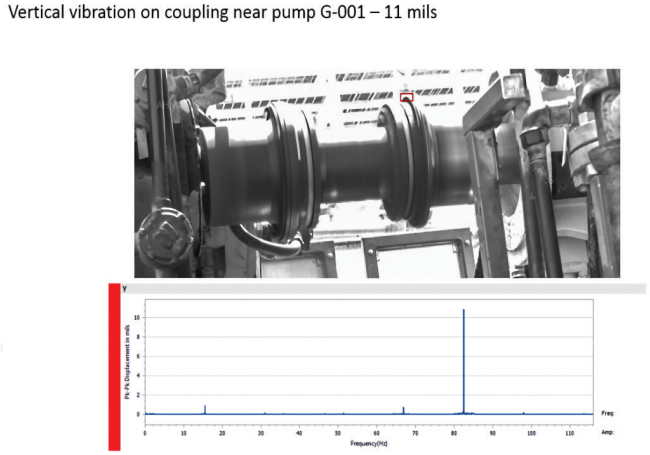

FIG. 5. Motion amplification shows high displacement at coupling I/B.

Results. The I/B vibration level reached a maximum of 1.7 mm pk-pk in the subsequent run (i.e., after the recommendations were implemented). This indicated a clear reduction in vibration level. However, there is still room for improvement, especially for trim balancing. HP

ACKNOWLEDGMENTS

Special thanks to the support of Saudi Aramco for permission to publish this article and to the specific individuals who contributed: Khaleel Al Hussain, Rehan Farooqi, Abdulkarim Rinawi and Salman Al Salman.

WESAM A. ALHARBI has been working as a Vibration Engineer at Saudi Aramco's Consulting Services Department since 2015. He provides technical consultations to resolve complex rotating machinery and static equipment vibration issues. His scope covers all Saudi Aramco oil and gas facilities in Saudi Arabia. Mr. Alharbi holds several international certifications in the field of condition monitoring and reliability and has a wide experience in technology evaluation and deployment of pilot programs.

AHMED GHAZAL is the Technical Lead for Saudi Aramco's additive manufacturing strategy and responsible for deployment and value creation. He has more than 6 yr of experience in the oil and gas industry. He began his career as a dynamic analysis engineer, providing technical consultations to Saudi Aramco facilities and resolving issues related to machinery and structural vibrations.

DR. DORU C. TURCAN is a vibration engineer. At present, his role includes vibration analysis, conducting vibration analysis trainings, standards and procedures development and conducting a company-wide vibration monitoring benchmarking program. He has more than 20 yr of rotating equipment troubleshooting experience.

H. P. BLOCH, Reliability/Equipment Editor

Modular reed valve technology for reciprocating compressors

Hydrocarbon processing plants use reciprocating compressors for process gases in a certain flow and differential pressure range, and double-acting cylinder-piston arrangements are almost always involved. These arrangements include inlet and discharge valves on both the head end and the frame end (also called the "crank end") of the cylinder. Inlet valves act as check valves that allow the gas to enter the cylinder during volume expansion; the valves close off during compression. Discharge valves stay closed during volume expansion and begin to open after the gas has reached a pressure higher than that of the opposing (delivery-side or process-side) pressure.

The back-and-forth movement of the piston inside the cylinder is done mechanically by means of a traditional slider-crank mechanism. Since these compressors are double-acting, compression takes place on one of the two sides of the piston while gas is aspirated on the other side. Upon stroke reversal, the cycle is reversed, and the other side of the cylinder is now involved.

Reciprocating compressors offer several advantages, and four of these usually come to mind first:

- Design flexibility, as these machines can be manufactured in vertical or horizontal configuration. The internal packing, including piston rings and rider bands supporting and sealing the piston, can be lubricated or non-lubricated. The piston can be configured with integral labyrinths for vertical reciprocating compressors, thereby eliminating piston rings.
- Excellent efficiency even for small compressor sizes operating at high pressures, and at partial loads.
- Operating flexibility over a wide range of gases and gas conditions for a given configuration.
- Wide range of throughput volumes achievable by keeping suction valves open during all or part of a cycle.

Today's leading compressor designers focus much attention on operating flexibility and ease of maintenance. In most cases, the design includes several crank mechanisms activated by a single crankshaft. Many cylinders (or "crank throws") can be installed on a single frame, all driven by one driver.

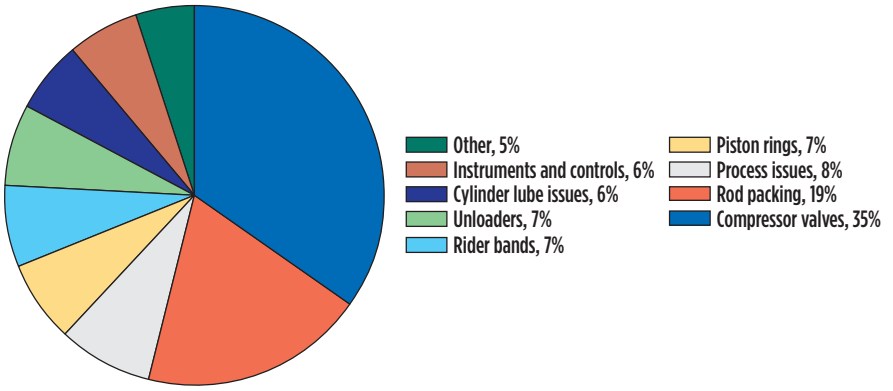

FIG. 1. Failing components in reciprocating compressors

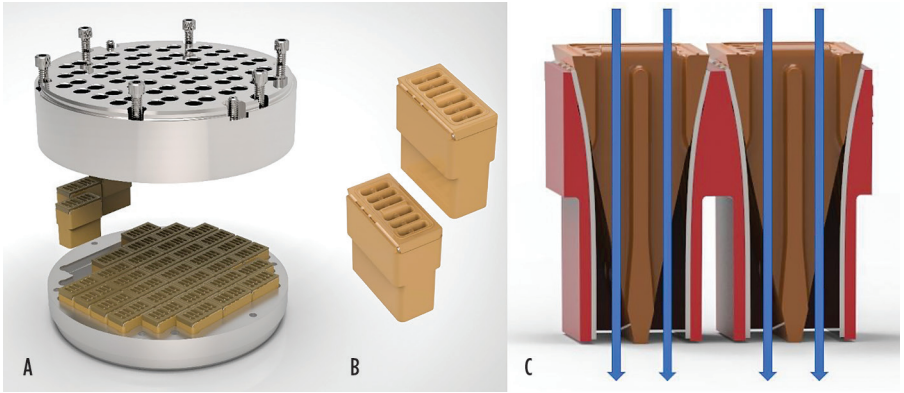

FIG. 2. Proprietary valve[a] (A); close-up of high-performance polymer flow elements (B); two straight-through flow elements illustrate the design principle (C).

The main function of reciprocating compressor valves is to control flow in and out of the compressor cylinders. However, valves are critically important components for reciprocating compressors; their functional integrity usually governs the availability and efficiency of these displacement compressors. FIG. 1 shows them at the top of failing components in reciprocating compressors.

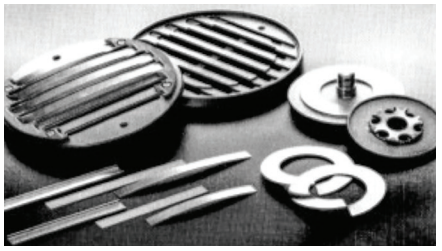

FIG. 3. A generic channel or reed valve, legacy style.

FIG. 4. A generic ring valve.

FIG. 5. A generic plate valve.

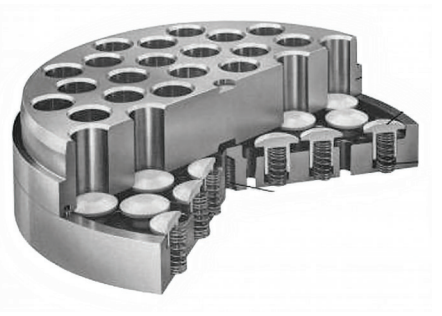

FIG. 6. A generic poppet valve.

FIG. 7. A modular reed valve, one of many possible drop-in replacement arrangements.

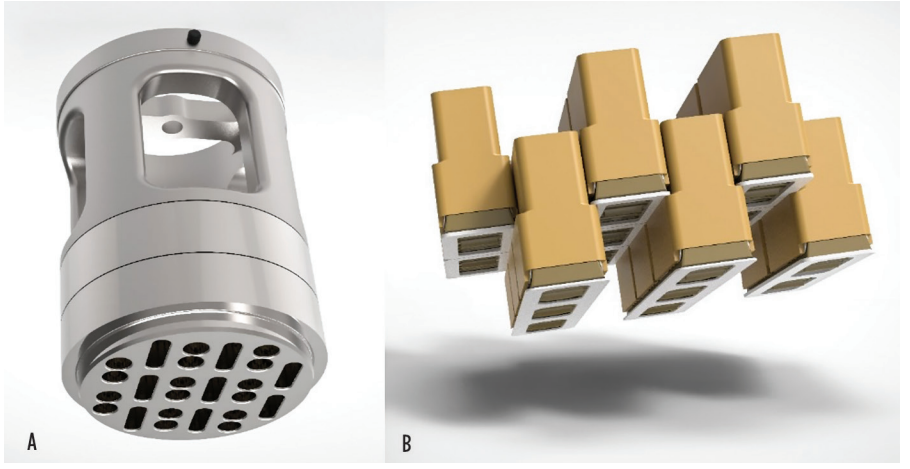

FIG. 8. A stacked proprietary valve[a] (A) and staggered element/insert arrangement in the stacked proprietary valve[a] (B).

Four or five styles of valve configurations are normally used in reciprocating compressors. Except for suction valve unloaders, which use mechanisms to physically keep a valve open during partial or entire stroke length (displacement) of a piston, valves are actuated by differential gas pressure. Valves open when the pressure on one side of the cylinder is greater than the pressure on the opposing side. Most living creatures breathe oxygen based on the same principle.

The compressor designer's and knowledgeable user's choice of valve depends largely on the type of process application. While valve type and size should be specified by the compressor manufacturer, the user-purchaser should also be involved. Although new or novel approaches are not entering the market every year, these products nevertheless exist and are well worth considering.

Reliability-focused users will be interested in understanding why certain, radically new modular reed compressor valves (FIG. 2) have been making inroads since about 2014, when they were used on offshore platforms. As of 2017, and after initially concentrating on oil exploration and production facilities, these modular-design straight flow-through valves have made excellent progress in oil refineries and other downstream facilities. Many modular reed valves are presently installed in hydrogen compressors, with some individual machines approaching 20,000 bhp.

Being aware of a wide spectrum of readers and their different levels of experience, we opted to begin this article with a brief compressor valve refresher.

Types of valves.

The most prevalent "traditional" valve types are described here. Note that these would often be labeled legacy valves, and that some of these have probably changed little, if any, in the five decades from 1970 to 2020.

Channel and reed valves: Channel and reed valves (FIG. 3) are now considered obsolete; they are used only in small air compressors. While they can be used at the highest practical speeds, they will require higher-than-average maintenance. Moreover, they exhibit below-average efficiency, meaning above-average power losses.

Ring valves: Ring valves (FIG. 4) are generally used in slow-speed, high-pressure process applications. These valves use concentric rings, which open and close the valve ports. Ring valves share with plate valves the distinction of best suitability for high speeds of 1,000 rpm–1,800 rpm

Plate valves: Plate valves (FIG. 5) are typically used for high-speed separable compressors. Note: In this context, "separable" means compressors not integral to a gas engine driver. Plate valves resemble ring valves, but with the rings connected by ribs. Instead of individual elements opening and closing, all valve ports open and close in unison. They share the high-speed suitability characteristic with ring valves.

Poppet valves: Poppet valves find frequent use in low-compression ratio applications, such as pipeline booster compressors. They are preferred at low speeds of 250 rpm–600 rpm. These valves (FIG. 6) function by each individual poppet lifting with very low differential pressure action; they then allow gas to pass through the flow openings in the stop plate. Standard poppet valves are generally used in the speed range of 250 rpm–600 rpm; modified poppet valves are in use up to 1,200 rpm.

FIG. 9. A standard straight flow-through valve.

Design considerations. Since many factors will affect reliability, straightforward valve comparisons are difficult. We advocate that reliability-focused owner-purchasers look for demonstrated experience in virtually identical services elsewhere. An educated user should insist on viewing comparison data, and a cooperative vendor or manufacturer will not withhold this information from reliability professionals engaged in due diligence.

In the pursuit of comparison, a well-managed user-purchaser applies the principles of up-front machinery quality assessment (MQA). Among many other tasks, the MQA engineer verifies that the vendor's material selection is appropriate for the purchaser's gas conditions, operating temperature profile, and the end user's expectations of low power losses. Corrections and/or knowledge updates may be required by either party; reaching early agreement during MQA will save time and settle potential issues long before the compressors leave the factory.

A gain of 0.5% efficiency in a 6,000-kW reciprocating compressor where power costs $0.06/kWh and where machines are expected to accrue 8,700 operating hr/yr is worth more than one

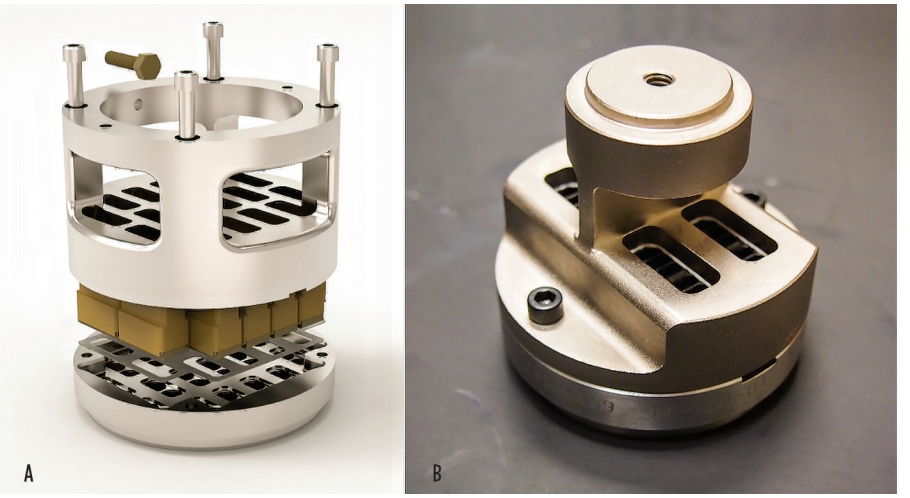

FIG. 10. A typical (A) and less-typical (B) integral cage proprietary valves[a].

FIG. 11. Demonstration of self-cleaning attributes of proprietary valves[a]; top (A) and (B), bottom (C) and (D).

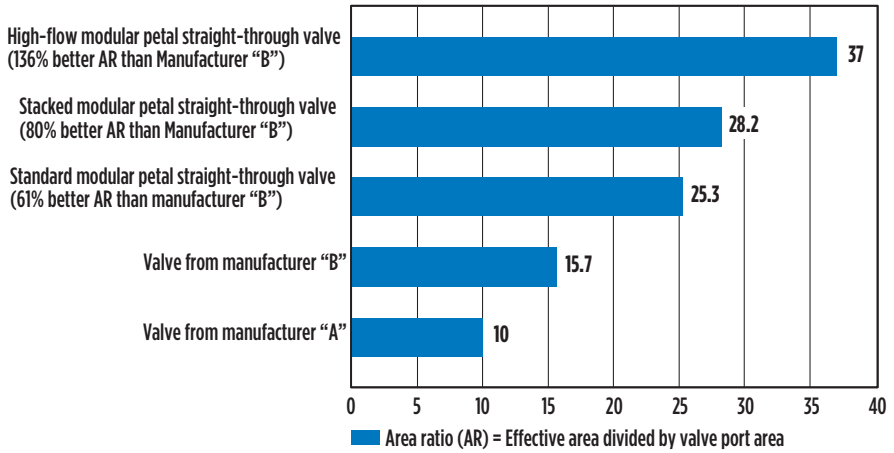

FIG. 12. Area ratio comparison for two widely used valves vs. three modular straight-through flow valves.

might think. Downtime avoidance also has value and should be part of the payback calculation. Again, clarification obtained during the MQA should not be viewed as burdensome; it will prove valuable to both the owner-purchaser and manufacturer-vendor.

Sharing knowledge. During scheduled pre-award meetings, a competent valve vendor or manufacturer will explain design compromises, gas velocity limitations, the meaning of valve lift (distance from seated to fully open, absence of valve flutter), tolerance for liquids and solid impurities carried in the gas, and overall valve operation in clean vs. fouling services.

Recall that there are bone-dry gases in some, and oil carryover in quasi-moist services. Explore if and how compressor valves tolerate these extremes. Find out before a sequence of premature failures tells you that experimentation with operating machinery is rarely acceptable when important assets are involved.

Examining modular straight-through flow valves. A new approach to compressor valve technology was introduced to refineries and petrochemical plants in 2017. The old legacy valves, **FIGS. 3–6,** can now be replaced by modular reed valves developed by a Houston-based manufacturer.[b] Modular reed valves can serve as drop-in replacements for virtually any predecessor valve. The novel technology is shown in **FIG. 2** and **FIGS. 7–11;** the modules (or modular elements) are an enhanced reed design incorporating high-performance polymers under compressive stresses. The inventor chose the generic term modular straight-through flow valve.

The author found considerable evidence that the manufacturer's advertised ease of service, improved compressor flowrates and other claims were correct. Servicing by lower-skilled workforce members, operating performance over an unusually wide speed range, and generally well-above-average availability/reliability were factually proven. While the first applications were in upstream facilities (oil exploration and gathering), modular straight-through valves have since made considerable inroads in downstream facilities, such as oil refineries and petrochemical plants.

The success of these valves is largely attributable to their straight-through design. Other advantages are intuitively evident; these include self-cleaning, an estimated 80% reduction in inventory, and validation through rigorous analyses. Test reports are among the various items of backup documentation; they reaffirm that the inventor's understandable enthusiasm was (and is) fully justified. A high-flow version is shown in **FIG. 7;** a stacked valve is depicted in **FIG. 8.**

Taken together, the seemingly small advantages in this or that measurement add up. Both standard and integral cage modular flow-through valves are shown in **FIG. 9** and **FIG. 10.** Either style adds value that cannot be ignored.

The flow area ratios of two widely used valves are compared with three modular straight-through flow valves in **FIG. 12;** the percentage area improvements are significant. Elementary physics explains that, for a given volume of gas, larger flow areas have less pressure drop than smaller flow areas. Lower maximum pressures in cylinders reduce pressure ratios by a small amount. These ratio reductions and larger areas of gas passage save energy and increase compressor throughput.

We were able to verify that the success of modular reed technology in proprietary valves[a] is linked to well-instrumented tests. It could be ascertained that the reports did not refer to comparisons of new modular straight-through flow valves with old and/or worn valves. Instead, the comparisons were for unused, old-style valves vs. unused, new-style valves.

The tests also showed sizeable improvements in energy efficiency, valve flutter, vibration, noise, pressure drop needed to activate valves, trouble-free operating time and necessary maintenance outlays. The self-cleaning attributes of the proprietary valves[a] (**FIG. 11**) were convincingly demonstrated. **FIG. 11A** shows one of the old, fouled valves removed from an oilfield compressor after less than 6 wk of operation, while **FIG. 11B** shows a modular reed valve removed from the same compressor after 31 mos of operation. **FIG. 11C** shows a traditional valve from an oilfield compressor in dirty natural gas service after 4 wk of operation—note that the valve is no longer repairable. In contrast, a modular reed valve from the same compressor taken out after 4 wk–5 wk can be field-cleaned in 10 min (**FIG. 11D**). HP

NOTES

[a] Zahroof's StraightFlo valve
[b] Zahroof

HEINZ P. BLOCH resides in Montgomery, Texas. His professional career commenced in 1962 and included long-term assignments as Exxon Chemical's Regional Machinery Specialist for the U.S. He has authored or coauthored more than 770 publications, among them 23 comprehensive books on practical machinery management, failure analysis, failure avoidance, compressors, steam turbines, pumps, oil mist lubrication and optimized lubrication for industry. Mr. Bloch holds BS and MS degrees (cum laude) in mechanical engineering from the Newark College of Engineering (NCE) and is one of 10 inaugural inductees into NCE's Hall of Fame, which honors its most distinguished alumni.

A. CURETON, Emerson, Minneapolis, Minnesota

How to support condition monitoring with wireless instrumentation networks

When *Wireless*HART first hit the market in 2008, most of the native devices using it were process measurement instruments. A pervasive sensing approach using these wireless instruments is now being embraced as companies deploy wider Industrial Internet of Things (IIoT) solutions as part of larger digital transformation efforts. The following are seven practical examples.

Pump monitoring. Pumps are critical to any process involving liquids, as is evidenced by the number of installations with two, or even three, redundant units supporting a single application. Pumps are maintenance intensive, suffering a failure or some level of degraded operation once every 12 mos. on average. Maintenance is typically reactive, costing approximately 50% more than detecting and resolving a problem prior to failure.

While strategic pumps frequently have some existing monitoring equipment installed, there are many others that should also be monitored. Before the advent of wireless instruments and networks, this monitoring was often too expensive; however, pumps can now be equipped with sensors to detect problems early so that appropriate actions can be taken. Such wireless sensors include those designed to monitor:

- Vibration
- Bearing temperature
- Inlet/outlet pressure
- Strainer clogging
- Seal fluid pressure/level.

Devices using *Wireless*HART networks are available to perform all these functions. The approach used to monitor a given pump will depend on its size and configuration, but the range of sensors illustrated is typical. It is important to use a multi-measurement approach because the various sensor technologies tend to overlap, working together to help diagnose problems.

For example, increased vibration might be caused by shaft misalignment or bearing deterioration. If the bearing temperature and noise have not increased, then the technician doing the troubleshooting might verify alignment first, since it is consistent with the symptoms.

Heat exchangers. Getting the most efficiency out of a common shell-and-tube unit (FIG. 1) requires process measurements. The main operating parameters are defined by:

- Inlet and outlet temperatures for both the process and transfer fluids
- Differential pressure (DP) readings across the inlet and outlet of the process fluid
- Flowrate for the transfer fluid.

The following is a typical setup using *Wireless*HART instrumentation:

- Temperature transmitters capable of sending data from four sensors on one wireless signal, reporting each reading in turn. The host system

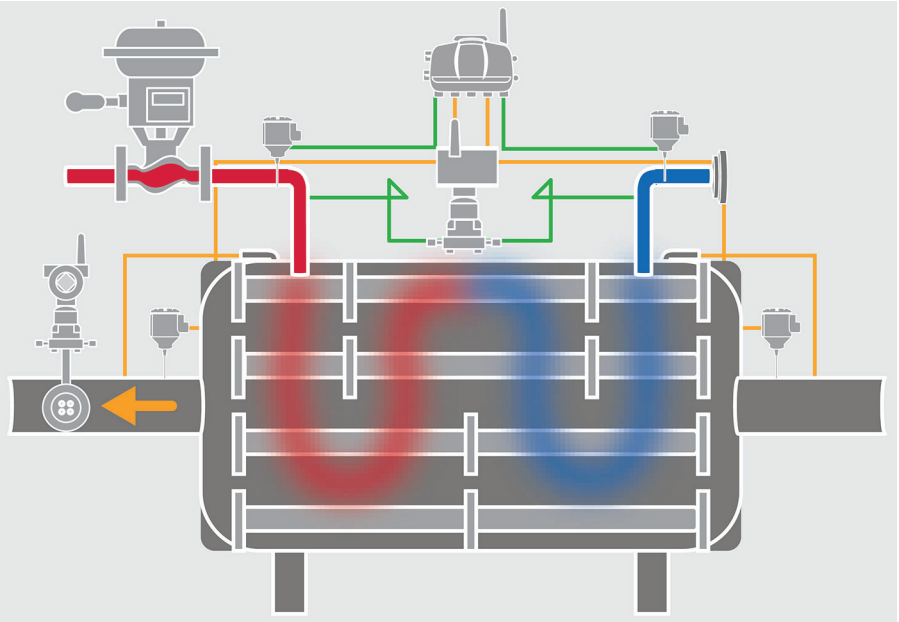

FIG. 1. A small group of strategic sensors can indicate both heat exchanger efficiency and condition.

updates each sensor reading individually. This covers all four temperature measurements.

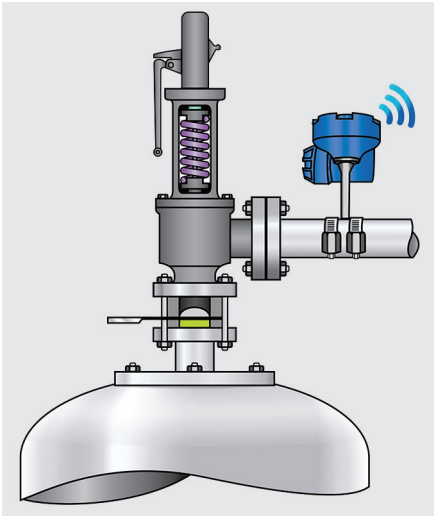

FIG. 2. An acoustic monitor mounted on the valve outlet can detect a full opening or slow leakage.

- The DP reading across the tubes uses a native *Wireless*HART DP transmitter.
- The flow meter for the transfer fluid can use a self-contained DP transmitter that is available with a native *Wireless*HART network.

When the temperature change and flowrate of both fluids are known, it is possible to determine how close the heat exchanger is running to its theoretical limit. If efficiency is low due to fouling, then information from the instruments can help determine which side of the tube wall is experiencing deposit formation. If there is a rise in the DP reading across the tubes unrelated to a change in flow, this suggests that the deposits are on the process side. A DP reading across the shell side is not recommended, since the internal free-passage flow is much larger. If there is enough depositing to cause a significant change on the shell side, this could cause a drastic loss of efficiency.

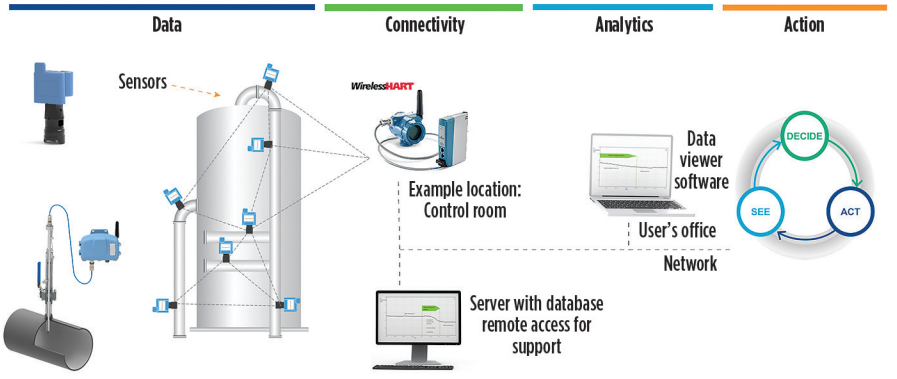

FIG. 3. Wall thickness sensors, combined with monitoring software, can provide data on real-time conditions and metal loss rates.

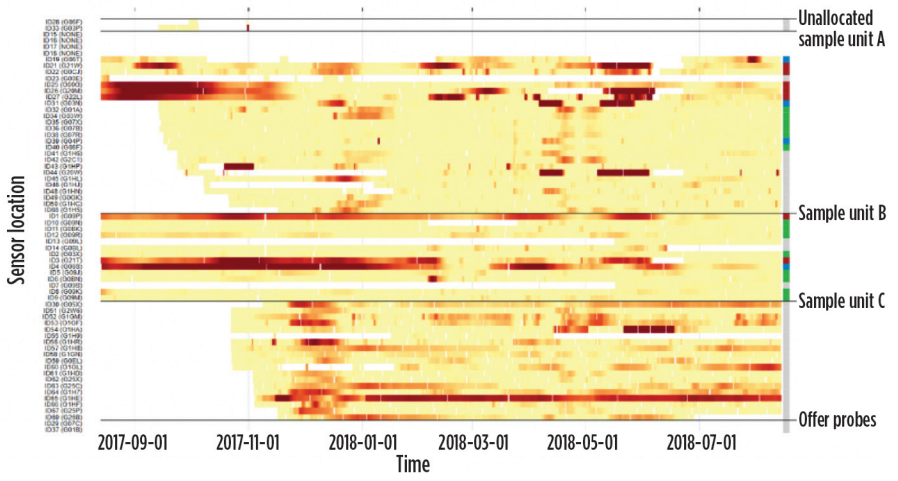

FIG. 4. Output from multiple sensors can be synchronized in time, using specialized software to provide a heat map of metal loss.

Pressure relief valves. Pressure relief valves (PRVs) have no built-in mechanism capable of reporting their condition or activity, so operators have little indication of their status. A PRV retains its seal by having a spring hold the stem against the seat. A fully closed valve is quiet because nothing is flowing through it. When the system pressure exceeds the setpoint, it opens, releasing the contents of the system—either liquid or gas (or both). This creates turbulence, generating noise that an acoustic monitor (**FIG. 2**) can hear and report to the automation system.

When pressure recedes, the valve should close again, and the noise should cease. Data from the acoustic monitor can report the time that the discharge began and ended, while indicating how serious the discharge was, based on sound amplitude.

The problem is getting the valve to reseal. Since overpressure incidents are often related to process upsets, particulates can be stirred up and blown out with the contents. Some can lodge in the valve seat, leaving it in a perpetually leaking state, which operators call "simmering." An acoustic monitor hears the simmering, so operators can tell if a given PRV has fully reseated itself after an incident. Maintenance can then decide when to address the issue.

With continuous monitoring, technicians can tell if a pressure release is underway or if a valve has not fully reseated itself. With prompt action, the overall effectiveness of the unit's safety system can be assured, while avoiding product loss and potential environmental consequences.

Steam traps. Steam traps are deployed throughout steam distribution systems to remove condensate. They are subject to mechanical problems, either failing open (resulting in a steam leak) or failing closed (causing condensate slugs to back up into steam lines).

Most plants monitor steam traps on manual rounds, where maintenance technicians look for signs of leaking, either visually or with handheld acoustic monitors. Condensate slugs are usually discovered when they damage equipment. Estimates suggest that 18% of the steam traps in a typical large refinery or petrochemical plant fail every year, each causing about $16,000 in extra fuel and steam costs.

By installing *Wireless*HART acoustic transmitters, plants can quickly identify

steam traps that fail open or closed, and determine if they are leaking or working improperly.

These transmitters listen in ultrasonic ranges and can recognize sounds made by units in various states by using an algorithm to identify failure modes and conditions (such as "good," "blow through," "cold" or "inactive"), and can also send warnings of malfunctioning units.

Corrosion monitoring. Understanding the effects of corrosion requires monitoring pipe and vessel wall thickness to determine how much metal has been lost and when containment will be lost. The traditional monitoring approach involves technicians taking manual thickness measurements by using a handheld ultrasonic device.

A large plant may have several thousand locations scheduled for inspection at periodic intervals that can range from every few weeks in high-risk locations to once every 5 yr in other less-critical areas. Manual inspections incur costs for the technicians to gain access to the desired measurement location, which may involve erecting scaffolding and removing insulation, among other requirements.

Even if the inspections are performed fastidiously, manual methods are notoriously inconsistent, and no data is available between inspections. Variability of ±1 mm (.04 in.) is typical, but if a pipe wall is 5-mm (0.2-in.) thick, the engineer may lack confidence when trying to determine when that pipe will reach its retirement thickness. Achieving consistent, reliable readings requires a different method.

Permanently installed, ultrasonic sensors monitoring wall thickness (**FIG. 3**), and which are designed specifically to work in harsh environments, can send data on a *Wireless*HART network. The installation cost of ultrasonic sensors is low because they are non-intrusive and can be mounted nearly anywhere without any cabling.

These corrosion monitoring systems allow even small levels of corrosion or erosion to be detected. Advanced signal processing software, along with its data visualization and analysis features, makes data interpretation significantly easier and quicker. Data from multiple sensors can be visualized on a single screen as a corrosion heatmap (**FIG. 4**).

Safety showers and eyewash stations. Companies often call people their most valuable asset, so monitoring the condition of human beings is critical. Safety showers and eyewash stations are scattered throughout process units, but are typically unmonitored. A distressed worker reaching a station may have to call for help on the plant radio or hope to be spotted by a colleague. With a simple *Wireless*HART valve monitoring device (**FIG. 5**), however, any activation of a safety shower or eyewash station can immediately be reported, along with its location, to the control room and first responders. This monitoring also helps protect equipment, as a leak or spill might be in progress.

The water supply must be monitored for temperature and pressure. If piping feeding the shower systems is exposed to the sun, it can get hot. These systems should use lines with enough flow to avoid solar heating or should automatically dump water when necessary. Similarly, monitoring pressure confirms that an operator has not inadvertently closed a valve and rendered a station inoperative. This can be done with a *Wireless*HART DP transmitter or pressure gauge.

Location awareness. If plant managers want a mechanism to indicate who is in the plant and where each individual is at any given moment, using Wi-Fi for this application is expensive. *Wireless*HART networks can support location monitoring at a lower cost, using a different technology than what is used when adding new process instruments to the network.

Location triangulation functions operate with a device that is called an "anchor" (**FIG. 6**). These devices communicate with

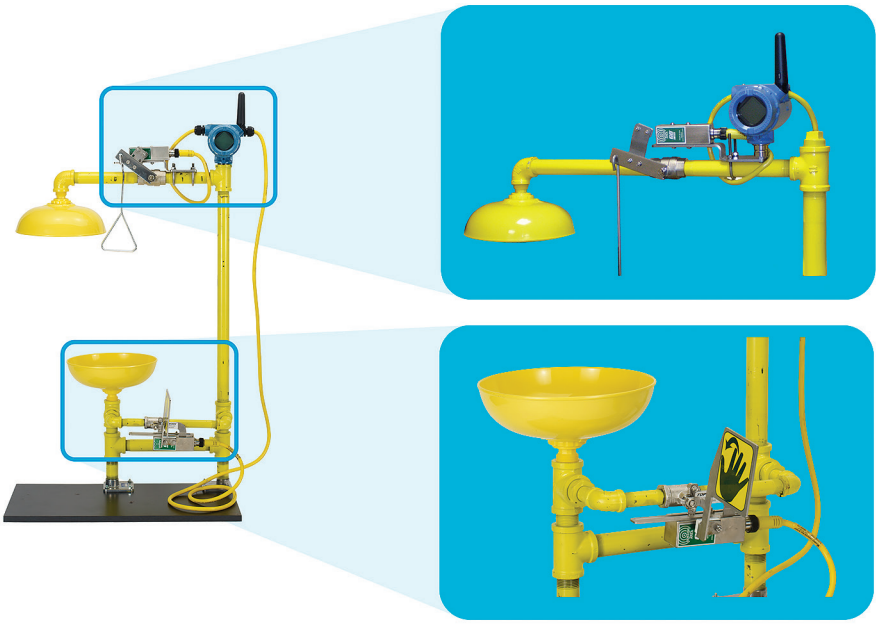

FIG. 5. Simple valve position indicators combined with a *Wireless*HART transmitter can warn the control room and first responders when a safety shower or eyewash station has been activated.

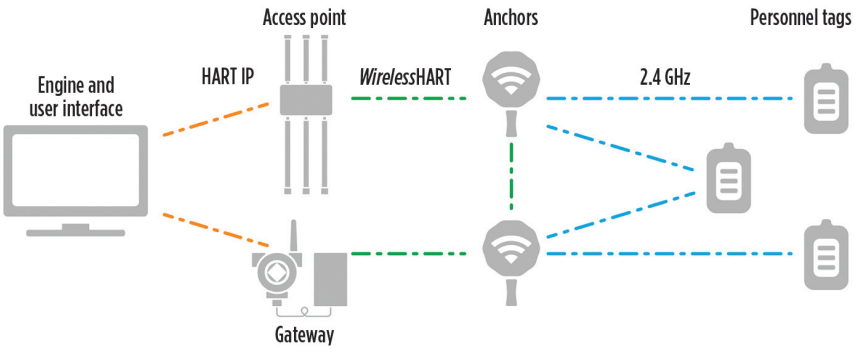

FIG. 6. Location anchors communicate with individual workers' tags, with each other and with the *Wireless*HART gateway.

each other and with the *Wireless*HART access points, in a manner similar to conventional *Wireless*HART instrument transmitters. Anchors communicate with the location tags worn by individual workers, providing the means to triangulate and determine where each tag/worker is located.

Location anchors are small, light and self-powered. Their Class 1/Division 1/Zone 0 rating allows them to be deployed throughout process plant environments. Rechargeable tags worn by each worker communicate with the anchors, and the anchors communicate with each other and with access points.

The *Wireless*HART approach is easily scalable to match head counts. It can also support the multi-level resolutions required for tall installations. This provides an exceptionally high level of flexibility to achieve the required coverage and overall worker safety.

Preconfigured software (FIG. 7) supports several useful functions, including:

- Geofencing indicates if individuals have moved into areas where they do not belong.
- Safety mustering lets first responders know which people have moved to the correct safe areas during a drill or an incident.
- Safety alerting allows a worker who is injured to hit a button on the tag to indicate an emergency in progress and the location.
- Social density can be monitored to ensure that large groups of workers are not gathered in a small area.

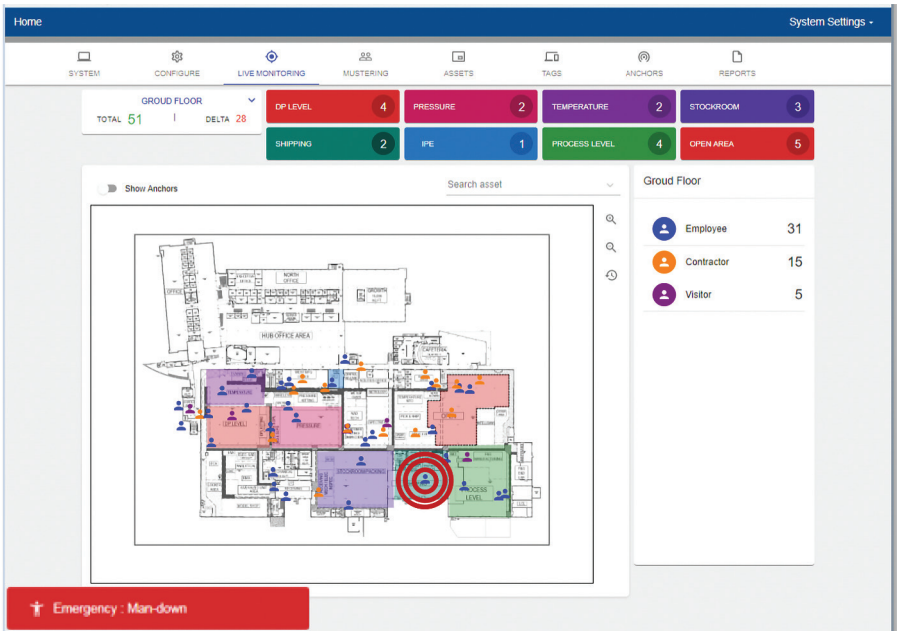

FIG. 7. Location monitoring platforms can indicate multiple functions, including emergency "worker down" situations.

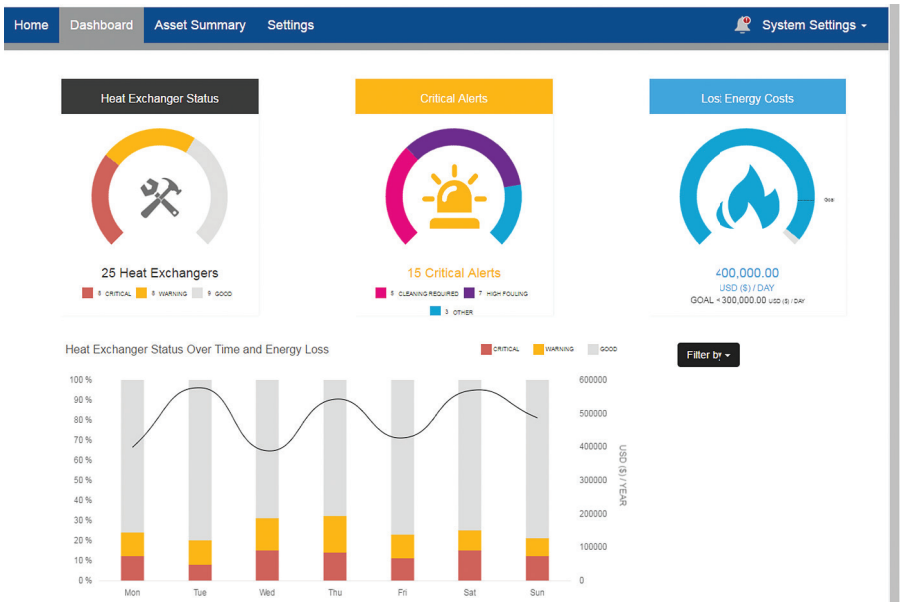

FIG. 8. Preconfigured applications (such as the one shown[a]) make data management and analysis far easier and less expensive than in years past.

Sensors for monitoring.

Sensors themselves do not ensure effective monitoring, as the data they provide must be collected and analyzed to be useful. Historically, this called for large-scale software installations, which made launching such a program a major undertaking and not cost effective for monitoring only a few items of equipment.

A new type of tool[a] has emerged (FIG. 8), drawing from concepts developed by the consumer electronics industry where sophisticated apps make user interactions simple. These are designed for specific functions, such as the seven just discussed.

Each application performs highly sophisticated analysis by focusing on their specific function, and includes preconfigured user interfaces and graphics, thus eliminating the need for custom software configurations. When provided with some basic values related to the equipment configuration and data from the wireless sensors, it becomes a simple matter to follow, record and analyze how the assets are performing.

*Wireless*HART sensors, whether used with existing control and monitoring systems or with new technical applications, provide the data required to improve process efficiency and safety. HP

NOTE

[a] Emerson's Plantweb Insight solution

ANDREW CURETON has been a Product Manager for Emerson's Pervasive Sensing applications for 4 yr and has been its go-to technical expert for the support of hundreds of wireless deployments in North America. His background includes quality engineering, computer networks and data analytics. Mr. Cureton earned a BS degree in industrial engineering from the University of Minnesota.

J. A. ZURLO, SUEZ Water Technologies & Solutions, Houston, Texas

Improving asset utilization by closing the corrosion window

Driving profitable refinery operations often requires owner-operators to balance production flexibility and product optimization with asset availability and equipment reliability. Many refineries face periods of severe corrosion and fouling in their crude unit distillation overhead systems. The exact cost of refinery corrosion is unknown; various analysis reports by NACE International and others estimate annual profit losses due to refinery corrosion to be $2 B–$12 B. Regardless of the exact value, it is not argued that corrosion is expensive and there is ample room for improvement to benefit both safety and profits. Overhead system corrosion is an ongoing phenomenon, but often occurs as a series of short episodes where intense corrosion occurs, separated by long periods when little to no corrosion occurs. These short, intense periods are known by some as the "corrosion window" and their episodic nature is one reason why corrosion can be a challenging issue to tackle.

Applying a collection of new tools, some of which have been developed in only the last several years, enables additional visibility, faster response and more informed decisions regarding which corrective actions to take for greatest effect. The overarching goal is to close the elusive corrosion window and shut out corrosion altogether. Today's technology innovation has created additional on-stream sensors to continuously monitor system performance and treatment levels, new methods to measure previously hidden properties, and expanded analytics capabilities to better predict issues before they happen. It is now possible to close the corrosion window to an extent previously considered impractical or uneconomical. Continuous system performance monitoring and automated alarming allows for near instantaneous response to changing conditions, enabling refiners to react faster and with better direction than previously possible. As will be illustrated, several refiners are applying one or more of the techniques for positive impact on their bottom line, while achieving safer, more reliable operations.

Corrosion causes and improvement strategies. Overhead corrosion can be complex to control. Three common corrosion mechanisms account for the majority of problems: acidic attack, salt-induced corrosion and velocity-assisted corrosion. Multiple factors are often involved, such as chemistry, contaminant concentration, contaminant types, operating conditions and mechanical factors. To clarify, an example of a mechanical factor is high overhead vapor flow, which can induce velocity-assisted corrosion.

Sometimes, one or more issues are perceived to be related to crude quality changes and are considered largely unavoidable, leading to overly conservative solutions at the exclusion of more complex, but more effective, options. This ultimately leads to increased costs and operational risks at a refinery. Despite the recognized high impact of corrosion, both the measurement and control of primary driving factors often fall short, frequently resulting in inconsistent performance across systems, making both the rapid understanding of driving forces and the consistent application of structured mitigation less effective. One possible explanation is that corrosion control programs were designed initially to prevent acidic attack. Advancements in chemistries and approaches to control corrosion have changed, but monitoring and control practice advances have lagged, leading to the gaps in recognizing and effectively responding to the intense corrosion episodes occurring during episodic corrosion windows.

Using modern equipment, sensors and techniques, it is now possible to effectively mitigate overhead corrosion while also maintaining flexibility, production and reliability. By taking advantage of the improved measurements, rapid testing and sophisticated analytics available today, much more granular and dynamic processing schemes can be effectively utilized where they were previously not possible.

While each overhead is unique, a common approach to recognizing, responding to, and ultimately overcoming corrosion can be used to reduce the size of the corrosion window or completely close it. The key elements in the approach include:

1. Reduce contaminants allowed into the overhead system—crude quality, desalting and contaminants introduced from outside the crude unit (e.g., amine contamination/recycle)
2. Corrosion control chemistry selection to improve performance and operating flexibility
3. Appropriate measurement frequency to respond to events faster
4. Ability to control the system within well-defined, safe operating ranges
5. Adopt a dynamic, safe operating window to avoid corrosion, moving away from using a fixed

safety margin based on "typical" safe practices.

Contaminant reduction. Contaminants found in an atmospheric distillation tower that contribute to corrosion can originate from a variety of sources—crude oil quality, upstream additives, poor desalter performance, amine compounds recycling via wash water and/or introduced from operations outside the crude unit battery limits.

While controlling and reducing contaminants that end up in the crude tower overhead system are a vital component of corrosion control, this is a broad topic best suited for a dedicated, standalone discussion (several published articles address these topics). Therefore, for the purposes of this article, we will assume that these external factors are addressed sufficiently and are out of scope, and instead focus on the overhead system itself.

Chemistry selection. Chemistry used to manage and control corrosion in an overhead system typically uses a three-pronged strategy: injecting controlled amounts of ammonia or organic neutralizing amines, a filming inhibitor and a water wash. Each individual corrosion control application will utilize these three elements to varying degrees based on the unit design, crude diet and operating envelope.

A neutralizer product is generally injected into the overhead vapors to control the pH of the condensing overhead waters within a range. This control helps balance the minimization of corrosion rate with the tendency for salt deposition caused by reaction with acids. Since there is a fundamental limit on the amount of corrosion reduction that can be achieved with the neutralizer alone, a filming inhibitor, or "filmer," is further used to reduce the corrosion rate of the system. Filmers function by coating the metal internals of the system with a hydrophobic barrier. The overall strategy is to use the minimum amount of the appropriate neutralizer possible to maintain pH in a slightly acidic region near 5.8, and then use the filmer to reduce corrosion rates to an acceptable level.

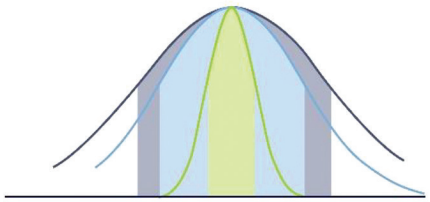

	Manual lab	Auto-monitor	Auto-control
Median	7.3	5.8	7.1
Standard deviation	3.8	2.9	0.9

FIG. 1. Chloride concentrations in boot water.

Further complicating the situation is that the neutralizer interacting with the acidic species can form a depositing salt, which can be very corrosive. In some circumstances, salts formed upstream of the natural water dewpoint of the condensing steam in the overhead system give rise to under-deposit corrosion. To control the deposition and corrosion potential of depositing salts, a water wash stream can be injected to dissolve, dilute and wash away the corrosive salts from the overhead system. In these cases, the salts are scrubbed and removed to the water boot of the overhead condenser.

Each acid neutralizer salt forms at a unique location determined by a thermodynamic state change, known as a "salt formation point." If the driving factors change in the system, then the salt formation point will also change. If the temperature characterizing the salt formation point for any of the amine species in the system is upstream of the water wash injection point or the natural dewpoint of the condensing steam, then there is little to prevent the depositing salt from causing corrosion in the condensing system—or in the distillation tower itself, in more extreme cases.

One method to prevent this corrosion is to modify the operating conditions of the tower. Traditionally, this means increasing the tower top temperature. While this can work, it reduces the flexibility of tower operation to maximize yield of the most in-demand or profitable products. A more powerful approach is to control salt formation through appropriate selection of neutralizer chemistry. A neutralizer program that effectively maintains pH but forms salts only in areas where sufficient liquid water exists will mitigate acidic attack, prevent salt formation in undesirable areas and preserve operating flexibility.

Three main issues can limit the effectiveness of filming inhibitors:

1. Coverage
2. The ability to maintain an effective film at low pH conditions
3. Water emulsification leading to degraded distillate product quality.

Filmers can generally be classified as semi-polar molecules. They possess hydrophobic and hydrophilic qualities. Classic filmers have a straight-chain hydrophilic tail, while newer filming technologies utilize a branched tail to provide a more complete barrier coverage at lower concentrations. Furthermore, while older filmer technologies struggle to maintain an effective film during dips below a pH of 4, newer technologies can maintain greater than 90% film persistence down to a pH of 2. An example when this may occur is during an uncontrolled high-chloride excursion where there is suddenly not enough neutralizer to keep the pH elevated—exactly the time that the filmer is needed most.

Finally, the semi-polar nature of the filmer molecules means they can act as surface active agents (surfactants), migrating to any interface, such as a metal surface or the surface of a water droplet in a hydrocarbon stream. Filmer molecules can surround a water droplet and make it hydrophobic, thereby preventing coalescing of smaller drops of water into a larger drop and preventing separation from the oil. The "emulsification tendency" varies over a wide range from one product to another. Products with a high emulsification tendency can interfere with product specifications, promote overhead accumulator emulsification, upset tower operations and/or cause fouling, and should therefore be avoided. One method to rank filmer chemistries for emulsion tendency is to perform a water saturation index modified test, or WSIM, to compare relative water emulsifications.

Measurement and control improvements. Introducing onstream measurement equipment to replace manual sample collection and testing of overhead parameters—for example, pH, chlorides and corrosion rate—can reveal a variety of short-term, episodic system fluctuations with significant impact on corrosion. Using the onstream measurements for automated, closed-loop control dramatically helps maintain the system within control limits on a continuous basis. This eliminates, or at least significantly reduces, time out of compliance as compared to the traditional manual testing and adjustment methods.

FIG. 1 shows the distribution curves of chlorides concentrations measured in a system during three separate time periods, using three different measurement scenarios. In all three scenarios, caustic is injected downstream of the desalter and adjusted to limit the chloride content in the overhead accumulator vessel. The median of all three data sets are essentially identical, at 6 ppm–7 ppm, which is considered appropriate. However, the standard deviation of the data in the scenarios is quite different, depending on the way the data is obtained and how the caustic injection rate is controlled.

The purple curve in FIG. 1 shows manual sampling and analysis in a refinery onsite laboratory, while the blue curve uses an onstream analyzer. Manual adjustment of the caustic rate was used in both scenarios. While a slight improvement to the standard deviation is seen when sampling and analysis moves from manual spot testing to automatic onstream analysis, manual adjustments to the caustic injection rate limit much of the potential for improvement. In contrast, the green curve uses the same onstream detector for measurement, but now the caustic injection rate is controlled using automatic closed-loop control, and the resulting variation of chloride concentration is significantly smaller than the measurements obtained using the other two methods. The advantage of this is dramatically lower overall salting potential, the ability to easily change chloride setpoint on an as-needed basis, and opening the opportunity to both expand and take advantage of a dynamically changing, safe operating window to allow more naphtha or kerosene/diesel to be produced as the market and margins dictate.

In parallel, more frequent and more rigorous amine speciation analysis with rapid generation of results brings a much larger amount of ongoing information about crude contaminant changes and their subsequent impacts on the corrosion behavior of the overhead system. The diversity of organic amine compounds used for a variety of chemical treatments and unit operations, both throughout the refinery and in the upstream/midstream segment, has increased over time in attempts to solve specific problems. As a result, the number of amine compounds detected in overhead systems has increased. In a modern refinery environment, it is not uncommon for six or more amine compounds to be detected in an overhead boot water sample within a short timeframe. Not all compounds react to form problematic salts, but the common practices of infrequent rigorous measurement or frequent measurement for a limited set of compounds leave significant gaps that often lead to undetected corrosion events.

FIG. 2 evaluates salting above the dewpoint temperature across five refineries that have experienced transient corrosion episodes. Each dataset was taken over a 4-mos period. Rigorous amine analysis was done 1–3 times per week in each system. The color scale indicates the frequency for each amine chloride salt that resulted in salting above the dewpoint for each system. Uncolored cells indicate that the amine was not detected in any analysis over the evaluation period. Clear variation is seen from system to system in both the amines detected and the ones that produce detrimental salts. Even when an amine is detected across most systems, the frequency of detrimental salt is not the same. While not specifically shown in FIG. 2, it is also notable that the amine species that produce detrimental salts in a given system often change significantly over time. Therefore, to provide adequate information about salting corrosion in a system, many amines should be tested on a frequent basis to accurately assemble a picture of salting and how the salting changes as time and conditions fluctuate.

Moving the rigorous analysis of multiple amines from a remote laboratory to the refinery site enables dynamic salting potential and safe operating window calculations in a near-continuous fashion. This is important, as many aggressive corrosion events are of a short-term nature and are missed otherwise. Coupling this with improved measurement of the salting state for the system allows more rapid identification of out-of-control events and the ability to make quantitative decisions for mitigation, further accelerating the ability to detect and respond to event-driven corrosion. Ultimately, lower corrosion, greater flexibility and extended equipment life result.

FIG. 3 shows three separate, 60-d periods where corrosion exceeded target on the same system. The blue region represents continuous corrosion measurement with manual control; the yellow region shows the value of closed-loop control of the chemical treatment and automated alarming of corrosion rates; and the gray region shows further improvement from dynamic system salting calculations, using local onsite amine analysis and subsequent automated salt

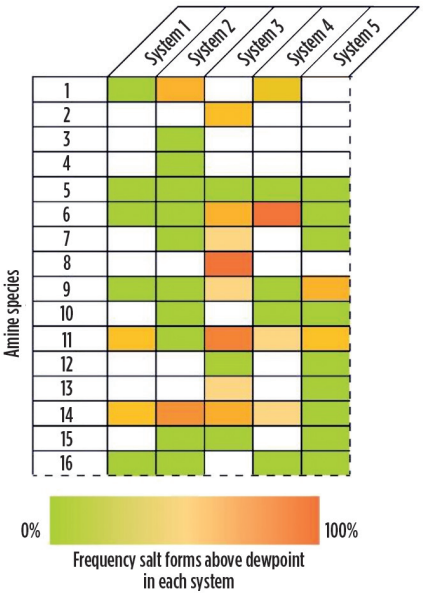

FIG. 2. Salting frequency in multiple systems.

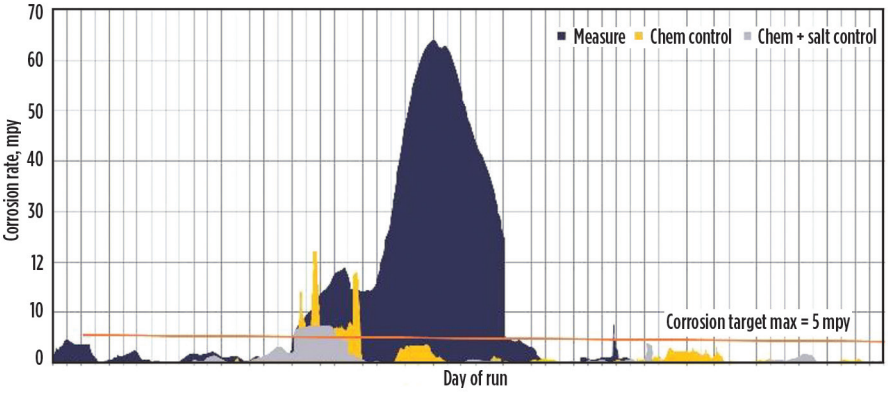

FIG. 3. Corrosion excursion improvement.

point calculations. **Note:** The time windows are arranged so that the measured events occur at the same spot on the graph. Each technology advancement reduces the duration above the target corrosion rate by improving response to uncontrolled events. Although these are specific examples from one system over time, they are representative of general improvements seen across multiple systems. The results, again, are lower overall system corrosion, longer equipment life and improved production yields.

Dynamic vs. fixed safety margin. The industry typically seeks to operate the atmospheric distillation tower upper section in such a way as to prevent a salt formation point from occurring inside the tower. The common method used is to calculate the salt formation temperature of the system and control the tower top operating temperature at a fixed safety margin that is higher than that of the salt formation temperature. Each refiner decides what safety margin to use, but generally a 25°F–40°F difference is specified. Based on the number of systems that experience premature failures and short equipment life, and the overall cost of corrosion, this approach does not appear adequate to effectively prevent ongoing corrosion, especially the type driven by transient events.

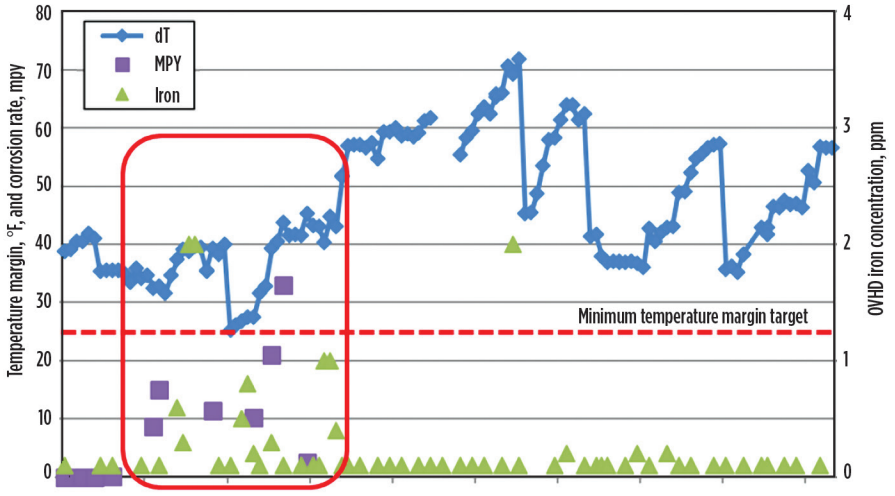

FIG. 4. Corrosion event.

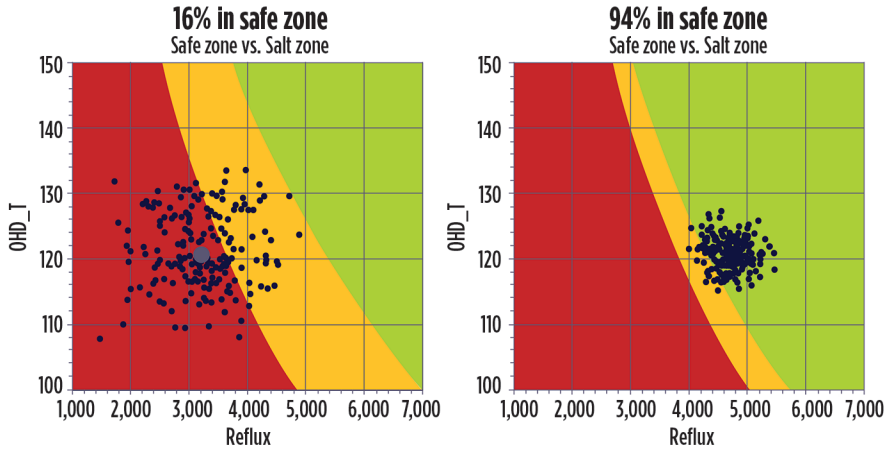

FIG. 5. Salting potential analysis.

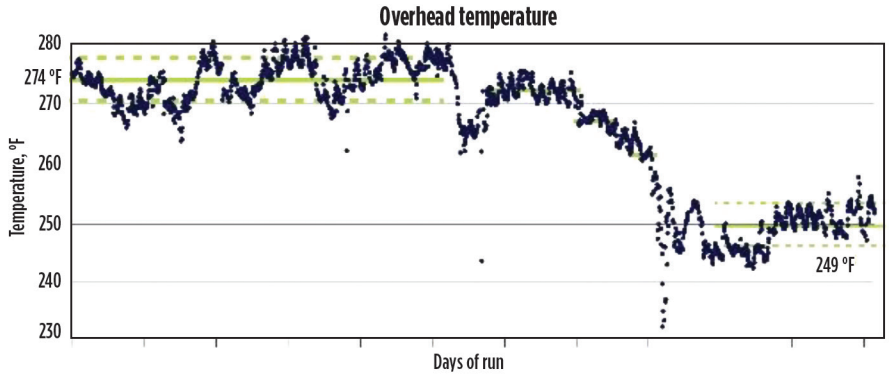

FIG. 6. Safely increasing distillate yield.

The issues surrounding the use of a fixed-temperature safety margin to mitigate ongoing corrosion are two-fold. First, calculating salt formation temperatures at fixed intervals leaves gaps that often do not catch episodic events. Second, using a fixed margin of safety on a dynamically oscillating parameter leads to control inefficiencies. When the safety margin is insufficient to protect against an uncontrolled event, corrosion occurs. To illustrate, FIG. 4 shows a system always operating above the targeted safety temperature margin of 25°F (red line), but the data inside the red box identifies a clear corrosion event indicated by a temporary rise in both corrosion rates (purple square markers) and iron in the boot water (green markers). Conversely, when a system is well controlled and salt formation temperatures are sufficiently low, the safety margin becomes larger than necessary to avoid corrosion, and the reduced yield optimization flexibility results in operational giveaway.

Together, the advantages of the technology developments described in the aforementioned sections with parallel advancements in data handling and quantitative, risk-based analytics have opened up a new path. They have allowed for movement beyond fixed-margin temperature targets to dynamic determination of system corrosion potential and use of current, safe operating margins. A key foundation has been the development of computational engines to process the large amount of incoming data, evaluate sensitivities and impacts, and reduce potential actions to a structured priority list based on a quantitative evaluation of risk and reward. FIG. 5 charts the over-

head salting potential of a crude unit during two separate operating periods at the same overhead temperature. The system salt formation temperatures are calculated at all operating times during the data acquisition window for each period. The green region represents the safe operating window, the red is unsafe and the yellow is the safety margin for the period.

The left chart in FIG. 5 shows a period of unsafe operation; the system is only in the safe operating region 16% of the time and has a wide operating variation (the spread of data points away from the center). During this period, a wide and potentially infeasible safety margin (yellow region) would be required to ensure safe operation. The right chart, on the other hand, shows much better performance with tighter operational control and, subsequently, is characterized by a narrower and economically feasible safety margin (yellow region). This type of computational technique and data visualization allows improved operating state visibility and the ability to operate closer to the optimum for improved profit, maintenance, and safety potential with reduced capital costs over time.

Using this different definition of safe performance and the other technology advancements discussed earlier, a U.S. refiner moving from a fixed safety margin-based operation to dynamic control was able to safely reduce overhead column top temperature by approximately 25°F (FIG. 6). This operational change allowed the refiner to increase distillate yield without sacrificing reliability, in a consistent and long-term manner. Due to favorable distillate margins, captured additional distillate profit alone was conservatively estimated at $1.5 MM/yr.

Takeaway. Progressive refiners are adopting new approaches that combine technology, chemistry and analytics to shift how performance is measured and controlled, with the result of more favorable operating windows, improved reliability and, ultimately, higher profits. The methods and approaches described here, while relatively new, have proven effective in the industry over the last several years at multiple refineries. These advancements have enabled refiners to not only better recognize the previously hidden corrosion window, but also act to close the window altogether on uncontrolled corrosion in crude unit overhead systems, while gaining opportunity to maximize profitable yields. Finally, while each aspect of advancement discussed here has benefit when deployed independently, greater gains are seen when all are implemented together. HP

ACKNOWLEDGMENT

The author thanks Dr. Collin Cross and Dr. Keyur Patel for their help with technical information, data and editing support.

JEFFREY A. ZURLO is a Senior Marketing and Commercialization Lead for SUEZ Water Technologies & Solutions. He has more than 30 yr of experience in engineering, technology, business development and marketing across several hydrocarbon processing technologies. Prior to joining BetzDearborn (now SUEZ) in 1997, Mr. Zurlo held various process engineering positions at Sunoco Inc., Koch Refining and Hercules Inc. He holds a BEng degree in chemical engineering from Stevens Institute of Technology in New Jersey.

T. WEBSTER, XRG Technologies, Tulsa, Oklahoma

Reasons for vibration issues in boilers and furnaces

A conversation with a long-time colleague at an industry trade show inspired me to think about one of the most confounding problems that occur in boilers and furnaces: vibration. Our discussion revolved around the fact that systems today seem much more prone to vibration problems than in the "good old days." A number of industry trends over the last several decades have contributed to this issue.

Trends contributing to vibration. Vibration in combustion systems has been studied for hundreds of years, from Dr. Higgins in the 1700s to Lord Raleigh in the 1800s and even NASA, as part of the Apollo program in the late 1900s. Despite all that research, it is still difficult to predict when vibration problems will happen and how to solve them when they do. The issue is complex for several reasons:

1. Vibration can be caused by a single component of the system or the interaction of multiple components.
2. Where vibrations manifest in the system may be far from the source.
3. "Identical" units do not exhibit the same behavior (i.e., one may vibrate and the other may not).
4. Vibrations may come and go with almost imperceptible changes in wind, temperature, humidity, barometric pressure or a combination of these conditions.
5. Solutions that have worked in the past do not necessarily work for today's problems.

Despite the difficulty in determining up front if a system will experience vibration problems, we have identified qualities that increase the likelihood of vibration occurring. The combustion process serves as a major participant in most vibrational problems. Flames generate noise across a wide range of frequencies and introduce a large amount of energy to these systems. This means that they can act as either sources of vibration or amplifiers for vibrations from other parts of the system.

Efforts to reduce NO_x. The drive to reduce NO_x emissions has further increased the role that burners play in vibration problems. Natural gas is now the most common fuel used and, unlike coal or oil, where most of the NO_x formed comes from nitrogen in the fuel, most of the NO_x from gas combustion is a function of the temperature within the flame (aka "thermal NO_x"). Burners now employ a variety of techniques to lower flame temperatures, but this also negatively impacts some operational characteristics.

Since lower NO_x burners also tend to have narrower windows of operation for excess air level, they can cause vibration when operated outside of these windows. Let us consider the example of a conventional burner from the 1970s producing 150 ppm of NO_x. Although high in NO_x emissions, this burner may have reliably operated with excess air levels between 5% and 60%. Compare this with a 30-ppm low-NO_x burner, which now must be kept between 10% and 40% excess air, or a 9-ppm ultra-low-NO_x burner, which must operate between 15% and 25%. Failure to keep these newer burners in the proper ranges can result in "rumble" (vibrations between 10 Hz and 60 Hz) when the excess air is too low, or "panting" (vibrations less than 10 Hz) when excess air levels are too high. Systems with high degrees of variability, due to changes in fuel composition or rapid load swings, may have trouble finding control devices that respond quickly and accurately enough to keep them within this required window. In these cases, higher-NO_x burners and the use of back-end cleanup systems, like selective catalytic reduction (SCR), may be a better operational choice.

When sound waves travel inside a vessel, their speed is a function of the temperature of the gases through which they travel. With a very hot burner flame in the center of the furnace and cooler flue gases near the walls, the sound waves within the furnace travel at different speeds. When low-NO_x or ultra-low-NO_x burners try to lower these peak temperatures to reduce thermal NO_x formation, they often spread out the heat more effectively in the furnace, thereby making the temperatures more uniform. This creates optimal conditions for a "standing wave" to form inside the furnace, as all the sound waves travel at the same speed. This is often seen as a high-frequency multiple of the fan speed. For example, a system with a fan operating at 60 Hz might experience a loud "whining" noise at 180 Hz, 240 Hz or 300 Hz. While this high-frequency vibration may not be as damaging to components as rumbling or panting, it can still make the area around the furnace a loud and unpleasant environment.

Sizing considerations. The competitive forces of the market push manufacturers to continuously optimize designs and efforts to reduce costs. When it comes to boilers and furnaces, this generally means making them smaller. The smaller

the furnace section for a given capacity, the higher and more uniform are the temperatures in the furnace. Both conditions increase the potential for vibration, especially when coupled with lower-NO_x burners.

A simple way to correlate this is by taking the total heat release of the burners and dividing it by the volume of the radiant section. For example, compare two boilers with a burner heat input of 100 MMBtu/hr. Boiler A has a radiant furnace section that is 6 ft wide × 9 ft tall × 28 ft long, and boiler B has a radiant furnace section that is 7 ft tall × 7 ft high × 20 ft long. This gives a furnace heat release for boiler A of $100{,}000{,}000 \div (6 \times 9 \times 28) = 66{,}137$ Btu/ft^3, and for boiler B it is $100{,}000{,}000 \div (7 \times 7 \times 20) = 102{,}041$ Btu/ft^3. While both units could be capable of meeting the performance requirements of a project, boiler B has a much higher probability of developing a vibration problem.

Fan alterations. Historically, systems that use forced-draft fans to supply the combustion air were commonly supplied with a damper on the outlet of the fan to control the airflow. To improve electrical efficiency, especially when operating at lower load, these outlet dampers are now often replaced by inlet vane dampers or variable speed drives.

However, the outlet damper acted like a resistor in the system, helping prevent vibrations from being transferred from the fan to the burner and vice versa. Eliminating it removes a critical tool that prevents or mitigates vibration problems. Since vibration problems occur when the driving forces in a system exceed the dampening forces, it is better to build more dampening into a system, rather than less. Another area where this can be helpful is having draft control dampers in the stack or breeching. Often, these are used only when multiple units share a common stack or on very tall stacks; however, when present they can be another key tool to tune out vibration issues.

Many of these tools, like the installation of fan outlets and stack dampers, are expensive to add in the field. Additionally, some of the selection decisions—e.g., burner type, NO_x control strategy and furnace or boiler selection—are even more difficult to change after the equipment is in the field. Therefore, it is best to include this analysis up front in the project. Spending a little extra money to include a couple of dampers, or not choosing the smallest and cheapest unit, may prevent higher costs and numerous headaches down the line. HP

TIMOTHY WEBSTER has more than 25 yr of experience in the combustion industry and brings a wealth of experience and technical expertise across a wide range of industries to XRG Technologies. He graduated with a BS degree in mechanical engineering from San Jose State University in California and received an MS degree in engineering from the University of Wisconsin. Mr. Webster began his career engineering custom combustion systems for a wide range of applications including boilers, heaters, furnaces, kilns and incinerators. He is a licensed professional mechanical engineer in the states of California, Texas, Louisiana and Oklahoma, has authored numerous articles and papers and has co-authored several combustion handbooks.

MIKE RHODES, MANAGING EDITOR
Mike.Rhodes@HydrocarbonProcessing.com

Real-time hydrogen monitoring in synthesis gas applications

H2scan has released its latest product in the HY-OPTIMA™ line of sensors. The HY-OPTIMA 2745 hydrogen-specific analyzer is designed to deliver real-time measurement of hydrogen levels in synthesis gas (syngas), with no cross sensitivity to high concentrations of carbon monoxide (CO).

Increasing global energy demand has driven interest in syngas, which can be used as an alternative energy fuel. Syngas also provides a way to turn waste gases, such as carbon dioxide (CO_2) produced by power plants or factories, into usable fuels. Syngas is composed of CO and hydrogen (H_2), with CO_2 sometimes also present. There are various methods of producing syngas, such as gasification from different feedstocks (coal, natural gas or biomass/waste products), partial oxidation, steam methane reforming or autothermal reforming.

The most common use of syngas is for production of H_2, with the H_2 then sold as a separate product and the residual gases recycled to be used as fuel for a steam methane reformer. Additionally, syngas can be used for production of synthetic petroleum, as a fuel or lubricant for internal combustion engines or as an intermediate for the production of other chemicals.

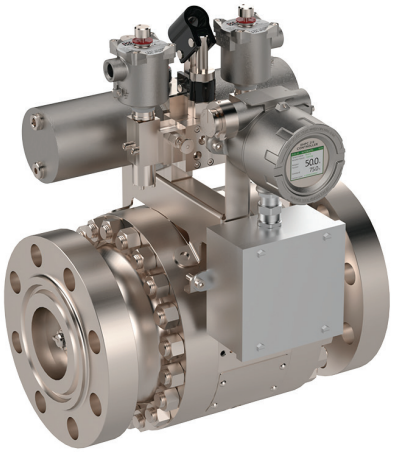

FIG. 1. Oxford Flow's ES axial flow isolation valve.

H_2 measurement in syngas is important as it indicates the quality of the syngas produced. Historically, this was done using either a thermal conductivity device to measure H_2 or by measuring the other components and assuming everything else was H_2. This assumption can result in costly inefficiencies in the production process.

H2scan's HY-OPTIMA™ 2745 hydrogen-specific analyzer is a measurement solution that provides a cost-effective and real-time measurement of H_2 in syngas streams. The solid state, non-consumable sensor technology, which is used in thousands of successful installations worldwide, provides continuous H_2 concentration data with no cross-sensitivity to other gases in the stream, including CO (up to 50% CO tolerant). No reference or carrier gas systems are required to reliably and accurately report real-time H_2 measurements with fast response times.

Real-time H_2 measurement allows an end user to adjust the hydrogen and carbon ratios to ensure maximum efficiency.

Axial flow valve fugitive emissions breakthrough

Oxford Flow has revealed that its ES axial flow isolation valve (FIG. 1) for the oil, gas and petrochemical sectors has excelled in fugitive emissions testing, offering a viable option to eliminate fugitive emissions from valves in critical processes.

ISO 15848-1 testing, performed at the Score Cowdenbeath laboratory in Scotland, demonstrated that the ES valve had a leakage rate of 100x less than allowed by level AH C03, which is the highest ISO performance level for isolation valves. It is notable that most valve manufacturers test in Class B, which allows 10x more leakage than Class A.

Using helium as a test medium, the results indicated that helium levels around the valve and hydraulics were not exceeding those normally found in the atmosphere. Therefore, the ES provides dramatically better fugitive emissions performance than the industry-standard for isolation valves.

Unlike traditional valve designs that utilize a mechanical drive train, the ES valve does not have an external stem and is instead operated by an integral hydraulic power unit. By removing the mechanical drive train and linkages, the ES design significantly enhances the long-term mechanical integrity and reliability of the valve and eliminates maintenance costs related to stem packing. Ideal for severe service applications, the valve provides repeatable tight shutoff across a wide range of processes.

Asset performance management software update

Coding challenges faced by operators implementing asset performance management (APM) software are to be significantly reduced or even removed, according to Lloyd's Register. Recognizing the staff, resource and cost challenges faced by many operators due to COVID-19, Lloyd's Register's latest update to its asset performance management software, AllAssets (FIG. 2), will help drive efficiencies and cost savings, mitigate risk and simplify implementation.

By re-emphasizing its innovative software development strategy of a low-code approach, Lloyd's Register hopes to empower companies to take control over their APM program and reduce the burden of deploying the resources needed to optimize operations and maintenance.

Low code removes the need for operators to pay to adapt software to their requirements and the need for outsourced technical expertise to implement it. The approach emphasizes shifting the power from the technology provider to the user, making software, such as APM platforms, much more straightforward and systematic and less time intensive, not only to implement but to update in line with

constantly changing business and regulatory requirements.

More broadly, adopting a risk-based approach using APM software can help operators of all sizes adapt to the new working conditions brought on by COVID-19. By optimizing the maintenance schedule, staff will only be required onsite when it is absolutely necessary, helping to reduce their exposure.

In addition to an emphasis on low code, the latest AllAssets release—v2.8—enhances user-journeys and performance with specific attention given to:

- Risk-based inspection journey
- Maintenance optimization journey
- Administrator journey.

By looking at how companies were using AllAssets capabilities in each journey, Lloyd's Register significantly optimized parts of these journeys with improvements of over 30% in some areas through simplified navigation and improved load time. The platform's dashboard now comes with hyperlinks, allowing users to access key parts of the platform in as little as one click. The new dashboard features also make it easier to dive into the data, helping users to more quickly understand which maintenance and inspection tasks to focus on.

Wireless monitoring of tension in critical joints

Maintenance engineers in critical environments charged with condition monitoring have long wished the bolts themselves could start the conversation. Now they can. Valley Forge & Bolt has taken its SPC4® Load Indicating Technology to a new level with the latest addition to the company's RTM™ (Remote Tension Monitoring) series of meters—the UHF Band RTM™ Meter, a wireless bolt monitoring system (FIG. 3). The UHF Band RTM Meter operates in 433/868/915 MHz frequencies, which includes the industrial, scientific and medical (ISM) frequency.

This wireless sensor detects and collects the tension level in a bolted joint as read by the company's SPC4® fastener, and then relays the data to a facility's condition monitoring/SCADA system. Users can also program the sensor to take measurements at prescribed intervals and send alerts if a bolted joint falls out of chosen tension parameters.

The UHF Band RTM™ Meter facilitates close monitoring of new fasteners during and immediately after install. The early hours after an initial tightening sequence can be critical to long-term performance because an unexpected loss of tension can affect bolt life.

In the long term, all bolts can be set to broadcast alerts when a chosen tension threshold is crossed. Managers can also program alert windows during "interest" periods, such as times of suspected greater vibration in a process, to gauge how fasteners are reacting.

With a web-based user interface, users can change parameters for each wireless sensor remotely. In addition, the UHF band attribute will improve battery life and enable increased distance from the probe to the collection device. SPC4® fasteners make it possible to measure the actual tension from within a fastener, providing real-time knowledge of critical joint tension and performance from installation through fastener life. A variety of sensors and meters are available to read, display and relay this tension information.

New range of comprehensive edge systems management capabilities

Stratus Technologies has launched enhancements to its ztC Edge computing platform with the release of Stratus Redundant Linux (SRL) version 2.2 and a preview of a new, comprehensive edge systems management solution, ztC™ Advisor. These enhancements enable optimal infrastructure performance, utilization and faster time-to-value to ensure simple, protected and autonomous business operations.

Stratus Redundant Linux 2.2, ztC Edge's core operating system, features an enhanced application interface, REST API, that provides more information via the web about ztC Edge's virtual machines (VMs) and their current state. This capability allows teams to remotely optimize infrastructure performance and utilization. SRL 2.2 also includes additional software and security updates.

With ztC Advisor, Stratus introduces a new edge systems management solution to simplify centralized monitoring and management of a customer's entire ztC Edge computing infrastructure. The new solution offers a secure web-based portal that anyone in operations or IT can use to view

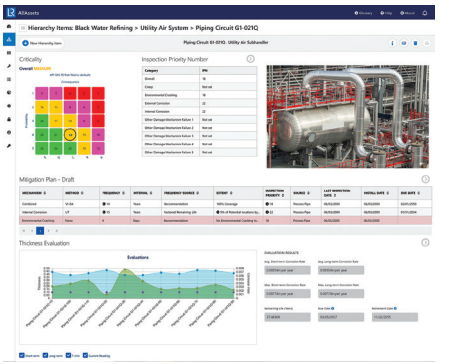

FIG. 2. The latest AllAssets release—v2.8—from Lloyd's Register.

FIG. 3. Valley Forge & Bolt's latest addition to the company's RTM™ (Remote Tension Monitoring) series of meters—the UHF Band RTM Meter.

the health and utilization of their entire ztC Edge inventory, remotely triage issues, improve productivity and mitigate risk.

ztC Advisor's first features include:

- A comprehensive asset management overview of all ztC Edge platforms owned by a customer, including systems that have been deployed but have not been provisioned. The overview makes it easier for administrators to holistically maximize resource utilization and optimize their hardware refresh and software patching schedules.
- A centralized dashboard view of individual system status and resource utilization presented in real time, enabling administrators to easily see platform status at-a-glance.
- User-defined groups for customers to assign individual systems to groups and use the ztC Advisor dashboard's built-in sorting and filtering functions to quickly access information from specific platforms.
- Secure-push technology between

ztC Advisor and ztC Edge. The web-based solution is architected so that ztC Edge platforms initiate sessions and periodically push information to ztC Advisor, which minimizes cybersecurity risk by limiting data transfer.
- Integration with Stratus Service Portal and ztC Edge platforms, allowing customers with portal access to use their same credentials to access ztC Advisor. One-click enablement from the ztC Edge Console automatically sets up the corresponding ztC Edge platform to be visible and present data through ztC Advisor, minimizing setup and configuration time.

ztC Advisor and its remote system monitoring capabilities are compatible with ztC Edge platforms running SRL 2.2, and build on updates to ztC Edge platforms, released earlier this year, that address customers' most pressing needs for enhanced security, monitoring and performance at the edge.

FIG. 4. New Hydra-Cell Q330 Series pumps by Wanner Engineering Inc.

FIG. 5. Sensirion's SCD30 CO_2 sensor.

Seal-less pumps without seals or packing

Wanner Engineering Inc. has introduced its new Hydra-Cell Q330 Series pumps (FIG. 4) that feature a seal-less design to avoid the maintenance problems of mechanical or dynamic seals and packing that can leak and wear. They are designed for a variety of high-capacity applications, including saltwater disposal (SWD), saltwater injection, bulk transfer and hydraulic lift in oil fields, as well as steam generation, reverse osmosis in water and wastewater treatment, mine dewatering, boiler feed and high-pressure cleaning. Models are available to meet API 674 performance standards.

The new Q330 medium-pressure models offer flowrates up to 153 gal/min (579 l/min; 5,247 bpd) and a maximum pressure rating of 3,500 psi (241 bar). New high-pressure models offer flowrates up to 118 gal/min (446 l/min; 4,047 bpd) and a maximum pressure rating of 4,500 psi (310 bar).

The seal-less design means that Hydra-Cell Q330 pumps do not have a leak path and therefore eliminate hazardous VOC emissions and the clean-up and disposal costs of packed-pump leakage. This also eliminates the need for external lubrication and maintenance as well as plunger wear problems associated with packing.

Hydra-Cell Q330 Series pumps can run dry without damage, will operate with a closed or blocked suction line, and can pump hot abrasive fluids effectively. The patented, seal-less Hydra-Cell Q330 Series pumps employ hydraulically-balanced, multiple diaphragms that enable the pump to handle high pressures with low stress and process abrasive particulates up to 800 microns in size.

CO_2 monitoring device

Cleveron AG has chosen Sensirion's SCD30 CO_2 sensor (FIG. 5) for its new CO_2 monitoring device. CLEVER Sense enables effective and smart ventilation in closed rooms and impresses with its top measuring accuracy and reliability.

More and more studies indicate that CO_2 can serve as a good indicator for monitoring the air quality in closed rooms. Since CO_2 in indoor spaces almost always originates from humans, conclusions can be drawn about the risk of infection with viral diseases such as COVID-19.

Especially in the cooler months of the year, it is important to keep the air quality high as people stay indoors longer than in summer. Air quality in classrooms, offices, meeting rooms, restaurants and many other spaces quickly becomes poor. Proper ventilation is therefore becoming increasingly important.

This is where Cleveron and Sensirion come into play. With CLEVER Sense, Cleveron AG offers a smart solution for monitoring CO_2 concentration indoors. With three levels that are based on a traffic light—red, yellow and green—the device shows the air quality in the room at any given time. Operation is user friendly via a web app or the integrated button.

The sensor used in CLEVER Sense is Sensirion's SCD30 CO_2 sensor. The sensor, based on the established CMOSens® technology, impresses with its top accuracy and reliability, as well as a small form factor that allows easy integration into applications.

New large enclosure system for purge and pressurization

Pepperl+Fuchs has introduced a Bebco EPS® purge and pressurization system (FIG. 6) designed specifically for use with large enclosures in Zone 1 hazardous areas. The 6100 series purge and pressurization system can purge an enclosure of more than 450 ft^3 (12.2 m^3), making it the largest purging system available from Pepperl+Fuchs. The 6100 series system is ideal for applications in the chemical/petrochemical and oil and gas industries.

The 6100 series is a fully automatic system that does not require an operator to initiate purging or pressurization. It offers optional temperature sensors that can be mounted around the enclosure for alarm notification or cooling. Additionally, there is automatic pressure compensation for excess leakage from the enclosure.

The 6100 system consists of a control unit, vent, low-pressure sensor and optional temperature sensors. The control unit allows users to configure the system for size of motor, temperature switch points, pressure switch points for leakage compensation and shutoff pressure, extra output for control or alarm, two selectable intrinsically safe inputs for various actions, and up to three temperature sensor inputs that can monitor various points

within the enclosure. The intrinsically safe user-interface can also be mounted in a separate enclosure near an operator for quick access and easy system monitoring.

The 6100 series purge and pressurization system features include:

- Certified for ATEX and IECEx Zone 1
- Fully automatic
- Maximum flowrate of 14,000 l/min
- Intrinsically safe user-interface for system programming and monitoring
- Control unit monitors system operation and controls enclosure power
- Auxiliary contact outputs for alarm or control
- Multiple temperature inputs for monitoring and control
- Automatic pressure compensation for excess leakage from enclosure
- Keeps enclosure pressure low during purging.

The intrinsically safe pressure sensor provides an accurate enclosure pressure reading for safe operation within the hazardous area. The pressure sensor, which can measure internal pressure from 0 mbar–25 mbar, can be remotely located at the enclosure's low-pressure section for correct, safe pressure readings.

The EPV-6100 vent can be ordered to detect various flows for purging and then feedback the signal to the 6100 series control unit to start the purge timer. There are five flowrates to choose from (14,000 l/min maximum) to meet any application requirement in large enclosures and some large motors.

Additional features of the 6100 series include system bypass, manual enclosure power on/off, temperature activation of purging for cooling purposes, and delay of power shutdown upon loss of pressure for pressure correction for shutdown procedures.

The 6100 Series Phase I is designed for large enclosures to keep the pressure low during purging. Phase II will be designed for large motors where the purge and pressurization pressure must be higher to compensate for the rotating machinery inside.

Enhanced thermal imaging flare stack solution

AMETEK Land has enhanced its flare stack monitoring thermal imaging solution (FIG. 7) with the inclusion of its advanced image processing IMAGEPro software to deliver accurate and reliable monitoring of the flame and the pilot light at the flare stack.

AMETEK Land's flare stack monitoring solution includes an infrared imager that produces high-resolution thermal images of the target, from any distance. This allows the camera to be positioned at a safe distance from the flame and makes it easily accessible for installation and maintenance.

The solution's IMAGEPro software monitors, captures and displays data from multiple thermal imaging cameras simultaneously to provide real-time analysis and exceptional functionality, delivering protection against unwanted emissions. Detailed visualization of the thermal data and the ability to set alarms enables the system to warn if action needs to be taken.

In addition to producing a visual image, AMETEK Land's imager also detects the infrared radiation emitted from the flame. This means the camera sees the flame, whether it is colored or clear, no matter the weather.

With a wide detection range from 100°C–1,000°C (212°F–1,832°F), even if the gas composition changes and affects the temperature of the flame, the imager continues to supply an accurate measurement. The range is high enough to ensure that background heat is ignored, and it operates in ambient temperatures from –20°C–60°C (–4°F–140°F), making it suitable for installation in almost any location.

The ability to select multiple regions of interest ensures that measurements continue to be made even when the flame is moved by wind conditions. By delivering accurate and reliable monitoring, the solution helps ensure that plants can meet flare stack emissions requirements in a safe and efficient operation.

Monitoring solution for carbon capture and storage

Silixa has launched Carina® CarbonSecure™, its distributed acoustic sensing (DAS)-based solution for continuous or on-demand monitoring of all stages of carbon capture and storage (CCS) operations. The new solution (FIG. 8) offers offshore and on-land operators the necessary monitoring measures with a reduced cost and environmental impact of their CCS facilities. The solution enables operators to provide the assurance to regulators and communities necessary to expand CCS adoption worldwide.

Carina CarbonSecure delivers ultra-high resolution, densely sampled acoustic data for real-time continuous and/or on-demand monitoring. Elements of the solution include micro-seismic monitoring and passive seismic throughout the lifetime of a CO_2 storage facility. The system also includes 3D vertical seismic profiling (VSP), time-lapse seismic, well-integrity and leak detection to ensure maximum safety over the various stages of CCS development.

Carina CarbonSecure is a reservoir management tool and can be deployed to:

- Assess the viability of geological formations for carbon storage during site characterization
- Monitor micro-seismic activity

FIG. 6. The Pepperl+Fuchs Bebco EPS® purge and pressurization system.

FIG. 7. AMETEK Land has enhanced its flare stack monitoring thermal imaging solution.

during the injection phase
- Ensure well and storage integrity when CO_2 is being injected
- Provide 4D monitoring of the CO_2 plume migration throughout the lifetime of the facility.

At the core of Carina CarbonSecure is Silixa's Carina® Sensing System, a patented, precision-engineered, fiber-optic acoustic sensing system that is proven to achieve 20 dB or 100x improvement in signal-to-noise ratio compared to standard DAS systems.

Carina CarbonSecure requires minimal seismic sources on land and fewer seismic shots offshore to acquire seismic data, meaning it can significantly reduce a project's environmental impact and cost. The system can be fully automated, enabling unmanned and remote seismic surveys on demand, lowering costs further while increasing employee safety.

In addition, Carina CarbonSecure's fiber array delivers high-resolution temperature data, is permanently installed and, because it has no mechanical parts, can be used without maintenance for decades in line with mandated CCS monitoring periods.

One device, two temperature instruments

The Ashcroft Model K dual-sensor thermometer (FIG. 9) combines two independent temperature sensing devices into a single instrument. For local indication, a silicone-dampened mechanical ANSI/IEC/EN classified bimetal system drives the pointer over an 80-mm, 100-mm, 130-mm or 150-mm diameter dial. Your choice of a stem from 90 mm–2,000 mm also contains a type K thermocouple to signal a remote readout, data acquisition device or control system. While providing these two distinct capabilities, the Ashcroft Model K only requires a single-process connection point. This multi-capable design will save both installation time and the cost of purchasing two separate instruments.

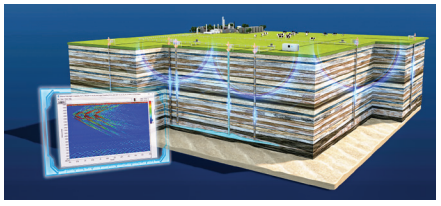

FIG. 8. Silixa's distributed acoustic sensing (DAS)-based solution, Carina® CarbonSecure™.

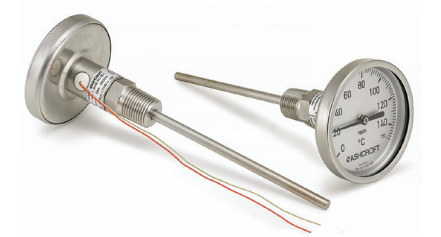

FIG. 9. The Ashcroft Model K dual-sensor thermometer.

Upgraded UTL process visualization and worker productivity platform

AIS Software has released its Version 8.2 release of the Universal Tag Locator (UTL) software that incorporates significant operations, productivity and safety enhancements based on requests and recommendations from its global clients.

UTL is an enterprise-level process visualization and reporting platform that aggregates real-time alarm, instrument, target, lab and exceedance information across a facility's stand-alone data silos into site-specific shift reports, operator dashboards and worker communications. Positive client experience has proven the value of leveraging one central communication tool for displaying operational data, reducing critical alarm floods, targeting key process values and removing the subtle barriers to process optimization. Since 1995, AIS Software has been consistently improving the client experience with rich shift logs, stronger operator communications and a wider range of functions.

Version 8.2 enhancement highlights include:
- Image manager
  - Insert user-captured images directly into shift reports, logs and operator instructions
  - Share images with other users
  - Link images to specific units, areas, systems or groups
- Alarm module improvements
  - Export alarm metrics data into new formats
  - Create custom line, bar and pie charts of tabular alarm data
  - Option to bulk enter external alarms
- Schedule target changes and IOW/DOW off-limit overrides
  - Schedule target changes and overrides in the future
- Register module expansion
  - Create blank paper forms that can be completed in Class I Div I environments
  - Improve register searches to capture more results over longer time intervals
  - Delete and archive registers in bulk.

More than 150 enhancements have been incorporated into the UTL platform, including improvements to register field logging and column formatting, expanding status change email notifications, better support for setting targets based on PI tags, and custom handovers embedded in shift reports. For more than 20 yr, these annual product enhancements have been distributed free of charge to UTL clients worldwide.

Glass tube variable area flow meters

Brooks Instrument has added the GT1600 Series of glass tube variable area flowmeters to its family of variable area flowmeter products.

Suitable for a wide variety of industries from chemical manufacturing to pharmaceutical production to water treatment and distribution, the GT1600 is ideal for low- and high-flow gas and liquid applications where viewing the process is important.

The rugged flow meter features high-quality design and materials, such as 316 stainless-steel construction and a polycarbonate shield, to ensure safety and longevity for both indoor and outdoor use.

For ease of use, the adjustable, transparent scale improves readability and allows for offset correction to compensate for process variation. In addition, the process connection can be rotated 360 degrees so users can view from all directions. An alarm option is also available for automatic monitoring of critical flow conditions.

Configured for simple installation, the GT1600 is available with a variety of connections to fit existing piping arrangements or mount to a panel or wall. It can also work as a drop-in retrofit for the Brooks Instrument GT1000, GT1300 and Full-View® 1100 Series of flow meters, which have been widely used for decades.

The GT1600 is fashioned for easy maintenance. For in-situ cleaning, the glass tube and float can be replaced without removing the flowmeter from the piping, saving time and cost. HP